

Master's thesis

2022

Master's thesis

prem kumar sherman

NTNU
Norwegian University of
Science and Technology
Faculty of Engineering
Department of Energy and Process Engineering

prem kumar sherman

SUSTAINABLE PRODUCTION OF FISH PROTEIN HYDROLYSATES: OVERALL SYSTEM ARCHITECTURE AND FOOTPRINT

June 2022



Norwegian University of
Science and Technology

SUSTAINABLE PRODUCTION OF FISH PROTEIN HYDROLYSATES: OVERALL SYSTEM ARCHITECTURE AND FOOTPRINT

prem kumar sherman

Sustainable Energy

Submission date: June 2022

Supervisor: Armin Hafner

Co-supervisor: Ignat Tolstorebrov

Norwegian University of Science and Technology
Department of Energy and Process Engineering

Preface

This is the Master Thesis report of **Prem Kumar Sherman** written during the final year masters study program in Sustainable Energy of **Department of Energy and Process Engineering** at the Norwegian University of Science and Technology (NTNU). The research work was carried out during the spring semester of the year 2022.

The main part of the work involves determining the energy efficient production technologies for fish protein hydrolysates and investigating the technology and economic feasibility. More effort has been taken with system modelling tools, optimizing the simulation, performing 3D modelling. I believe that the generated outcomes will be of value in future development and a guidance document to further researchers.

I would like to express my sincere gratitude and hearty thanks to my supervisor Professor **Dr. Armin Hafner** and co-supervisor **Dr. Ignat Tolstorebrov** for their continuous guidance throughout the thesis work. I would also like to thank Professor **Dr. Trygve Magne Eikevik** for his guidance and encouragement.

Finally, I would thank my parents **Sherman** and **Sugirtha Leela** and express my profound gratitude for their motivation and support.

Trondheim, June 2022



Prem Kumar Sherman

Abstract

Nowadays, there is a growing interest to use the fish rest raw materials in a more economical way. The **Fish Protein Hydrolysates** (FPH) produced from the rest raw materials have increasing application in the food and medicine industry. The production and stabilization of final FPH using conventional moisture removal techniques like spray drying and evaporation are energy-intensive. Process sustainability requires energy optimization in the process chain involved in the production of FPH, which greatly reduces greenhouse gas emissions and its environmental impacts. Hence, in this research work, the most efficient and energy-saving techniques for FPH production are investigated from cradle-to-gate in-terms of overall heating, cooling demand and energy demands.

Different alternatives in concentrating and drying steps are studied in detail to identify the process combinations with less energy use. It was observed that the process with direct drying consumes significant energy between **1.53 to 1.8 kWh/kg of water removal**. Concentrating before the drying stages helps to reduce the overall energy demands. Methods like freeze concentration (FC), three-stage evaporator (MSE/3SEV) and mechanical vapor recompression (MVR) evaporators consume less energy. In the results, it was observed that freezing the water using a freeze concentrator, takes less energy of around (0.076 kWh/kg water) **273 kJ/kg of water**. Two-stage system 'TWICE' was studied as a process for achieving maximum concentration in freeze concentration. In comparing the different processes, the mechanical vapor recompression cycle, requires the lowest energy of around **150 kJ/kg of evaporated water** (0.04 kWh/kg water), since the process works on the energy recovery principle.

Heat pump application covers heating and cooling demands which significantly reduces the overall energy needs. The energy recovery solutions are investigated with integrated heat recovery using a transcritical two-stage CO₂ system in Dymola & EES. The simulation results have **the heat pump COP of 3.5**. Also, the High-Temperature Heat Pumps (HTHP) were studied as an alternative for evaporation techniques. When integrating heat pumps with the spray drying process, significant **energy reduction of up to 50%** was achieved.

The energy study indicates, when producing the hydrolysates with energy-efficient equipment at the concentrating stage results an energy reduction of 60%. Also, the calculated CO₂ emissions levels are in a lower range. The investment analysis resulted a payback time of **4.8 to 5.7 years** for processes with freeze concentration and different dryers, **3.4 to 4.2 years** for processes with three-stage evaporators and dryers and **2 to 2.2 years** for processes with MVR and dryer's combinations. Finally, the economic sensitivity analysis has been carried out and the process representation is presented in 3D schemes modelled in SOLIDWORKS.

The thesis work was presented and published at the **7th IIR conference** on sustainability and the cold chain and **secured best paper award** for the research work.

***Keywords:** Fish protein hydrolysates, Energy demands, Sustainable production, CO₂ Heat pumps, process optimization, Freeze concentration, Evaporation process, High-Temperature Heat Pumps, Drying methods, Economic Analysis.*

Sammendrag

Nå for tiden er det en voksende interesse for å bruke restmaterialer fra fiskeproduksjon på en mer økonomisk måte. Fiskeproteinet hydrolysat (FPH) blir produsert av avfallet og får økende bruksområder i mat- og legemiddelindustrien. Produksjonen og stabilisering av FPH med konvensjonelle vannfjerningsmetoder som spraytørking og fordampning er energi-intensive. For at prosessen skal bli mer bærekraftig, må hele prosesskjeden fra restmaterialet til FPH energi optimaliseres. Dette fører til at klimagassutslipp og miljøpåvirkning tilknyttet produksjonen reduseres betydelig. I denne oppgaven blir derfor prosesskjeden for FPH undersøkt fra start til slutt med tanke på totalt oppvarmingsbehov, kjølebehov og energibruk.

Forskjellige metoder for konsentrert frysing og tørkemetoder blir studert på detaljnivå for å identifisere prosesskombinasjoner med lavt energibruk. Det ble observert at tørkeprosessen bruker mellom **1,53 til 1,8 kWh per kg vann** fjernet. Konsentrering før tørkestegene reduserer det totale energiforbruket. Metoder som frysekonsentrering, tre-steps fordampning og mekanisk rekompresjon (MVR) bruker mindre energi. I resultatene ble det observert at ved å fryse vannet ved bruk av frysekonsentrering, brukes det (0,076 kWh/kg vann) **273 kJ/kg av vann** fjernet som er mindre energi. I den mekaniske rekompresjons-syklusen var det gjennomsnittlige energibehovet på 150 kJ/kg for fordampet vann (0,04 kWh/kg vann) siden prosessen benytter energigjenvinningsprinsippet.

Varmepumper dekker behovet for oppvarming og kjøling, som reduserer energibehovet. Potensialet for energigjenvinning av varme og kulde ble undersøkt ved å simulere et 2-steps transkritisk CO₂-system i Dymola & EES. Effektfaktoren eller COP til den transkritiske varmepumpesyklusen er 3.5. Høytemperatur-varmepumpe ble også undersøkt som et alternativ til fordampningsmetoder. Ved å integrere varmepumper med spraytørkingsprosessen kan **energiforbruket reduseres med nærmere 50 %**.

Energistudien indikerer at produksjon av hydrolysatene med energieffektivt utstyr i konsentreringsstadiet resulterer i en energireduksjon på 60%. Dessuten er de beregnede CO₂-utslippsnivåene i et lavere område. Investeringsanalysen resulterte i en tilbakebetalingstid på **4,8 til 5,7** år for prosesser med frysekonsentrasjon og forskjellige tørkere, **3,4 til 4,2** år for prosesser med tre-trinns fordamper- og tørkeralternativer og **2 til 2,2** år for prosesser med MVR- og tørketromskombinasjoner. En sensitivitetsanalyse ble deretter gjennomført og 3D-modeller av prosessen er fremstilt i SOLIDWORKS.

*Oppgavearbeidet ble presentert og publisert på den 7. IIR-konferansen om bærekraft og kjølekjeden og sikret **prisen for beste papir** for forskningsarbeidet.*

***Nøkkelord:** Fiskeprotein hydrolysate, Energibruk, Bærekraftig produksjon, CO₂ varmepumper, Prosessoptimalisering, Frysekonsentrering, Fordampningsprosess, Høytemperatur varmepumper Tørkemetoder, Økonomisk analyse.*

Table of Contents

List of Figures.....	x
List of Tables	xii
Chapter 1: Introduction	1
1.1 Research significance.....	1
1.2 Motivation and project background	3
1.3 Task description	3
1.4 Overview	4
1.5 Report structure.....	5
Chapter 2: Theory and literature review.....	7
2.1 Pre-treatment	7
2.1.1 Thawing process.....	7
2.1.2 Grinding & mincing	7
2.2 Enzymatic hydrolysis technique	8
2.3 Filtration.....	9
2.3.1 Centrifugation.....	9
2.3.2 Micro, ultra and nano	9
2.4 Concentration	10
2.4.1 Multi-stage evaporation:.....	10
2.4.2 Mechanical vapor recompression evaporator.....	11
2.4.3 Freeze concentration.....	12
2.4.4 Membrane reverse osmosis.	13
2.5 Drying methods.....	13
2.5.1 Spray dryers.....	13
2.5.2 Vacuum freeze-drying	14
2.5.3 Roller drum drying	15
2.5.4 Heat pump assisted drying:	16
2.5.5 Reversed Brayton cycle.....	18

2.6 High-Temperature Heat pumps (HTHPs)	19
2.7 Economic analysis.....	20
2.7.1 Feasibility study	21
2.7.2 Fixed capital investment.....	22
2.7.3 Variable cost during production	24
Chapter 3: Thermo-physical properties	26
3.1 State equation.....	26
3.2 General specific heat (C_p)	26
3.3 Specific enthalpy (h)	27
3.4 Latent heat (L).....	27
3.5 Thermal diffusivity (α)	28
3.6 Density	28
3.7 Influence of ice and C_p in thermal properties.....	29
Chapter 4: Methodology.....	31
4.1 General Process flow diagram	31
4.1.1 Mass balance	32
4.1.2 Energy balance	34
4.2 Calculation models for freeze concentrator	34
4.3 Calculation equations for multistage evaporation with three effects	36
4.4 Calculation equations for mechanical vapor recompression evaporation.....	38
4.5 Calculation equations for spray drying	39
4.6 Calculation models for vacuum freeze-drying.....	41
4.7 Calculation equations for rotary drum drying.....	43
4.8 Softwares used	44
4.8.1 Engineering Equation Solver (EES).....	44
4.8.2 Dymola	44
4.8.3 SOLIDWORKS.....	45
4.8.4 MATLAB	45

4.9 Energy recovery solutions.....	45
4.9.1 Model description.....	46
4.9.2 Thermo-dynamic process and the state points	48
4.10 High-temperature heat pump (HTHP) system design	50
4.11 Economic analysis	51
4.11.1 Capital costs estimating methods.....	52
4.11.2 Depreciation cost.....	55
4.11.3 Profitability analysis	56
4.11.4 Sensitivity analysis.....	58
Chapter 5: Results.....	60
5.1 Concentration using freeze concentration	60
5.1.1 Two-stage freeze concentration process and block freezing	62
5.1.2 Freeze concentration (30%) with different drying methods.....	65
5.2 Concentration by multistage evaporation (three effects).	68
5.2.1 Three stage evaporation drying combinations.....	69
5.3 Mechanical vapor recompression evaporation (MVR)	72
5.4 Process scheme with direct drying	74
5.5 Heat pump assisted drying	75
5.6: Summary of overall energy demands.....	77
5.7 Carbon footprints of main electricity generation technologies	78
5.8 Process schemes represented in 3D models.	79
5.9 Simulation results.....	82
5.9.1 Performance-enhancing measures.....	87
5.10 HTHP’s results	88
5.11 Economic analysis results	91
5.11.1 Sensitivity analysis results.....	98
Chapter 6: Discussion	102
Chapter 7: Conclusion.....	110

Chapter 8: Further work.....	112
Bibliography	113
Appendix.....	119

List of Figures

Figure 1: Logo of the CoolFish project.....	3
Figure 2: Schematic flow of extraction of fresh herring by-products	8
Figure 3: Principal scheme of micro, ultra and nano-filtration.....	9
Figure 4: Three effect evaporator.....	10
Figure 5: Mechanical vapor recompression cycle.....	11
Figure 6: GEA Icecon freeze concentration plant.....	12
Figure 7: Spray drying method	14
Figure 8: Vacuum freeze dryer	15
Figure 9: Rotary Drum dryer	16
Figure 10: Refrigeration cycle	17
Figure 11: Log P-h diagram and Ts-diagram for a single refrigeration cycle	17
Figure 12: Closed loop heat pump drying process.....	18
Figure 13: Drying of Clip fish using Heat pump	18
Figure 14: Reverse Brayton cycle	19
Figure 15: Heat pumps in industrial process.....	20
Figure 16: Types of Feasibility study	21
Figure 17: Fixed capital investment types,	22
Figure 18: Changes of thermal properties during phase transition of water,	27
Figure 19: Density behaviour of different substances	28
Figure 20: Ice fraction predicting models at freezing temperature	30
Figure 21: Schematic representation of process flow diagram	32
Figure 22: Mass balances of fish rest raw materials at each process stage.....	33
Figure 23: Water phase diagram- Pressure-enthalpy	39
Figure 24: Two-stage CO ₂ heat pump simulation model.....	46
Figure 25: HTHP system: Propane-Butane cycle	51
Figure 26: Types of depreciation	55
Figure 27: Process flow diagram with freeze concentrator.....	61
Figure 28: Concentration vs Freezing point plot	62
Figure 29: Processes after freeze concentration.....	63
Figure 30: Energy demands & Heating capacity in process with freeze concentrator	66
Figure 31: Process flow diagram of freeze concentrator with drying methods	66
Figure 32: Process flow diagram in Three-stage evaporator	70
Figure 33: Energy demands and heating capacity required in process with MSE.....	70

Figure 34: Ph diagram of water with condensing pressure 1.5 bar	73
Figure 35: Ph diagram of water with condensing pressure 2 bar	73
Figure 36: Schematic process flow in direct drying method	74
Figure 37: Spray dryer energy demands against inlet air temperature.....	76
Figure 38: Process with three stage evaporator and spray drying.....	80
Figure 39: Process with mechanical vapor recompressor and rotary drum drying.....	80
Figure 40: Process with Freeze concentration and spray drying	81
Figure 41: Freeze concentration plant.....	81
Figure 42: Simulation model of Two-stage CO ₂ Transcritical cycle.....	82
Figure 43: Ph diagram and TS diagram of CO ₂ Transcritical model.....	83
Figure 44: Effectiveness of PI controller (COP vs Time).....	84
Figure 45: Counterflow of hot & cold fluids inside HX	84
Figure 46: CO ₂ discharge pressure vs Heat pump_COP.....	85
Figure 47: CO ₂ evaporating temperature vs refrigeration COP	86
Figure 48: Butane condensing pressure vs Heat pump_COP	89
Figure 49: Butane condensing pressure vs Discharge temperature	90
Figure 50: Investment costs of different process	92
Figure 51: Payback time of different processes	93
Figure 52: Process wide yearly energy costs	94
Figure 53: Yearly depreciation cost of each process	95
Figure 54: Different costs for process with freeze concentration with spray drying	96
Figure 55: Different costs for process multi-stage evaporator with spray drying.....	96
Figure 56: Different costs for process mechanical vapor recompressor with spray drying.....	97
Figure 57: Operating hours vs Payback Time.....	99
Figure 58: Influence of changes in investment cost in determining the payback time	99
Figure 59: Influence of changes in energy costs in determining the payback time	100
Figure 60: Energy demands vs Different processes for 1-ton RRM.....	103
Figure 61: Energy demands in different process with freeze conc, (FC) and spray dryer (SD)..	104
Figure 62: Yearly CO ₂ emissions electricity source: Hydropower.....	108
Figure 63: Yearly CO ₂ emission, electricity Source: Coal with CCS.....	109

List of Tables

Table 1: Typical applications of HTHP'S	19
Table 2: Direct and Indirect Costs	23
Table 3: Types of off-site costs.....	23
Table 4: Types of fixed costs	24
Table 5: Coefficients for calculating the regression equations	29
Table 6: Composition RRM initial and after separation	33
Table 7: Parameters initialization for freeze concentrator	35
Table 8: Parameters initialization for three-stage evaporators.....	37
Table 9: Parameters initialization for Spray dryer	39
Table 10: Parameters initialization for vacuum freeze-drying.....	41
Table 11: Parameters initialization for rotary drum drying	43
Table 12: CO ₂ properties.....	47
Table 13: Heat transfer coefficients used in the heat exchanger.....	48
Table 14: Hand factor for cost estimation.....	53
Table 15: Wroth Factor for cost estimation	53
Table 16: Equipment cost details	54
Table 17: Parameters for economic analysis.....	57
Table 18: Concentration vs Freezing point	61
Table 19: TWICE- Two stages FC process data.....	63
Table 20: Freezing load requirements for FC process with different conc,.....	65
Table 21: Energy and work requirement in freeze concentration with drying methods.	67
Table 22: Energy demands for different cases with freeze conc, process	68
Table 23: Three-stage evaporator energy requirement	69
Table 24: Energy and work requirement in three-stage evaporators with drying methods.	71
Table 25: Energy requirement in mechanical vapor recompression.....	72
Table 26: Energy requirement in the direct drying process.	75
Table 27: SMER values for Heat pump drying and other methods	77
Table 28: Summary of overall Energy demands.....	77
Table 29: Carbon footprints of different electricity production technologies.....	79
Table 30: Equipment details in 3D Modelled images.....	79
Table 31: COP and other data of the HTHP system	89

Nomenclature

Abbreviations

<i>FPH</i>	Fish Protein Hydrolysates
<i>RRM</i>	Rest Raw Material
<i>Hx</i>	Heat exchanger
<i>CO₂</i>	Carbon dioxide
<i>COP</i>	Coefficient of performance
<i>BPR</i>	Boiling Point rise
<i>ERS</i>	Energy Recovery Scheme/Solutions
<i>MEE</i>	Multi Effect Evaporator
<i>SE</i>	Steam Economy
<i>R717</i>	Ammonia
<i>R744</i>	Carbon dioxide
<i>MP</i>	Medium Pressure
<i>LP</i>	Low Pressure
<i>LT</i>	Low Temperature
<i>HP</i>	High Pressure
<i>TS</i>	Temperature Enthalpy
<i>MVR</i>	Mechanical Vapor Recompression
<i>DH</i>	Degree of Hydrolysis
<i>RO</i>	Reverse Osmosis
<i>SMER</i>	Specific Moisture Extraction Rate
<i>HTHP</i>	High Temperature Heat Pumps
<i>OC</i>	Operating Cost
<i>IC</i>	Investment Cost
<i>MC</i>	Maintenance Cost
<i>CAPEX</i>	Capital Expenditure
<i>OPEX</i>	Operating Expenditure
<i>PB</i>	Payback time
<i>DC</i>	Depreciation costs
<i>SD</i>	Spray Dryer
<i>VFC</i>	Vacuum Freeze Dryer
<i>RDD</i>	Rotary Drum Dryer

Symbols

<i>H</i>	Enthalpy [kJ/kgK]
<i>C_p</i>	Specific heat capacity [kJ/kgK]
<i>W_C</i>	Work Carnot [kW]
<i>U</i>	Overall heat transfer coefficient [m ²]
<i>m_f</i>	Feed mass flow rate [kg/h]
<i>m</i>	Mass flow rate [kg/h]
<i>m_v</i>	Mass flow rate of vapor [kg/h]
<i>T_{boil}</i>	Boiling temperature [°C]
<i>ΔT</i>	Temperature difference [k]
<i>x₁</i>	Solids in inlet feed [kg/h]
<i>x₂</i>	Solids in outlet feed [kg/h]
<i>Q_{net}</i>	Net heat transfer rate [kW]
<i>Q</i>	Heat transfer [kW]
<i>E</i>	Energy demands [kWh]
<i>π</i>	Pressure ratio -
<i>T</i>	Temperature [°C]
<i>L_{ice}</i>	Latent heat of ice [kJ/kg]
<i>K</i>	Thermal conductivity [W/m-K]
<i>T_{a1}</i>	Inlet air temperature [°C]
<i>T_{a2}</i>	Exit air temperature [°C]
<i>n</i>	Polytropic index
<i>u</i>	Specific internal energy [J/kg]
<i>V</i>	Volume [m ³]
<i>ε_{ap}</i>	Apparent porosity
<i>ε_{ex}</i>	Porosity with excess volume fraction
<i>ρ_t</i>	True density [m ³ /kg]
<i>ρ_{ap}</i>	Apparent density [m ³ /kg]
<i>x_p</i>	Fractions of proteins
<i>x_l</i>	Fractions of lipids
<i>x_{ash}</i>	Fractions of ash
<i>x_w</i>	Fractions of water

<i>ISBL</i>	Inside Battery Limits	x_{cc}	Fractions of carbohydrates
<i>OSBL</i>	Off-site costs	T_f	Temperature at freezing point [°C]
<i>FC</i>	Freeze concentration	M_R	Mass of remaining substance
<i>TWICE</i>	Two stage freeze concentration	S	Amount of solids
<i>RDD</i>	Rotary Drum Dryer	T_{P1}	Temperature of product at inlet [°C]
<i>3SEV</i>	Three stage evaporators	T_{P2}	Temperature of product at outlet [°C]
<i>EA</i>	Economic Analysis	E_v	Evaporated water [kg/h]
<i>IHX</i>	Internal Heat exchanger	T_c	Condenser temperature [°C]
<i>FCI</i>	Fixed Capital Investment	T_e	Evaporator temperature [°C]
<i>VC</i>	Variable Costs	S_x	Standard deviation
<i>FA</i>	Feasibility Analysis	x	Mean value

Greek symbols

ΔH_{vap}	Latent heat of vapor [kJ/kg]
ρ	Density [m ³ /kg]
η_c	Carnot efficiency -
μ	Viscosity [Pa s]
φ	Relative humidity [%]
Σ	Summation -
ΔP	Pressure drop [Pa]
λ	Volumetric efficiency
α	Heat transfer coefficient [W/m ² K]

Subscripts

l	liquid
v	vapor
w	water
f	final
l	low
h	high
sat	saturated
tot	total
br	breakdown

Chapter 1: Introduction

1.1 Research significance

Protein sources are high in marine and fish products and are widely used for wide range of human consumption. The fishery industry is growing over years which leads to an increase in fish wastes which ultimately demands the best utilization of the rest products into a valuable nutritional source. There is an increased interest among researchers to study the fish protein hydrolysates and peptides in terms of potential human benefits. Fish protein hydrolysates (FPH) are produced mainly from fish rest raw materials (RRM) through the protein hydrolysate technique (Petrova et al., 2018).

FPH can be used for different applications as a feed food for animals, aquatic fish, to high-quality protein mix for humans. Protein from fish can be used to produce bioactive peptides and FPH, which increases the economic value and lowers the environmental impacts (Himaya et al., 2012).

The liquid state of FPH has a high amount of water content, which is relatively unstable, and reduces shelf life, hence long-term storage and transport was limited. The removal of moisture from FPH is difficult and involves high costs. Drying can be performed either using spray dryers, vacuum freeze dryers or drum dryers which removes the moisture content and lowers the value to 1-3% (Petrova et al., 2018). Spray dryers which are widely used in industries, consumes the energy around 4500 and 11500 kJ/kg of water removed (1.25-3.2 kWh/kg). The process design modification can lead to reducing energy use (Mujumdar, 2007). Other pilot models proposed by Al-Mansour et al. (2011), have a minimum specific energy demands of around 5500 kJ/kg (1.53 kWh/kg). Freeze drying and rotary drum drying also consume high amount of energy. Hence drying process generally is highly energy intensive.

Concentration processes are performed before the final stages of product drying, which lowers the drying cost. Freeze concentration can be performed before the drying stages, to lower the overall energy demands. The freeze concentration procedure is a gentle way for dewatering food products with a concentration of 30%. Studies investigated by Miyawaki et al. (2005), stated in his research work, that the freeze concentrators consume the energy of around ~ 330 kJ/kg of water to freeze.

Other alternative methods used in concentration process, are evaporation techniques, membrane filtration methods. For evaporating 1 kg of water the energy value required is approximately 2,700 kJ/ kg (0.75 kWh/kg). With improvement in methods, multistage evaporation (MSE) method, Mechanical vapor recompression (MVR) method can be used, the energy reduction can be

achieved. [Han et al. \(2021\)](#), experimentally investigated the MVR system and concluded that with two effect evaporator 40% more energy saving was achieved than a single-stage MVR system.

The concentrating methods are used as a pre-step before drying methods. This combination results in greater energy savings. [Jeantet et al. \(2015\)](#), studied the energy demands by combining the vacuum evaporation and spray drying methods during production of dairy powders and established calculation equations which compute the lowest energy charges for dairy powders. They found that to produce the dairy powders, the energy costs are at 1.7 kWh/kg (6120 kJ/kg).

Studies related to integrated heat pump systems with energy recovery in producing the protein hydrolysates from fish rest raw material are limited. [Wang et al. \(2013\)](#), examined the transcritical CO₂ system along with an internal heat exchanger and twin expansions. In his study, he found that optimization of higher discharge pressure is required to achieve maximum refrigeration capacity.

When investigating the process, which is most energy conservative among the different processes, the investment analysis performs a major role in influencing the profitability and selection of the process. When studying the technological aspects of different processes, the economic feasibility must also be studied. [Bassoli et al. \(1989\)](#), in their chapters named coffee product and economic analysis in freeze concentration, where he compared freeze concentration methods with drying and evaporation techniques and mentioned that when comparing the freeze-dried coffee, a 25% reduction in production cost was obtained when freeze concentration method was implemented.

From the above literature review, it is identified that research findings related to energy-efficient techniques in the production of fish protein hydrolysates (FPH), and its optimization are limited and are available in scanty. Also, there is no well-established economic analysis of technologies associated with FPH production. Hence, in this study, the main objective is to identify the energy use in each process, identify the process with high energy use and suggest the energy reduction measures in a sustainable way.

Energy recovery solutions are simulated in Dymola & EES, and the applications of High-Temperature Heat Pumps (HTHP) as an alternative for the evaporation process are analysed in EES software. The economic analysis is performed in a well-detailed method including sensitivity analysis. Also, 3D Modelling has been performed to illustrate the process schemes on an industrial scale for better representation.

1.2 Motivation and project background

The main motivation for working in this research area is because the thesis addresses major societal problems and provides effective solutions. The thesis investigates sustainability issues and connects **people, profit,** and the **environment** by identifying **energy-efficient processes** for energy reduction, establishing ways for **reducing global emissions,** and indicating **how profitable the various process** alternatives are.

Also, the thesis provides an opportunity to participate in the technologies related to the development of energy-efficient processes, integrated climate-friendly cooling, freezing, and heating. Process efficiency is highly important to main the quality of fish products which is the important scope of the COOLFISH project. The new technologies can be both energy effective and are economically feasible which reduces greenhouse gas emissions and impacts.



Figure 1: Logo of the CoolFish project

The three main objectives of the project are:

- **Energy efficiency:**

To develop efficient refrigeration systems, combined with heating and cooling, thermal storage, and heat pump.

- **Industry design case:**

Improving the energy efficiency of the refrigeration process and other systems.

- **Climate and environment:**

To increase awareness of the effects on climate and environment of refrigeration systems, onboard fishing boats and to suggest better solutions.

The project is managed by the SINTEF Ocean in collaboration with SINTEF Energy Research and NTNU. Industry partners that are associated are Blue wild, Perfect Temperature Group, Danfoss, MMC First Process, GASNOR. Other organization include the International Institute of Refrigeration (IIR), London South Bank University and Johnson Controls

1.3 Task description

This master thesis work is a continuation of the project work which is performed during the fall semester of 2021. In the project work, understanding and identifying the overall energy demands involved in the production of powdered FPH from RRM were calculated, and the thesis work is

subjected to investigating energy and economic study in more detail. Schematic 3D representation of entire process schemes was modelling in SOLIDWORKS software, energy recovery solutions are developed in Dymola and EES software. Also, investigation of HTHP technologies as a substitute for evaporation technology is studied.

The following tasks which are included in the thesis work are:

1. Review of relevant literature e.g., alternative fish protein hydrolysates processes, freeze concentration, industrial CO₂ refrigeration, and industrial drying processes.
2. Investigation of the application of refrigeration technologies and heat pumps to determine sustainable and energy-efficient methods for processing and stabilization of FPH.
3. Develop a relevant system in the modelling environment, and able to simulate the process plant.
4. Perform design investigations, simulations, and experimental campaigns. Analyse the overall comparison of production lines with respect to the energy savings of different techniques.
5. Understand the areas of energy reduction and enhance the process efficiency by identifying the effective process.
6. Analyse and discuss the results in terms of system performance, footprint depending on capacity ranges and energy demands.
7. Master Thesis report including chapters, discussion and summary section.
8. Proposal for further work
9. Draft version of a scientific paper based on the results.

1.4 Overview

During the project work, the following tasks were accomplished.

- *Mass and energy balances are analysed in detail at each step.*
- *Heating and cooling loads were calculated based on operational parameters.*
- *Comparison of energy savings between different alternatives and identifying the best scheme.*

Thesis continuation

This master thesis will further investigate the technical and economic feasibility of the schemes. The process consequences, specifications and cost have been evaluated for each process choice. The possibility of technologies to integrate offshore and onshore has been studied. The combination of multistage (two-stage) freeze concentration methods was studied in the concentrating steps to understand the feasibility to produce the maximum solid content.

Hence, the relevant literature review, theory and other chapters from the project work are relevant for this master's thesis work. With the agreement with the supervisors, Armin Hafner and Ignat Tolstorebrov, the relevant chapters from the project are utilized. This provided an opportunity to invest greater time in developing the different models and analysing them in more detail. Significant efforts have been taken during 3D modelling and performing simulations & economic investigation. Simulation models using Dymola and EES of a two-stage transcritical CO₂ system have been simulated and the system performance with integrated heating and energy recovery has been studied.

1.5 Report structure

The thesis consists of nine parts which are explained below, all the tasks presented in Section 1.3 has been carried out during the thesis work.

Chapter 1: Introduction

The motivation and objective of the thesis work are explained. The problem statement is briefed, and the overview is provided. The task description and the report structure are provided.

Chapter 2: Theory and literature review

This chapter contains relevant literature regarding different production processes with concentration and drying stages. Also, the relevant economic studies, CO₂ heat pump and HTHP system literature are included.

Chapter 3: Thermo-physical properties

The thermo-physical properties determine energy needs during heating, cooling, or freezing applications. Hence, information about these properties is explained and their influence on calculating the energy use is explained.

Chapter 4: Methodology

In this chapter, first, the calculation equations for freeze concentration (FC), three-stage evaporator (MSE/3SEV), mechanical vapor recompression (MVR), spray dryer (SD), vacuum freeze dryer (VFD) and rotary drum dryer (RDD) are established. The procedure to calculate the energy for each process is provided in detail. Second, the Dymola system design was explained followed by the HTHP system model. Finally, the equations for economic and sensitivity analysis are provided.

Chapter 5: Results

This chapter includes the results which are carried out in methodology. Process wise energy calculations are provided. First, results of freeze concentration, TWICE process, and freezing into blocks were presented followed by combinations with the different drying processes. Then, the other concentration process MSE, and MVR are provided with drying combinations. Finally, the results from system modelling and economic analysis are presented in different subchapters.

Chapter 6: Discussion

Most of the explanations are discussed coherently in the results chapter itself. In this chapter, a detailed summary was provided addressing the major findings in the results. The technical analysis is provided in a broader perspective in comparison with the literature review.

Chapter 7: Conclusion

Concluding the major outcomes from the thesis work. Key findings from calculations and simulation models are provided. Energy requirements for each process, system COP, and investment analysis outcomes are included with other important data.

Chapter 8: Further work

Although the thesis work was very extensive it can further be expanded for improvement. Some of the techniques which are not discussed will be provided in further works. The further work will act as a proposed guideline for other researchers working in this research area.

Appendix

The relevant calculation models, 3D modelled images, EES simulation code and other important information are provided in this chapter. The scientific paper and the award certificate was attached at the end of the document.

Chapter 2: Theory and literature review

This chapter briefly explains the relevant theory and literature review. The production of the FPH process was briefly explained in this chapter. The relevant literatures regarding different production processes in concentration and drying stages are explained with references. Also, the economic studies; CO₂ heat pump and HTHP system literature are included.

2.1 Pre-treatment

The rest raw materials like fish leftover (skin, heads, bones, viscera) exist in two forms, a frozen state, and a chilled state. The rest raw material is frozen to temperatures of approximately -18 °C. The chilled form of RRM is maintained at temperatures +3 °C approx.

Pre-treatment steps have the following stages.

2.1.1 Thawing process

In this step, The RRM is first thawed from a lower temperature of -18 °C to 10 °C if it is in the frozen state. The energy demands during this process are relatively high since in addition to the sensible heat above and below freezing point, the latent phase change of the ice is also accounted.

2.1.2 Grinding & mincing

Once the RRM is thawed, the next step involves preparing the RRM for the hydrolysis process. In this process, the RRM is finely crushed into smaller mixtures. Crushing is usually powered using mechanical coarse grinders followed by fine ones. The proper grinding of the RRM is very important since this affects the hydrolysis time. The smaller the substances the more quickly the proteins in the structure dissolve. During this step, an equivalent amount of water, usually 1:1 was added to the mixture and minced properly for the hydrolysis process. When using Codfish heads, the water percentage can be lowered since the heads have a lot of moisture. The specific heat before mining and after mincing was determined based on state temperatures and are used in the calculation. The amount of water added during the process is highly important to have a better breakdown of protein molecules and this also determines the cost of drying during the process. The process flow representation is given below in *Figure 2*.

2.2 Enzymatic hydrolysis technique

During the hydrolysis process, the solution is heated to hydrolysis temperature of 50 – 55 °C and the enzymes were added to the RRM mixture. Heating the mixture to the hydrolysis temperature demands a higher amount of energy. Knowing the specific heat capacity of the solution and the mass flow rate, the heat flow and energy demand are calculated. Once the entire solution reaches the required hydrolysis state, the hydrolysis process begins. Generally, the hydrolysis process can take up to 60-120 mins and in some cases even longer time. The temperature and process parameters are well controlled during the entire process and the mixture is uniformly stirred during the entire process to have a uniform temperature distribution.

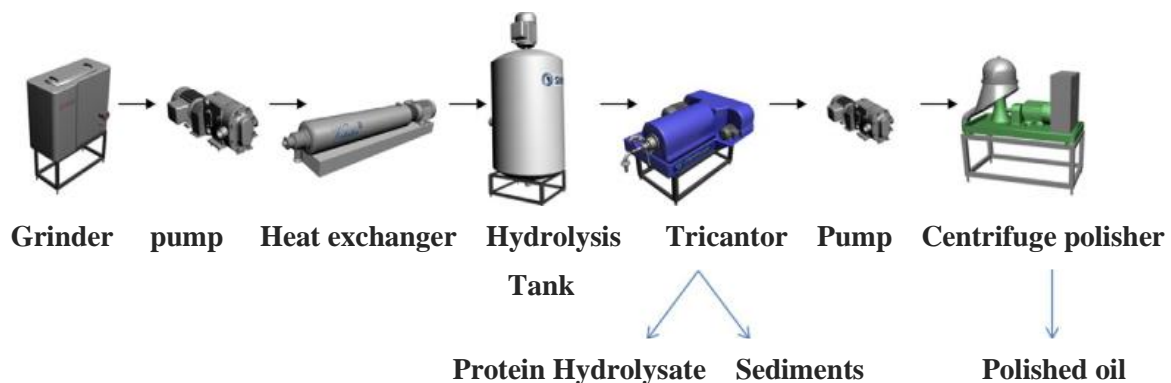


Figure 2: Schematic flow of extraction of fresh herring by-products (Carvajal et al., 2014)

The protein part in the solution was broken into the smaller structure of peptides and amino acids. The fish RRM is diluted with water and 0.1 % of enzymes were added. The degree of hydrolysis is defined as the ratio of breakdown peptide bonds (P_{br}) to that the net peptide bonds (P_{tot}). It is as follows,

$$\text{Degree of hydrolysis (DH)} = \frac{P_{br}}{P_{tot}} * 100\% \quad (2.1)$$

After the completion of the hydrolysis process, the solution is pasteurized to a high temperature of 90 °C and the mixture is stirred for another 15-20 mins. This process is carried out to reduce the microbial activity and to inactive the enzymes present in the solution.

FPH having larger fragments of proteins have some bitter taste. Hence, the further breakdown of larger peptides into amino acids of smaller size can lead to reduced bitterness. The hydrolysis process is adjusted based on final requirements and hence a hold of control is provided on the degree of hydrolysis.

2.3 Filtration

After the hydrolysis process was finished, the hydrolysates water mixture is filtered and separated into liquid hydrolysates, unsolved protein mixtures and lipids. Commonly used methods are given below,

2.3.1 Centrifugation

The hydrolyse mixture was separated into different fractions through the centrifuging process as in Tricantor. The primary working principle of centrifugation was based on centrifugal force. It has a main element called rotary which is a rotating part.

The hydrolysates were separated into liquid protein hydrolysates, sludge, and the solid layer of undissolved proteins. He et al. (2013), in their investigation reported, that the filtration was so detailed with oil and an aqueous layer, with oil on top, liquid in the middle and sludge at the bottom.

2.3.2 Micro, ultra and nano

To obtain fine separation of liquid FPH, techniques which selectively trap the solids based on particle size were considered. Membrane-based separation (Figure 3) was found to be the most widely used and effective filtration method in industries (Abejo'n et al., 2018). The membrane filtration selectively filters the substance in the range of 100, 10, and 1 nm for micro, ultra and nano filters respectively. Membranes are usually made of polypropylene, cellulose acetate polyvinylidene difluoride etc.

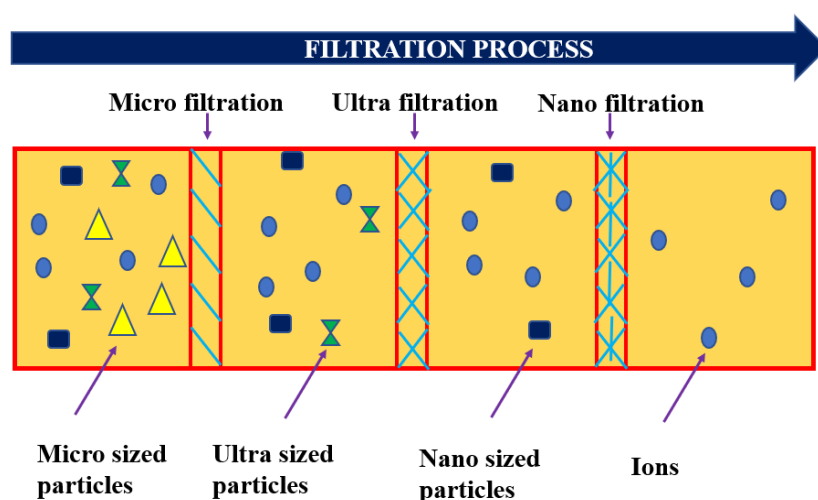


Figure 3: Principal scheme of micro, ultra and nano-filtration

2.4 Concentration

The liquid hydrolysates are further concentrated to lower the water content in the hydrolysates. The concentration process was carried out to reduce the final energy requirements before the drying process. Some of the widely used concentration processes in industries are freeze concentrators, evaporators (three effect evaporator, mechanical vapor recompression evaporator), and membrane reverse osmosis. The protein hydrolysates are concentrated up to 30 % in freeze concentrators and in evaporators they are concentrated up to 50~60%. (Pasupuleti and Braun, 2010).

2.4.1 Multi-stage evaporation:

Many industrial processes use multi-stage evaporators with three effects (Figure 4) for concentrating the liquid. Generally, evaporation is a highly energy-intensive process. Multistage evaporation (MSE) reduces the energy costs. Water can be evaporated in a series of flash vessels that operates at lower temperatures and pressure. To concentrate the feed liquid, a larger amount of energy is consumed during the evaporation process. Hence, the high energy demands in the single-stage evaporator are reduced by using a multiple stage evaporator (MSE) which increases the evaporation efficiency.

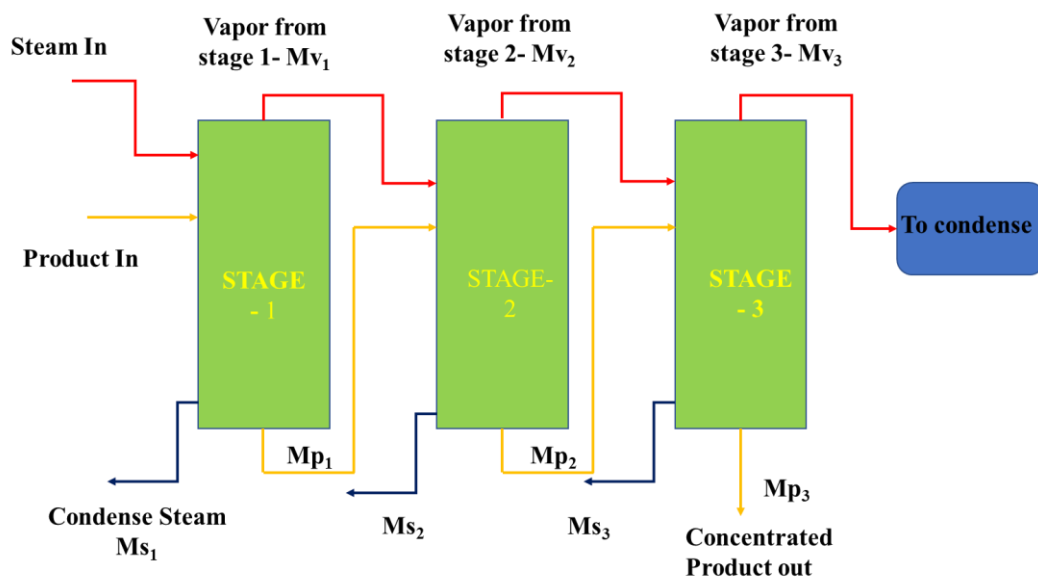


Figure 4: Three effect evaporator

Yun et al. (2013), analysed the film evaporation simulation to obtain the high purity in hydrolysate steam and optimized the energy demands in biodiesel production, Kern (1950), investigated concentration of the chemical solution using the triple effect evaporator (TEE) technology. His study focused on studying parameters like mass and enthalpy balance, minimal BPR, constant

solution physical characteristics, and varied U for separate effects. His results showed an enhanced evaporator performance.

2.4.2 Mechanical vapor recompression evaporator

Hang et al. (2021), studied mechanical vapor recompression technology to reduce energy demands by recovering secondary steam's latent heat in a steady evaporation process. Stable evaporation shows significant advantages in terms of energy savings of up to 40%. The typical process is represented in *Figure 5*.

The working principle of the process is the vapor from the feed solution is heated using a compressor or a blower fan which increases the pressure and the temperature sufficiently for energy transfer. A reheater can also be employed at the exit of the compressor based on temperature requirements. The steam vapor, after releasing the heat condenses inside the evaporator. This heat at a lower temperature from the condensate fluid can also be reused to preheat the inlet temperature of the feed flowing into the heat exchanger. The process is simple, with a high degree of product purity, compact equipment, and no external heating source is required. It also has greater thermodynamic efficiency. (Ettouney et al., 1999; Darwish et al., 1988; Al-Juwayhel et al., 1997).

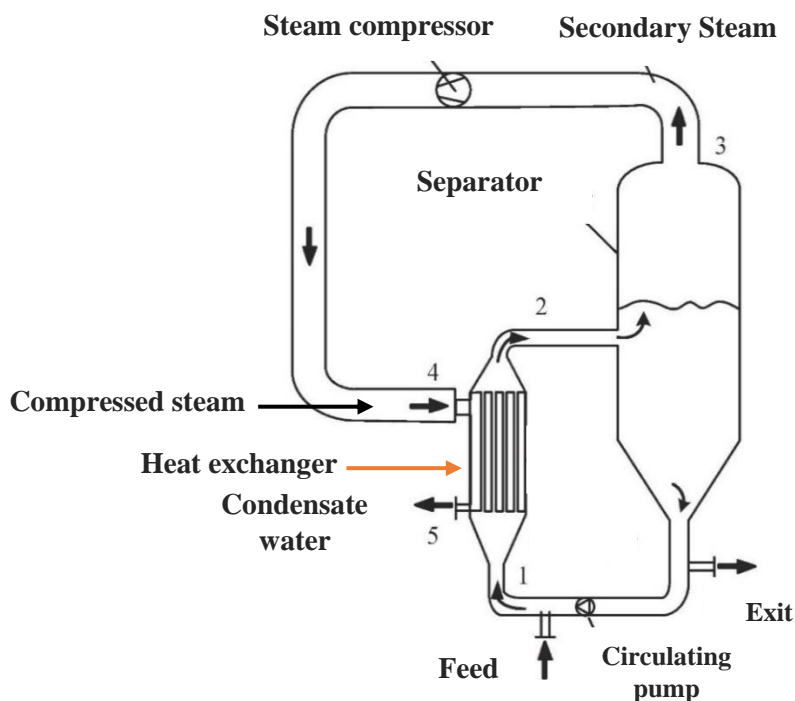


Figure 5: Mechanical vapor recompression cycle

2.4.3 Freeze concentration

Freeze concentration is a technique that involves freezing and removal of water by fractional crystallization of water into ice. It can be used as an alternative process to membrane filtration, evaporation, and distillation methods. This method provides significant energy saving measures when comparing the evaporation process. Because of this, many industries are widely using this method for the concentration process. [Auleda et al. \(2011\)](#), calculated the freezing point of concentrated fruit juices in freeze concentration and developed a model that forecasts fruit juice freezing points. [Miyawaki et al. \(2005\)](#), stated that freeze concentrators consume the energy of around ~ 330 kJ/kg (0.092 kWh/kg) of water to freeze. The freeze concentration process is given below in *Figure 6*. The steps involved in freeze concentration are:

1. Freezing
2. Recovery of crystals
3. Melting of ice.

In this method, the hydrolysates enter the heat exchanger, due to the lower temperature of the process, water starts to freeze and forms an ice structure, the hydrolysates are usually maintained at a temperature of -2 °C. Product freezing takes place in the crystallizer. The heat exchanger walls are refrigerated to provide the necessary low temperature for the entire process. The entire product is allowed to enter the separator column to separate the ice and concentrated hydrolysates.

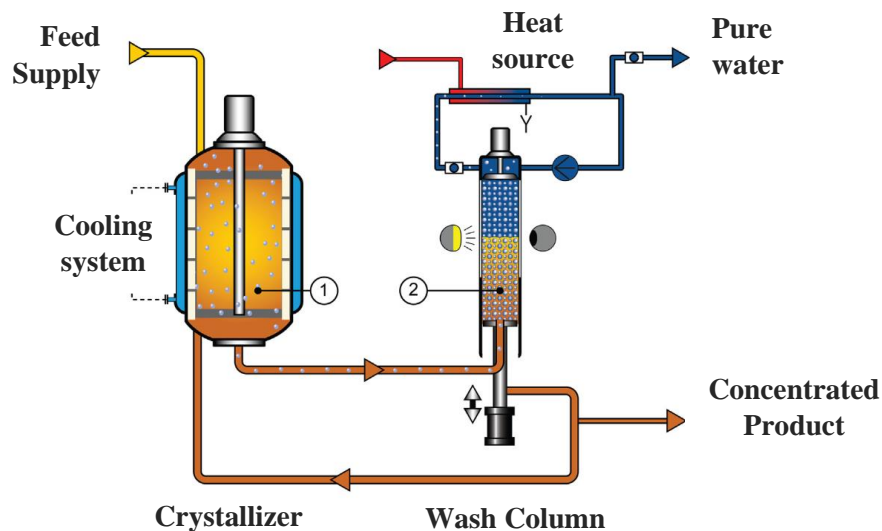


Figure 6: GEA Icecon freeze concentration plant ([Fellows et al., 2017](#))

Due to the density differences, the concentrated hydrolysates stay in the bottom while the ice is formed at the top. The ice is melted by the hot water which circulates at the top of the wash column. Finally, the concentrated hydrolysates are produced from the system with a concentration of 30%.

The low-temperature operation of the process is used to obtain high-quality products, without much change in their properties.

2.4.4 Membrane reverse osmosis.

Membrane filtration using reverse osmosis (RO) offers lower energy demands in removing the water and concentrating the product. This method was widely utilized in the desalination plant, and fruit juice industries. It is widely used as an alternative approach to the evaporation method. In evaporation, the process requires higher energy required to convert the water into vapor which makes the process more energy demands.

Madaeni et al. (2008, 2010), studied the reverse osmosis method as an energy-reducing option in the sugar sector. He evaluated the energy demands of the conventional evaporation technique against reverse osmosis paired with evaporation in his research and found a 33% energy savings when using RO together with the evaporation method. When enzymatic hydrolysate is processed, due to lower porosity, lower hydrophilicity, and higher surface roughness, the membranes lead to higher surface fouling.

In the RO system, the only energy consumers are the high-pressure pumps. Fouling is a major issue that affects the effectiveness of the system. Factors like porosity, membrane structure, pore size, and surface roughness largely affect the effectiveness of the separation. RO filtration is not widely used to concentrate feed on large volumes due to membrane clogging and the high process time. Hence, in this work, this method was not studied in detail for concentrating hydrolysates.

2.5 Drying methods

Drying was performed to completely remove the remaining moisture present in the product. The main reason to completely dry the product is to increase its shelf life of the product and to make the product stable. Typically, spray dryers, vacuum freeze dryers, and rotary drum dryers are widely used processes for drying the FPH. For large scale production rates, spray dryers are widely used in industries.

2.5.1 Spray dryers

It consists of a feeding system on the top of the equipment with a long cylindrical tube, the outlet session has a separator for separating the final dried product. The air was heated usually 150-220 °C to dry the product. Liquid FPH is fed into the inlet portion of the system. The feed flows

continuously into the sprayer chamber by the atomizer. A typical spray dryer is given in below *Figure 7*.

Atomizer was a special device that mixes the feed and sprays into fine droplets. Air is heated using the heater and is supplied into the spray chamber. Here, the liquid mixes with hot air and flows into the chamber and towards the separator. When the feed was sprayed into the chamber using an atomizer, the moisture and solids present in the liquids comes in contact with the drying air and the moisture was removed and carried out by the outlet air through the separator. Dryer design modification or heat recovery options can be integrated for energy reduction purposes. [Patel et al. \(2020\)](#), studied the process integration of spray dryer with heat recovery systems, he observed when compared with the base design, 74% energy savings was achieved through recirculation of air in a hybrid heat recovery system.

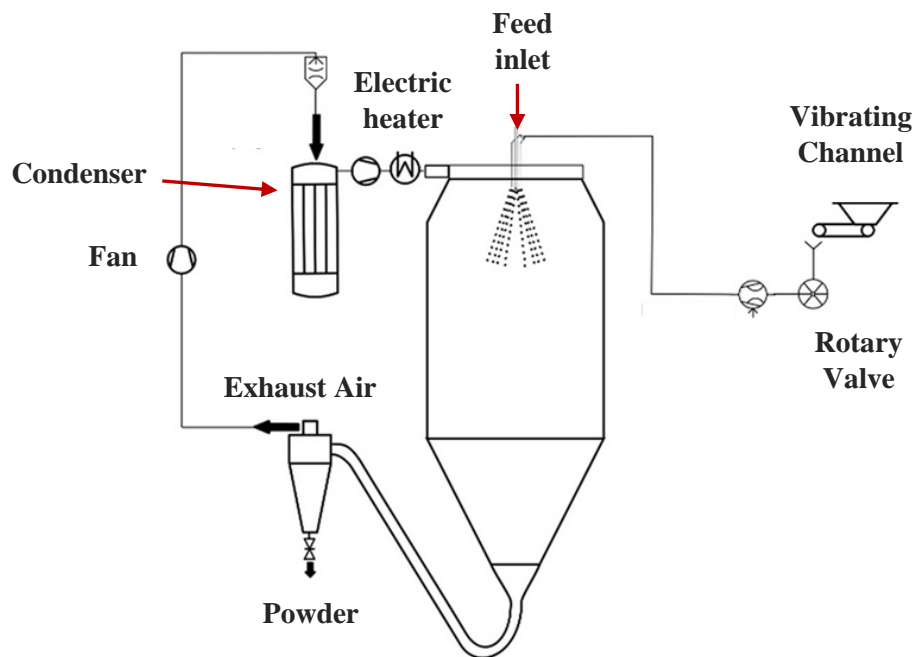


Figure 7: Spray drying method (Alfons et al., 2020)

2.5.2 Vacuum freeze-drying

The principle in vacuum freeze-drying (*Figure 8*) is the moisture sublimation of the product which occurs under lower pressure. The liquid hydrolysates are frozen to a lower temperature of -20 to -30 °C inside the freezing chamber. Sufficient low pressure was maintained inside the chamber using a vacuum pump (1.0 mbar). The moisture removal rate is based on product thickness, moisture content and thickness of ice formed on the surface of the heat exchanger. Primary drying

removes most of the water at the lower temperature, and the remaining water was removed in secondary drying where the drying temperature is increased.

[Stratta et al. \(2020\)](#), investigated the economics of a freeze-drying process and provided a methodology for calculating the different types of costs like operating and investment costs for a freeze-drying process.

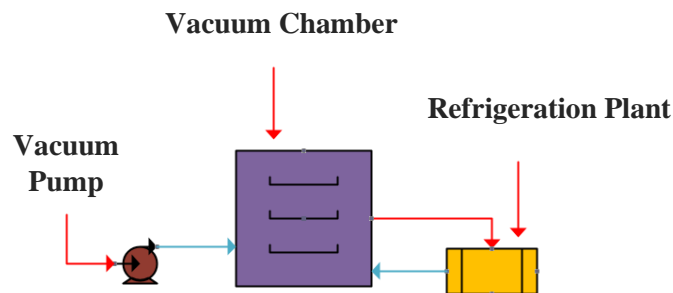


Figure 8: Vacuum freeze dryer

2.5.3 Roller drum drying

It consists of a horizontally mounted hollow cylinder. The cylinder can be a single piece of drum or with two hollow cylinders spinning in same directions (*Figure 9: Rotary Drum dryer*) or rotating in opposite directions (Twin drum dryer). Hot air at a very high temperature of 200 °C or above is supplied inside a hollow cylinder. Convection of heat occurs between the heating medium and the wall. The high-temperature air acts as a heating medium and provides the necessary heat for removing the moisture in the product. The cylinder diameters vary from 0.5 to 6 m, and the length is about 1 and 6 m. The product was heated and concentrated, and a thin film was formed over the heated surface. Finally, the concentrated FPH was scrapped using blades and removed from the surface.

[Almena et al. \(2019\)](#), optimised food dryness processes using a drum dryer as an energy-efficient operation. In their model, they observed thicker slurries require long residence times and high steam temperatures requirement contributes to significant energy needs.

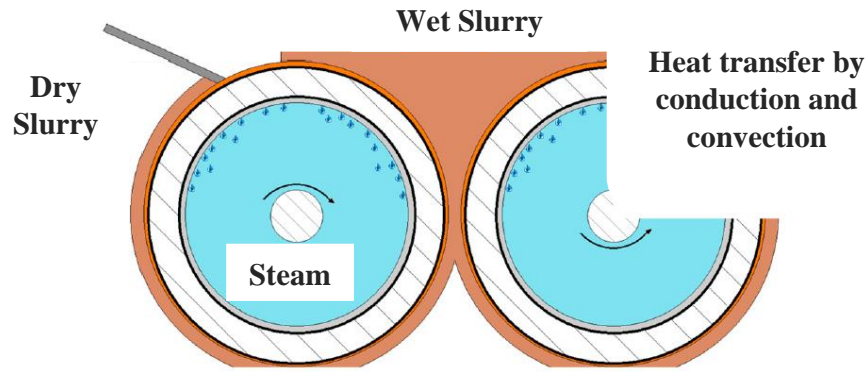


Figure 9: Rotary Drum dryer (Almena et al. 2019)

2.5.4 Heat pump assisted drying:

Heat pump assisted drying can provide greater energy savings for the drying process. The heat rejected from the system is used to heat the air to high temperatures and it can be used for drying the products. Natural refrigerants like Ammonia and CO₂ are widely used in the refrigeration industry due to their better thermodynamic properties and reduction in environmental impacts. CO₂ booster systems and ejector techniques are the advancements in CO₂ refrigeration which increases the system performance. An ejector technology can boost the COP by up to 17% (Hafner, 2019). High-temperature heat pumps are well suited for drying applications.

The simple heat pump cycle is shown below (Figure 10), it contains a compressor unit, condenser, evaporator, and expansion valve. It works on the principle of the vapor recompression cycle. In this system, the refrigerant which is at low temperature (LT) and low pressure (LP) absorbs heat in the evaporator and gets compressed in the compressor. For heat transfer to occur, the evaporation temperature should be lower than the ambient temperature. The high-pressure (HP) high temperature (HT) refrigerant leaving the compressor, condenses and provides heat at the condenser. The refrigerant will then expand through the expansion valve and flow to the evaporator at low pressure and low temperature and the process repeats. The thermodynamic states are represented in the below PH and TS diagram. (Figure 11),

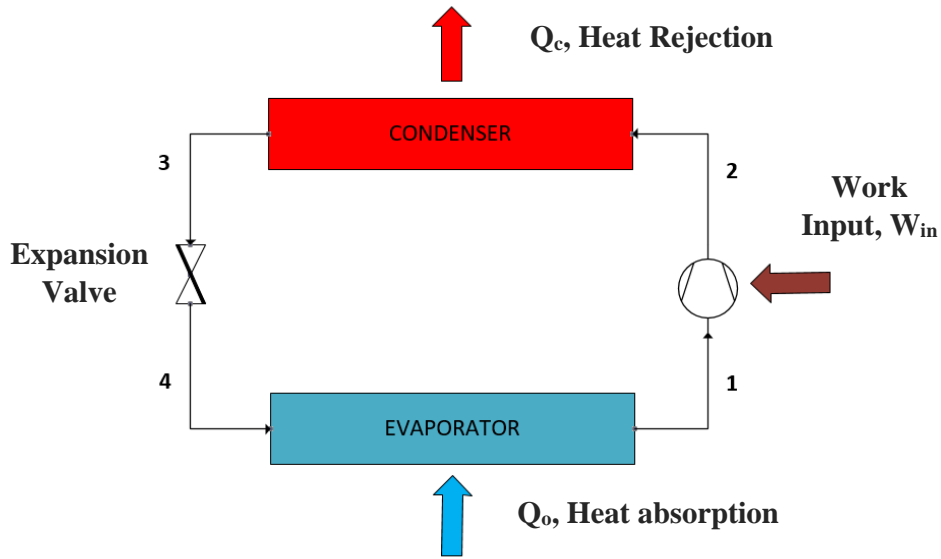


Figure 10: Refrigeration cycle

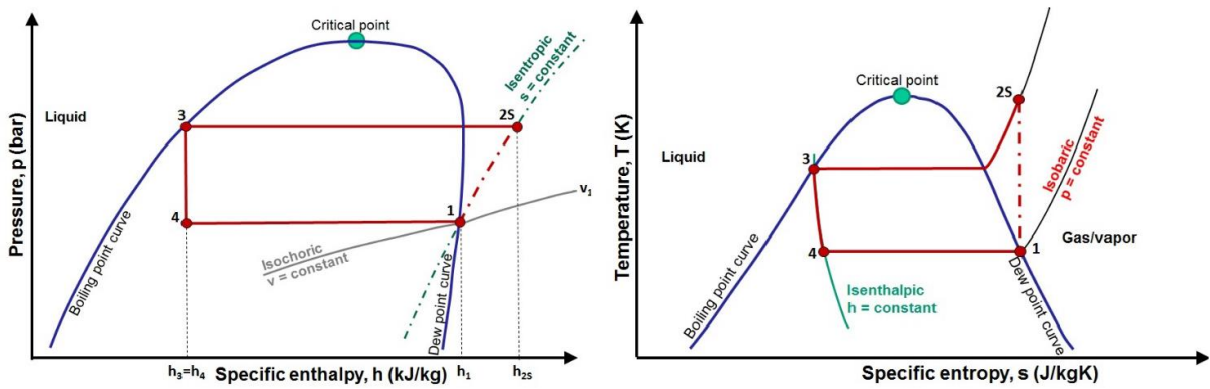


Figure 11: Log P-h diagram and Ts-diagram for a single refrigeration cycle (Eikevik, 2019)

The specific moisture extraction rate is given by

$$SMER = \frac{m_{evaporated}}{Energy\ input} \quad (2.2)$$

The system coefficient of performance is given by

$$COP = \frac{Q}{W} \quad (2.3)$$

COP indicates how efficiently the heat pump is running. From an industrial point of view, higher COP reduces energy costs. A typical closed-loop drying and drying of clip fish by heat pump process was shown in the following figures.

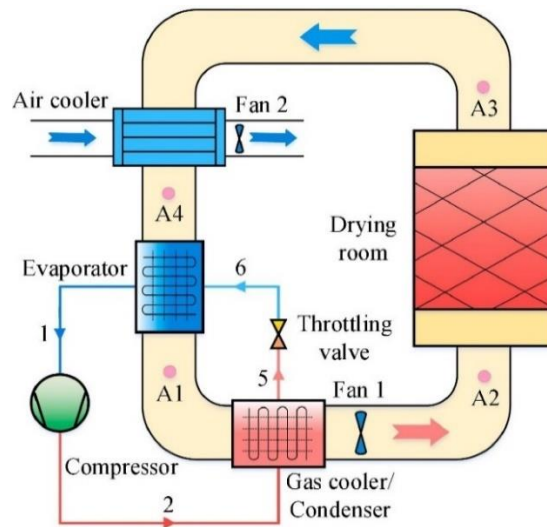


Figure 12: Closed loop heat pump drying process (Dai et al., 2020)



Figure 13: Drying of Clip fish using Heat pump (Bantle et al., 2013)

2.5.5 Reversed Brayton cycle

With reversed Brayton cycle, air can be heated to a very high temperature. The basic scheme is given below (Figure 14). Angelino et al. (1995), studied the possibilities of reversed Brayton cycles and considered them as a feasible substitute for heat supply at higher temperatures. The reversed

Brayton cycle has the same turbomachinery elements as a gas turbine, a compressor and a turbine but not a combustor.

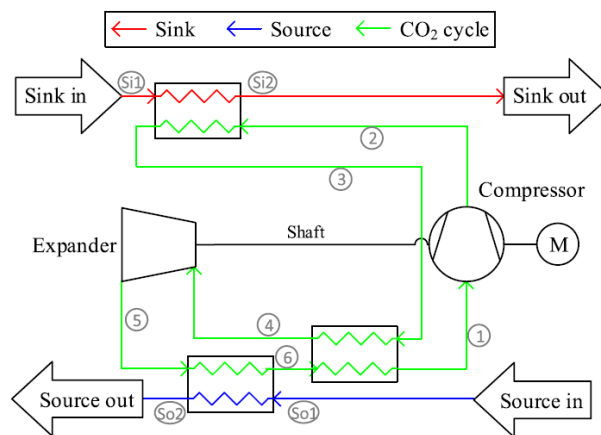


Figure 14: Reverse Brayton cycle (Zühlsdorf et al., 2019)

The compressor used is a turbocompressor which was mounted on the same shaft to recover the expansion work. Because of the high-pressure ratios and the fact that expansion takes in the gas phase, the recovery of expansion work seems promising. Due to an increase in compressor work and a decrease in turbine work output, the network input rises. As a result, the COP of reverse Brayton cycles will be much lower than the COP of ideal reverse Brayton cycles. The design of new compressors and turbines is essential to enhancing the system's COP.

2.6 High-Temperature Heat pumps (HTHPs)

Generally, heat pumps deliver heat for medium temperature applications. Conventional heat pumps, suffer incapability to deliver heat for high-temperature applications due to limitations like compressor design and working fluids properties. In the FPH production process, we need to provide heat at a higher temperature for several stages, either in evaporation or in final drying. Hence these can be either replaced or integrated with the HTHP system to reduce the energy demands. The advantages of HTHP are that it can deliver heat to a higher temperature, and are suitable for several applications in food processing as stated in the following table, (Arpagaus et al., 2018)

Table 1: Typical applications of HTHP'S

Drying process upto 250 °C	Evaporation (40-170 °C)	Pasteurization (60-150 °C)
Sterilization upto 140 °C	Boiling (70-120 °C)	Distillation (40-100 °C)
Concentration (60-80 °C)	Blanching (60-90 °C)	Tempering (40-80 °C)

Integration of heat pumps can improve the efficiency of the system, the dependency on fossil fuels can be reduced and industrial processes can be decarbonized. The process is represented in *Figure 15*. Combining the process heating and cooling needs with heat pumps will result in increased process efficiencies and lowers operating costs. The principle of high-temperature heat pumps is almost the same as heat pumps, it's the system design, operational parameters, suitability of working fluids, available heat source range and heat delivery temperatures determines the nature of HTHP. It is possible to operate the heat pumps at lower temperature lifts and can reach a higher COP. The HTHP based on the type of applications can have a slightly lower system COP due to the requirement of producing higher temperatures. (Higher temperatures require higher temperature lift, hence higher system pressure)

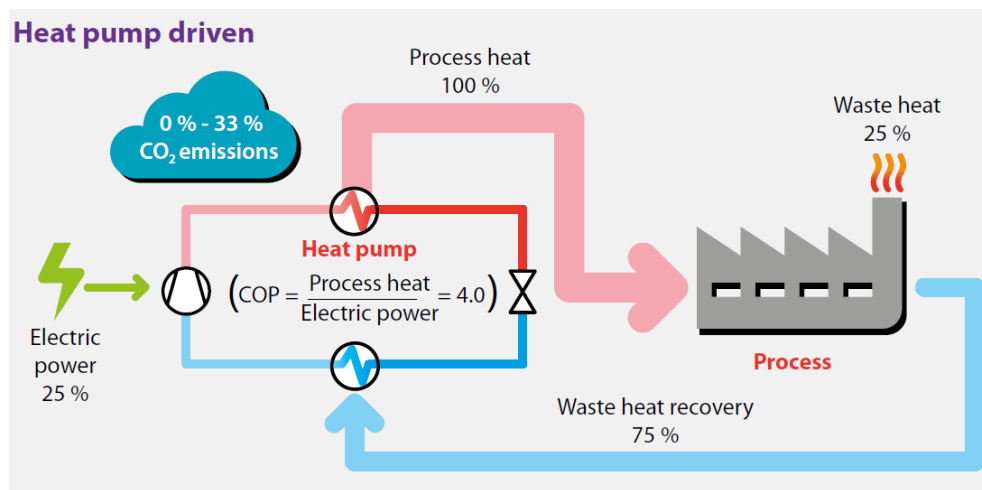


Figure 15: Heat pumps in industrial process (Boer et al., 2020)

For HTHP, the main technology restrictions are the compressor operating parameters (temperature and pressure). [Bamigbetan et al. \(2019\)](#), studied the prototype compressor and found that due to butane's favorable thermodynamic features the prototype compressor has an isentropic efficiency of 74 percent and a volumetric efficiency of 83 percent. They also observed that the operational parameters (pressure and temperature) were acceptable, with the potential of having higher temperature heat delivery.

2.7 Economic analysis

When analyzing the production process in a technological aspect like the type of process, principle of operation, energy demands etc., the economic study must also be performed to understand the various costs associated with the process and to determine the economic feasibility. It can provide information about the technology which is most economically suitable for a process. The

profitability, payback time, investment, operational, and depreciation costs are important to be considered when studying the available process.

Beek et al. (2018), investigated the technical-economic analysis of freeze concentration systems for temperature-sensitive biomolecules. In his economic analysis, he has studied the freeze concentration method along with the combination of spray drying and vacuum freeze-drying and observed that the operational cost of a freeze concentration plant is greatly influenced by the size of the facility and obtained a payback time of 4 years for a smaller plant capacity. The freeze concentration unit costs 1 million Euros for a dewatering capacity of 400 kg/h. Also, when compared with other processes, the running costs are greatly reduced.

Bae et al. (2022), experimentally studied the operating methods, economic study and environmental analysis of heat pump systems with heat source from a ground source. In his economic investigation results, it is seen that the initial investment cost can be lowered when the intermittent operational approach was performed. This could lower overall cost by up to 18.7% when compared to the continuous operation method.

Stratta et al. (2020), investigated the economic analysis of a freeze-drying process. They proposed a model for determining the capital costs and operational costs in the freeze-drying cycle. They observed that the freeze-drying method is expensive since it has a higher energy value cost. But the main factor which limits its consideration is its higher initial expenditure.

2.7.1 Feasibility study

Generally, the feasibility studies are explored by the project owners to validate the project projection and analyse various risks, and stability of the project before the actual commencement starts. These studies provide data which can be used in modifying the projects and enhancing their value. The feasibility study provides information on whether the proposed project will meet the minimum requirements established by the industry when considering the net investing capital.

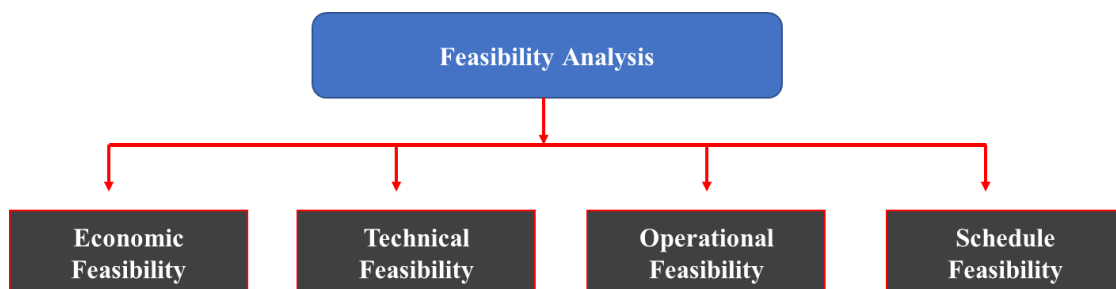


Figure 16: Types of Feasibility study

The feasibility study is broadly classified into several groups as follows,

1. Economic feasibility

The project cost and its benefits are evaluated in the Cost-Benefit analysis module.

2. Technical feasibility

Risk assessment of various technologies and their solutions are evaluated.

3. Operational feasibility

Study the process, operating modes, control, and improving the efficiency.

4. Schedule feasibility

Project completion times, planning resources etc.

If the feasibility study provides positive information, then the actual projects will begin as planned and detailed project engineering will take place. On the other hand, if the data is not so reliable then the project may be abandoned or recycled to an earlier stage, or an alternative project plan will be evaluated from the start. The plant size, its production capacity, operating methods, cost and source of raw materials, price of equipment, and effective utilization of resources are some of the factors which are studied in the feasibility study. The engineers and economists at each stage of the project, continuously monitor the design, costs, start-up facility and construction details. The knowledge about these is highly necessary for the firm owners to identify whether the industry is generating profit.

2.7.2 Fixed capital investment

It is defined as the net cost which consists of the cost of planning, building, and installation of the plant. It also includes the necessary cost of preparing the production plant site. It consists of the following,

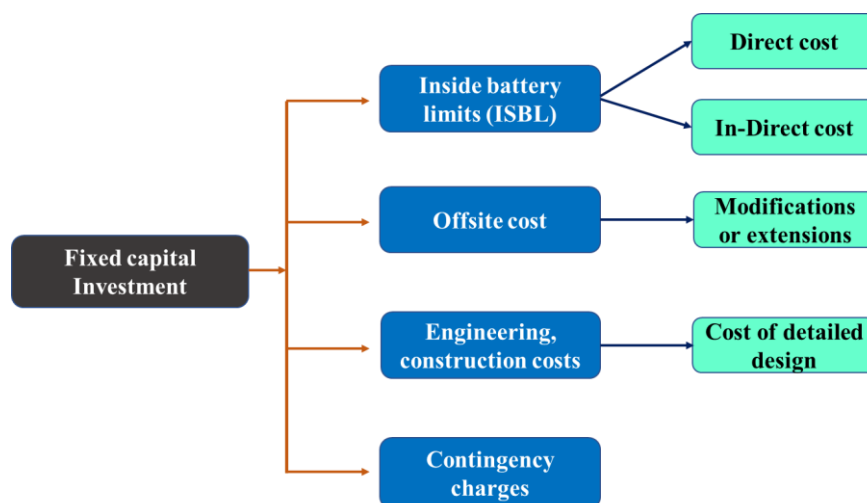


Figure 17: Fixed capital investment types, (Couper, 2003)

2.7.2.1 The inside battery limits (ISBL) investment

It includes the procuring cost and installing cost of all the equipment when constructing the new plant. It is divided into direct cost and indirect cost as follows,

Table 2: Direct and Indirect Costs

Direct cost	Indirect cost
Cost of all the process equipment	Temporary construction, temporary power and water, construction workshops
Cost of piping, insulations, structures, wiring, valves etc	Field services and expenses related to it such as overtime pay, and field canteens.
Cost of roads, foundations, piling etc	Construction insurance.
Installation and supervision cost.	Labour work compensation and benefits

2.7.2.2 Off-site costs (OSBL)

The cost which is associated with enhancing the capacity of an existing plant or adding an additional plant will be included in offsite costs., It includes the following,

Table 3: Types of off-site costs

- Transformers, power lines, electric main substations.	- Standby generators, turbine engines, Power generation equipment,
- Supply pumps, boilers, steam mains, condensate lines,	- Circulation pumps, cooling towers
- Water pipes, wastewater treatment plant	- Maintenance facilities.
- Offices, central control rooms, laboratories, canteens, analytical equipment, changing rooms	- Medical facilities, firefighting equipment Emergency services, etc.

2.7.2.3 Engineering and construction costs

It includes,

- The cost of drafting the plant layout, cost of engineering, and detailed design.
- Construction services and supervision
- Administrative charges including project management, engineering supervision,

For projects of a smaller scale, engineering costs are considered to be 30% of combined ISBL and OSBL cost and for larger projects 10% of ISBL plus OSBL cost. In our calculation, we have taken 10%.

2.7.2.4 Contingency charges

These are additional costs included in the project to consider any change from the planned valuation. Any modifications in project scope, fluctuations in prices, changes in labour pay, or other unanticipated coverages are generally covered in contingency charges. It is taken 8% for the present calculation and it is based on the stage of known information available when estimating or projecting the project cost. If the project is uncertain, then higher contingency charges (10-15%) are used.

2.7.3 Variable cost during production

These are certain costs which are associated with the plant operation requirements and are proportional to the additional cost required during the production process.

These include the following,

1. Utility requirements: steam, raw water, cooling water, nitrogen requirement, and other cost occurring at the site.
2. Raw materials costs.
3. Any consumables if used
4. Packing and shipping charges.

Fixed costs during production:

These are the costs which are fixed irrespective of the changes in the output of the plant process. Even though the plant cuts its production volume, these costs are fixed.

Table 4: Types of fixed costs

1. Labour working in the process plant.	2. Supervision charges,
3. Salary overhead	4. Insurances and property taxes., Environmental charges
5. Licence fees for running the plant.	6. Sales and marketing costs.

2.7.3.1 Maintenance cost

The Maintenance cost of the process is taken 5-15% of the total investment cost based on the project capacity. For our project volume and production capacity, 5% is considered in the calculation. This varies from case to case and the operational modules of the project.

2.7.3.2 Revenues

These are the monetary value or income earned through sales of main or by-products produced in the plant. At the initial stages of the design, the production rates and the plant capacity are calculated and hence the revenues are predicted at the design stages itself.

2.7.3.3 Margins

It is defined as the sum of revenues obtained by the main product sales along with by-product minus the raw material costs.

$$\text{Gross Margins} = \text{Revenues} - \text{Raw material costs} \quad (2.4)$$

2.7.3.4 Profit

It is defined as the main product revenues minus the sum of fixed and variable production costs.

$$\text{Gross profit} = \text{Main product revenues} - (\text{Variable cost} + \text{Fixed cost}) \quad (2.5)$$

However, the profit made by the production plant is subjected to taxation. Hence the gross profit is subjected to the taxes and the taxes rates are followed differently in each country and each location.

$$\text{Taxable income} = \text{Gross profit} - \text{Tax allowances} \quad (2.6)$$

Chapter 3: Thermo-physical properties

Chapter three explains the important thermo-physical properties and their importance in influencing heat and mass transfer analysis. Food processing involves heat and mass transmission between the product and the surrounding. The thermo-physical properties play a significant role in internal heat and mass transfer.

3.1 State equation

The main thermo-physical properties are included in the state (fundamental) equations, which are used for the determination of heat and mass transfer in food. The “heat equation” is the fundamental equation, and the general heat transfer equation in one dimension is given below,

$$\frac{\partial T}{\partial t} = \frac{k}{\rho c_p} \frac{\partial^2 T}{\partial x^2} \quad (3.1)$$

Where T represents the temperature in spatial co-ordinate (x) at a given time (t) and k , ρ , c_p denotes the thermal conductivity, density and specific heat of the substance respectively.

The diffusion equation describes the mass transfer in the food as follows,

$$\frac{\partial C_A}{\partial \tau} = \nabla(D_{AB} \nabla C_A) \quad (3.2)$$

Where, C_A represents the concentration of the substance ‘A’, D_{AB} denotes the diffusion coefficient and τ represents the time. The above state equations can be applied to model the heat and mass transfer in the food. The important thermo-physical properties of foods are temperature (°C), product composition and the state of the material like gas, liquid, amorphous or crystalline.

3.2 General specific heat (C_p)

It is generally defined as the quantity of energy necessary to raise the temperature of 1 kg of the product by one Kelvin ($\text{J kg}^{-1} \text{K}^{-1}$). For food materials, the specific heat is mostly measured at atmospheric pressure. Food compounds having high moisture content exhibit high C_p value since water has the highest C_p value among other food components. Most of the food components usually have a value between 1.0 to 2 kJ/Kg k. With the increase in temperature, the heat capacity of most of the components shows an increase in the trend, except for water. It is calculated based on the following expression,

$$C_p = \sum x_i C_{p_i} \quad (3.3)$$

3.3 Specific enthalpy (h)

It is the measure of the heat content of food per unit mass. The difference in enthalpy between the two state points indicates the heat or energy absorbed or extracted based on the heating or cooling of the product. The enthalpy difference between two state temperatures is given by the following expression,

$$\nabla h = \int_{T_1}^{T_2} C_p \partial T \quad (3.4)$$

3.4 Latent heat (L)

It is defined as the amount of heat absorbed or released when 1 kg of substances changes from one phase to another. The different phase changes occurring in the substances are the crystallization of water, melting of ice, crystallization of fats and their melting, change in liquid to vapor, and sublimation of ice crystals. The phase transition is described as the direct transition of thermal properties of pure compounds at the freezing point as described below in *Figure 18*. In the enthalpy curve, the latent heat of phase transition during product melting or freezing is represented as a vertical line.

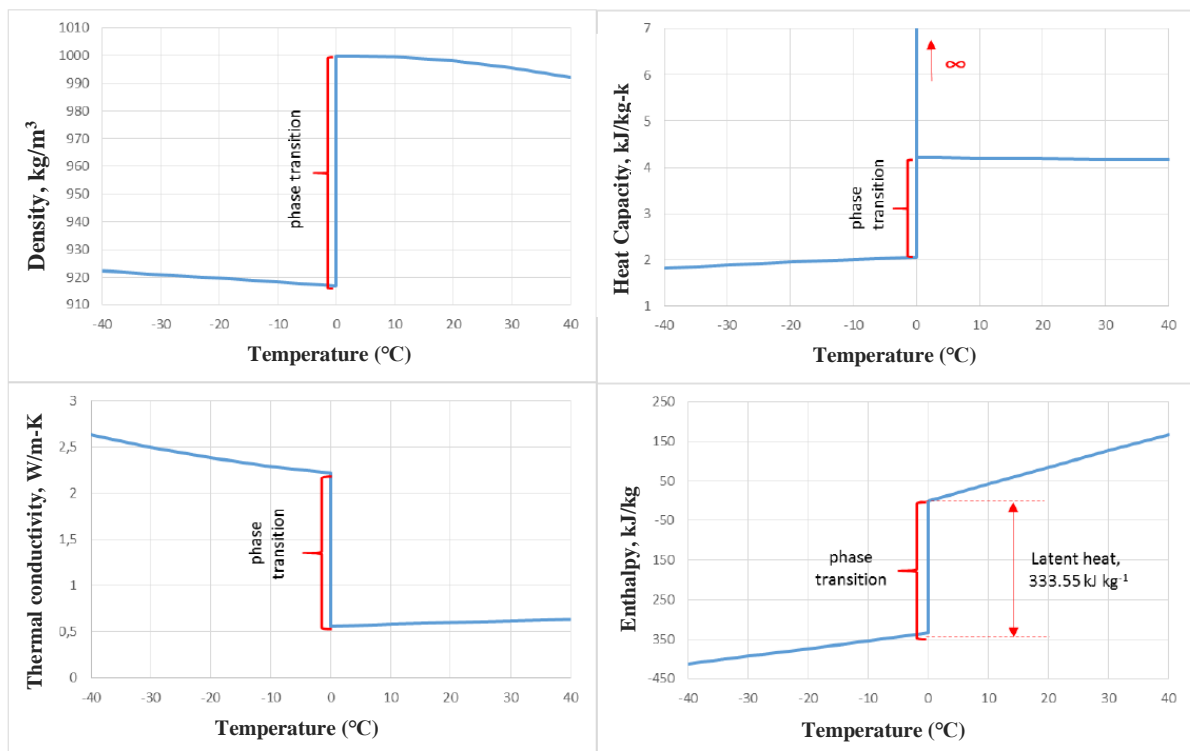


Figure 18: Changes of thermal properties during phase transition of water, (Eikevik, 2021)

3.5 Thermal diffusivity (α)

It represents how fast heat is diffused/transferred through the substances. It is given by the following equation,

$$\alpha = \frac{K}{\rho C_p} \quad (3.5)$$

3.6 Density

The density of a product is very important in the calculation of heat and mass transfer. It is the relation between the ratio of mass to volume of a product. The density of different compositions in food with respect to the temperature is represented below, since the food has lower thermal expansion and low compressibility, the influence of pressure and temperature on the density of the products is relatively small. With the increase in the temperature and pressure the density of fats, protein and carbohydrates are increased.

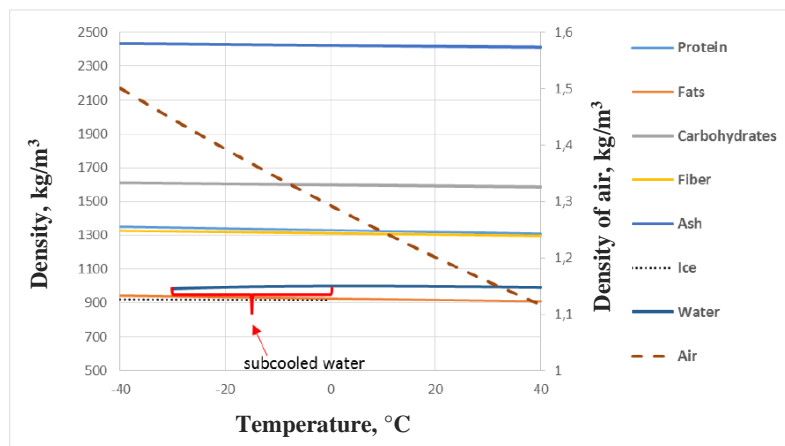


Figure 19: Density behaviour of different substances (Eikevik, 2021)

It is divided into apparent and real densities. Apparent density is termed as the true density (ρ_t) of the substances, without considering air gaps, porosity (ϵ_{ap}) and excess volume fraction (ϵ_{ex}) between the molecules. It is based on the following equation,

$$\frac{1}{\rho_{ap}} = \left(\frac{1}{1 - \epsilon_{ex} - \epsilon_{ap}} \right) * \frac{1}{\rho_t} \quad (3.6)$$

True density is defined as the ratio of the summation of densities of individual composition to that of the fraction of the same component. It is given as following,

$$\frac{1}{\rho_t} = \sum_{i=1}^m \frac{x_i}{\rho_{t,i}} \quad (3.7)$$

3.7 Influence of ice and C_p in thermal properties

For determining the energy flows, we should know the thermal properties of each product during the process. Different composition in the product has different thermal properties and this affects the overall energy needed during the heating or cooling process. The formation of structures with crystalline form is called crystallization. There is also the formation of crystallization of fats and carbohydrates.

Generally, the crystal is stable form. At normal conditions, the pure water freezes at 0.0 °C. During the freezing process, there is a release of the latent heat due to the formation of ice crystals. The value of latent heat 'L' during ice formation or melting is 333.55 kJ kg⁻¹ K⁻¹. On other hand, the food products do not have pure water. Generally, they contain salts in a dissolved state and other soluble substances. This solute affects the freezing point which decreases the value below 0.0 °C.

Ice: Determination of the amount of ice in a product is highly important for heat transfer relations. The mass of ice dependent on the product's temperature and the amount of water it contains. Free water is defined as the ability of the water to freeze completely at lower temperatures. Water and the amount of ice greatly influence the thermal properties of food. The heat capacity and thermal conductivity of the product are higher with high water content. The ice to water phase transition can increase the conductivity of the food. On the other hand, the density of the product is reduced. The regression equation can be applied to determine the thermo-physical properties in food between the temperature range +40 °C to -40 °C,

$$\rho_i, C_{p,i}, K_i = f(T) = \frac{(A_i + B_i * T + C_i T^2)}{1000} \quad (3.8)$$

The co-efficient for heat capacity in determining the thermal properties is given in the below table, (Eikevik, 2021)

Table 5: Coefficients for calculating the regression equations

	Protein	Fats	Carbohydrates	Fiber	Ash	Ice	Water
A	2008	1984	1549	1846	1093	2060	4210
B	1.2089	1.4733	1.9625	1.8306	1.8896	5.6732	-1.6297
C	-0.0013	-0.0048	-0.0059	-0.00465	-0.0037	-0.0103	0.0186

The knowledge of the amount of freezable and unfreezable water in the substances plays a significant part in the prediction of freezing point calculation. Freezable water is defined as the amount of water that freezes into ice at low temperatures below the freezing point. The unfreezable water will not freeze even at low and ultra-low temperatures but it forms concentrated solutions by mixing with other solvents present in the product which are soluble in water. The below *Figure 20* represents the comparison of different models of ice fraction formation rate with respect to different temperatures.

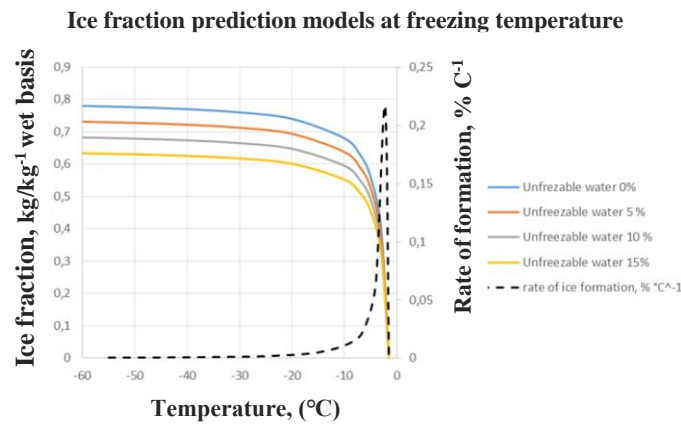


Figure 20: Ice fraction predicting models at freezing temperature (Eikevik, 2021)

Temperature Specific Heat capacity (C_p)

The theoretical value of the heat capacity of the product can be found using the summation of the product of individual heat capacity with the fraction of the components. It is given in the following equation,

$$C_p = x_p C_{p,p} + x_l C_{p,l} + x_{cc} C_{p,cc} + x_{ash} C_{p,ash} + x_w C_{p,w} + etc \quad (3.9)$$

Where $x_p C_{p,p} + x_l C_{p,l} + x_{cc} C_{p,cc} + x_{ash} C_{p,ash} + x_w C_{p,w}$ represents the sum of the product of fraction of individual fractions with that of specific heat of proteins, lipids, ash and water respectively. The specific heat below freezing must consider the sensible cooling below freezing and the phase change. Crystallization of water or melting of ice occurs due to a decrease or increase in temperature. Hence, the energy which is required to convert the product temperature should be determined by including the amount of latent heat.

$$C_{p, frozen, T} = C_p - (x_w - x_{un,w}) \left[\frac{LT_f}{T^2} + (C_{p,w} - C_{p,ice}) \right] \quad (3.10)$$

The C_p value will be calculated at the freezing point temperature, T_f , and L is the latent heat of water, and T is the initial temperature.

Chapter 4: Methodology

In this chapter, the schematic investigation, and the calculation equations for freeze concentration (FC), multistage evaporator- three effects (MSE) and mechanical vapor recompression (MVR), with the drying process are established in the first part. The process parameters and initialization values are provided at each process level. Second, the Dymola system design was explained followed by the HTHP system model. Finally, the equations for economic and sensitivity analysis are provided.

4.1 General Process flow diagram

The below scheme (*Figure 21*) represents the detailed process flow diagram of the production of fish protein hydrolysates. At all levels, the mass flow and heat flows are analysed to determine the energy values. The process diagram includes different ways of producing the FPH. Efficient techniques at concentrating and drying steps which can be used to produce the FPH sustainably and efficiently are considered in our investigations.

The energy study involves a detailed investigation of freeze concentration, multistage evaporation, and mechanical vapour recompression evaporation as an alternative in each process in the concentrating process. Similarly in the drying stage, the spray drying method, vacuum freeze drying, rotary drum drying, and heat pump assisted drying was studied. Different schemes are studied based on the alternatives at each stage and the energy required for the process was investigated in detail.

For instance, a typical process flow involves concentrating using freeze concentration and drying using spray drying as alternative 1, vacuum freeze-drying as alternative 2, and drum drying as alternative 3. Similarly, the study was extended for all combinations of alternatives with different concentrating and drying methods, like concentrating using multistage evaporation and drying with all combinations of alternatives, and concentration using vapour recompression evaporator with all drying alternatives. All the schemes are studied in terms of energy demands. The experimental work carried out during the production of FPH at the SINTEF mobile sea lab at Myre is given in ([Appendix 1](#))

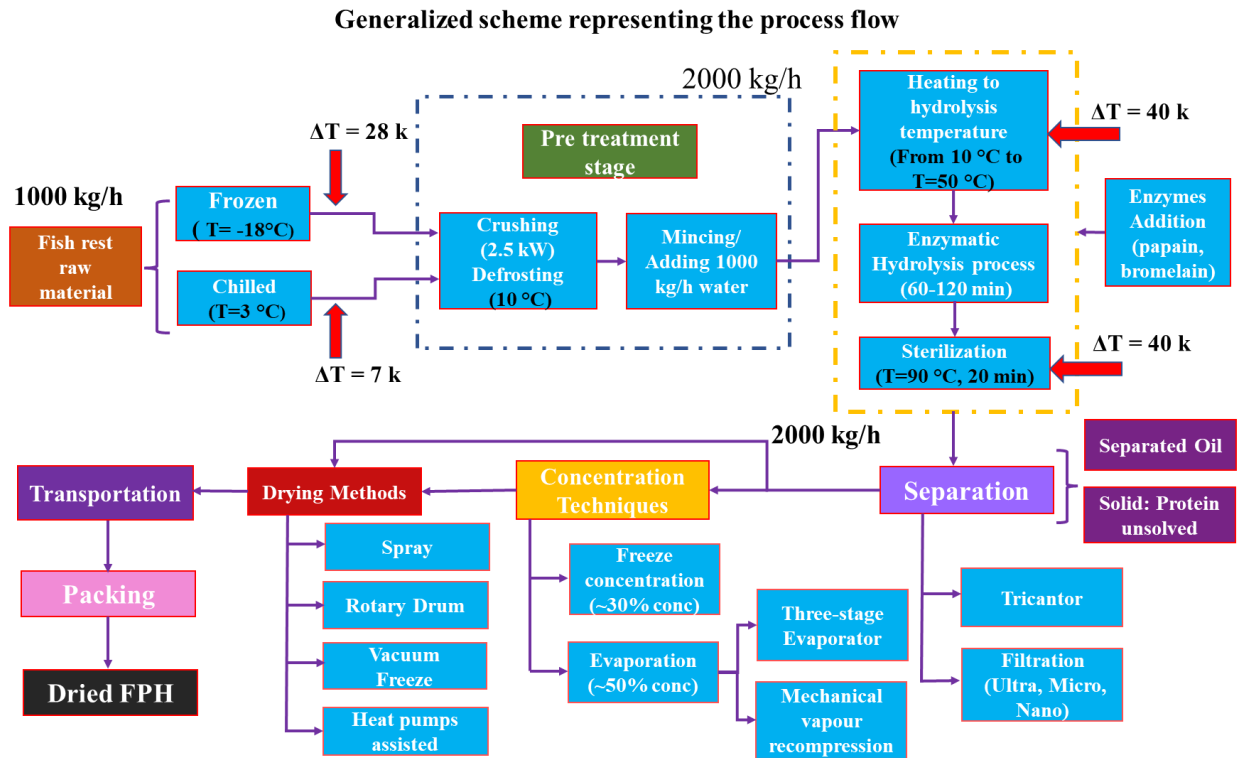


Figure 21: Schematic representation of process flow diagram

In the freeze concentration process, a concentration level of 30% was studied. Sulzer industry developed a process in which a maximum concentration of up to 60% is achieved in the freeze conc method. Hence in these analyses, the combination of suspension freeze conc. and static layer crystallization is studied theoretically. However, the removal of ice will be highly difficult from the wash column at a higher concentration and hence the technology should be validated. The study was performed only to understand the energy requirement at higher concentration levels.

Also, for onboard processing of FPH, the concentrated FPH can be further frozen to blocks and can be used based on the application. If further drying is required, the blocks are then processed in any of the drying methods located at land facilities. The decks in the fishing vessels are 2 and a half feet in height and hence the feasibility of installing the drying techniques is complicated. Hence for on-board vessels, freezing of blocks can be a good option for long term storage

4.1.1 Mass balance

It is important to specify all material flows when determining the mass balances during the production of FPH. The calculation for mass balance is based on the principle of conservation of mass. It states that at a given period, in a system with a defined boundary the total mass entering or leaving the system should be accounted for together with the mass which is already present in

the system. If there was no mass accumulated in the system, then the total mass entering the system is equal to the total mass leaving the system.

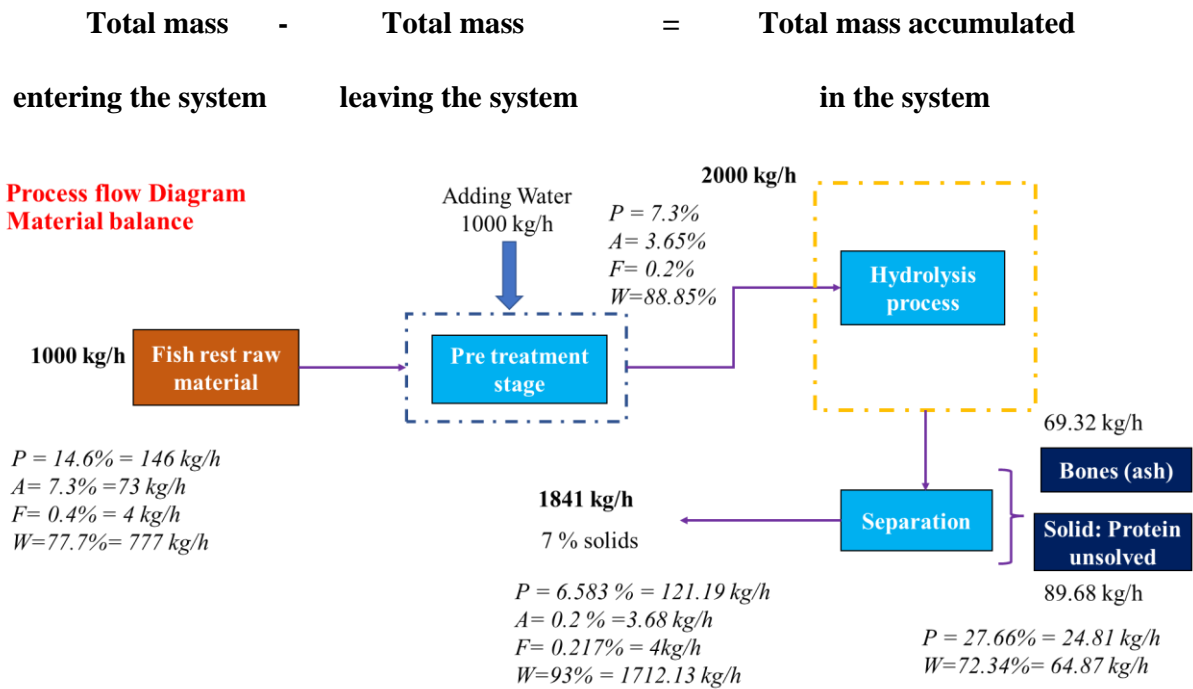


Figure 22: Mass balances of fish rest raw materials at each process stage.

For calculation, the assumption was considered for the input of 1000 kg/h of COD RRM, and 1000 kg/h of water (1:1 ratio). The initial composition of RRM was given in Table 6 (Petrova et al., 2018). After the hydrolysis process, the RRM water - mixture is fed into the separation process.

Table 6: Composition RRM initial and after separation

RRM input composition (1000 kg/h)	Percent	Liquid FPH after separation (1841 kg/h)	Percent
Water (W)	77.7	Water	93
Protein (P)	14.6	Protein	6.583
Fats (F)	0.4	Fats	0.217
Ash (A)	7.3	Ash	0.2

Here, in the calculation, it is assumed to have a maximum yield of liquid FPH after separation with a solid content of ~ 7%. The protein unsolved mixture has 80% protein and 20% water for initial calculation. The bones were almost separated during the separation process and the Liquid FPH has very negligible ash dissolved in it. COD RRM has a very less fat content. The composition of

the final FPH after separation was 1841 kg/h which is highlighted in the above *Figure 22*. These values are also given above for comparison with the initial RRM composition.

4.1.2 Energy balance

The main purpose of performing energy balance is to understand the flow of energy at each stage in the production of FPH and identify the potential area for energy conservation. The energy balance is performed based on the law of conservation of energy. The energy entering the system is equivalent to the energy leaving the system. The heat flow is given by the following eqn,

$$Q = m * C_p \Delta T \quad (4.1)$$

$$Q = m * \Delta h \quad (4.2)$$

Energy requirements for different processes

1. Heating/Cooling – It is the energy required for raising or lowering the product temperature from the initial to the final state.
2. Freezing/thawing — Energy for freezing/thawing of a product.
3. Refrigeration Energy— The necessary refrigeration capacity required to maintain frozen storage.
4. Pump energy— It is the energy required to pump fluid from one level to another. The pump energy is not considered in our calculation as it is assumed to be negligible when comparing the overall process energy. Vacuum pump on the other hand consumes huge energy for its operation and it is considered.

In the initial process, the energy required for thawing the frozen RRM product from -18 °C to 10 °C is calculated using models described in the freeze concentration, since both the sensible and latent heat has to be considered. After thawing, the RRM mixture with water was heated to a hydrolysis temperature of 50 °C from 10°C, and then heated to 90 °C for sterilization, here only the sensible part is considered as it does not involve any phase change.

4.2 Calculation models for freeze concentrator

The following data are initialized for calculation involving freeze concentration. The equations presented here are from relevant references and topics ([Eikevik, 2021](#)).

Table 7: Parameters initialization for freeze concentrator

Parameters	Value	Parameters	Value
Inlet Mass flow rate	1841 kg/h	Initial temperature	+4 °C
Desired Concentration	30 percent	Final temperature	-3 °C

Calculation of freezing point depression using empirical models.

The below equations are used to determine the freezing temperature.

$$\Delta T = 0 - T_f \quad (4.3)$$

For seafood,

$$\Delta T = \frac{x_w - 1}{0.0078 - 0.140x_w} \quad (4.4)$$

The amount of unfreezable water, $x_{un,w}$, (kg kg^{-1} wet basis) can be determined as below,

$$x_{uw.w} = 0.4(x_p + x_{cc} + x_{ash}) \quad (4.5)$$

here x_p , x_{ash} , x_{cc} , denotes the mass fraction corresponding to proteins, ash and carbohydrates present in product (kg kg^{-1} on wet basis).

The unfrozen water is a function of freezing time and temperature. This decreases with a decrease in the temperatures. At the end of freezing only the water which is in unfreezable form exists in a liquid state. The temperature-dependent unfreezable water can be calculated by the following equation, which is the difference between the net water content in the substance and the amount of ice.

$$x_{ice,w,T} = x_w - x_{ice} \quad (4.6)$$

The following empirical formula is employed to determine the ice fraction in the substance when considering the unfreezable water,

$$x_{ice,T} = (x_w - x_{un}) * \left(1 - \frac{T_f}{T}\right) \quad (4.7)$$

Where T , T_f denotes the initial product temperature and the product freezing temperature. Above the freezing temperature, the enthalpy change can be computed as follows,

$$\Delta h_T = (T - T_f) * C_p \quad (4.8)$$

The C_p value can be calculated as the sum of C_p values of individual products as explained above. Below the freezing point, Δh is calculated as follows,

$$\Delta h_{T,frozen} = (T - T_f) * (C_p - (x_w - x_{un,w})) * \left(\frac{L}{T} + (C_{p,w} - C_{p,ice}) \right) \quad (4.9)$$

Where L represents the latent heat of ice (333.5 kJ/kg), $C_{p,w}$, $C_{p,ice}$ represents the heat capacity of water and ice respectively which is calculated as a function of temperature, hence the total change in enthalpy is given by,

$$\Delta h_{total} = \Delta h_T - \Delta h_{T,frozen} \quad (4.10)$$

The net heat load to be removed to freeze the product in kW is as follows,

$$Q_c = M * \Delta h_{Ttotal} \quad (4.11)$$

Where M is the mass flow rate of feed in kg/s. During the process, the heat provided to melt the formed ice from -3 °C to 0.5 °C should consider the sensible heat and latent heat.

Carnot COP of the refrigeration capacity operating at $T_h = 0$ °C and $T_l = -40$ °C

$$COP = \frac{T_L}{T_H - T_L} \quad (4.12)$$

Carnot's work is given as below,

$$W_{car} = Q_o * \frac{T_c - T_e}{T_e} \quad (4.13)$$

The two-stage process TWICE from the SULZER industry is further investigated and the energy for freezing blocks is studied at onboard processing.

4.3 Calculation equations for multistage evaporation with three effects

In the evaporation process, the desired concentration level was 50%. The calculation is performed for two cases, Case1: 90 °C, since the temperature after the separation is expected to be 90 °C with no heat loss. In case 2, the hydrolysates are stored at room temperature of 0 °C.

The following data were initialized for calculation involving multistage evaporation.

Table 8: Parameters initialization for three-stage evaporators

Parameters	Value	Parameters	Value
Initial Mass flow rate	1841 Kg/h	Initial temperature	Case1: 90 °C, Case2: 0 °C
Concentration Level	~ 50 percent	Amount of water in the feed	93 percent
No. of effects	Three	Amount of water in the product	50 percent

The operation temperatures, pressure, and heat transfer coefficient of each stage in the system vary based on the system configuration and other factors. The actual energy is determined by the difference in enthalpy between the hot stream and cold stream of feed, concentrate and vapor at each stage. For an approximation, the energy required in multistage evaporation is halved by a factor of n when compared with a single-stage operation. Where n describes the number of the stages or effects. Here, the calculation was made to determine the minimum energy demands of the system.

To calculate the energy required in evaporation, the mass flow in and out of the system and the amount of moisture evaporated are to be determined and are provided by the following equations, (Toledo et al., 2007).

Mass flow out of the evaporator:

$$M_2 = M_1 \left(\frac{X_{feed}}{X_{product}} \right) \quad (4.14)$$

Where M_1 and M_2 represent the mass flow rate at the inlet and exit of the evaporator, X_{feed} and $X_{product}$ is the fraction of water at the inlet and outlet respectively.

The amount of vapor evaporated from the system is given by,

$$Vapor = M_1 \left(1 - \left[\frac{X_{feed}}{X_{product}} \right] \right) \quad (4.15)$$

The fraction of moisture removed in percent is given by,

$$X_{fraction,Vapor} \% = \left(\frac{Vapor}{M_1} \right) * 100 \quad (4.16)$$

The amount of heat required to evaporate in a single effect evaporator is the heat energy or heat load required to raise the feed temperature to boiling point (100 °C) and the latent heat required to evaporate from liquid to vapor which is given by,

$$Q_{net} = M * C_p * \Delta T + M_v * \Delta H \quad (4.17)$$

The heat input required for three effect evaporators in kW is given below,

$$Q = \frac{Q_{net}}{n} \quad (4.17.1)$$

Where n is the number of effects. Heat load to be removed from the condensing vapor is given by,

$$Q_c = M_v(h_3 - h_{liq}) \quad (4.18)$$

Where h_3 is the enthalpy of vapor at the third effect and h_{liq} is the enthalpy of the liquid at condensing temperature and pressure (0.2 bar and 30 °C)

Finally, the heat energy required to evaporate per kg of water is given by dividing the heat energy by the amount of moisture removed in kg/s.

$$E = \frac{Q}{M_v} (\text{kJ/kg of water}) \quad (4.19)$$

4.4 Calculation equations for mechanical vapor recompression evaporation

The inlet mass flow rate of the system is 1841 kg/h, here the concentration level was 50 %. The system can be operated at the increase in pressure and the corresponding heat output can be improved, on the other hand, the work input to raise the pressure is higher. The heat required to evaporate the product in vapor recompression evaporation is the heat required for raising the temperature of feed to boiling temperature and then to the latent heat of vapor as given by,

$$Q = M_v * (h_{100} - h_i) + M_R (h_{100 \text{ sat } L} - h_i) \quad (4.20)$$

Where, h_{100} is the enthalpy of gas at 100 °C, and $h_{100 \text{ sat } L}$ represents the saturation enthalpy of liquid at 100 °C, and h_i represents the enthalpy of the liquid at the inlet temperature. If the feed was at a lower temperature say 20 °C the heat energy required to raise the feed temperature is also considered.

The required heat energy to evaporate the moisture and to concentrate the feed is provided by the necessary work input to the vapor recompression system, which is represented in the phase diagram of water. The temperature and pressure levels are represented below *Figure 23*,

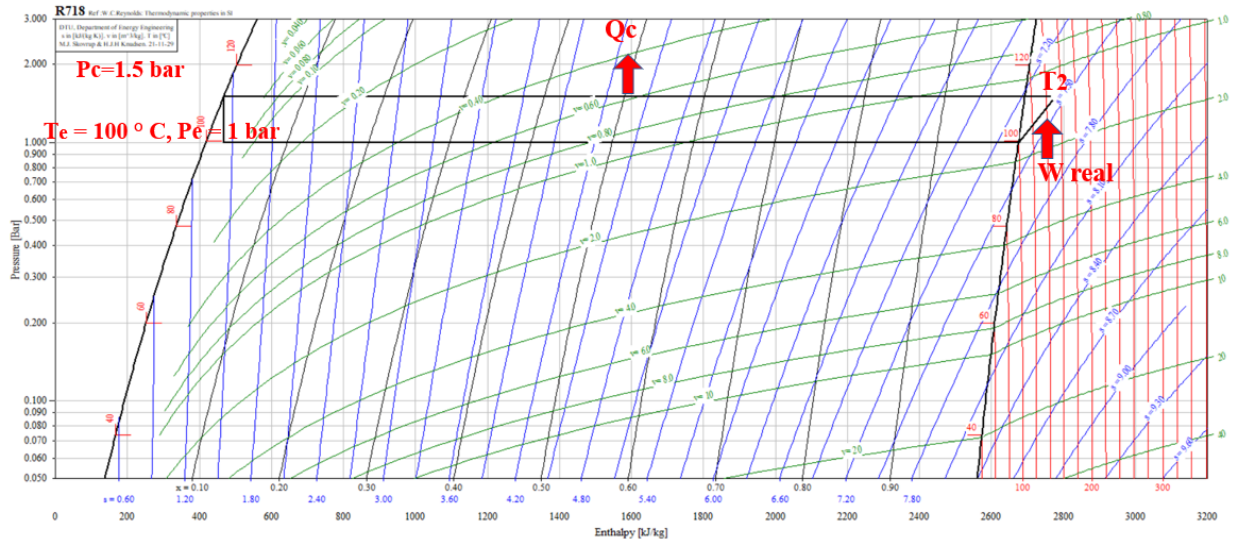


Figure 23: Water phase diagram- Pressure-enthalpy

The work input in kJ/kg in the vapor compression cycle is provided by,

$$W = \frac{h_{2s} - h_1}{n_{is}} \quad (4.21)$$

$$h_2 = h_1 - \left[\frac{h_{2s} - h_1}{n_{is}} \right] \quad (4.22)$$

The isentropic efficiency of the fan/compressor is usually in the range of 0.5 to 0.7. For our assumption 0.7 was considered. Hence, the heat demand Q (kW) is given by the product of the amount of evaporated vapor in kg/s with the work input.

$$Q = M_v * W \quad (4.23)$$

4.5 Calculation equations for spray drying

The following data was initialized for calculation involving spray drying.

Table 9: Parameters initialization for spray dryer

Parameters	Value	Parameters	Value
Initial Mass flow rate	Depends on the previous process	Product Initial temperature	0 °C (from storage temperature)
Desired Concentration	~98 %	Amount of water in the feed	Depends on the previous process
Hot air temperature	210 °C	Amount of water in the product	< 2 percent

The calculations equations used in the spray dryer are as follows, (Van't, 2011)

Let M_1 be the amount of feed entering the spray dryer, and it has S_1 of solids in it. The amount of water in the inlet feed is given by

$$W_1 = M_1 - S_1 \quad (4.24)$$

The exit air temperature is given by the following equation.

$$T_2 = 88.39 * \log_{10}[T_1 - 112.35] \quad (4.25)$$

The exit product temperature (T_{p2}) is given as the difference between the exit air temperature (T_2) and the inlet product temperature (T_{p1}). In most cases, this temperature is close to the exit air temperature.

$$T_{p2} = T_2 - T_{p1} \quad (4.26)$$

It is assumed that the amount of the solids entering the dryer is equal to the amount of the solids leaving the system (S_2).

$$S_1 = S_2 \quad (4.27)$$

The mass at the exit of the drier with a solid concentration of 98% is provided by the following relation,

$$M_2 = \frac{S_1}{0.98} \quad (4.28)$$

Water content in the exit feed,

$$W_2 = M_2 - S_2 \quad (4.29)$$

Amount of water evaporated,

$$Ev = W_1 - W_2 \quad (4.30)$$

Heat transfer calculation,

Q_1 is the heat input required for evaporating the water and heating the water vapor,

$$Q_1 = Ev * [2500 + (1.9 * T_2) - (4.2 * T_{p1})] \quad (4.31)$$

Let Q_2 be the heat required for heating the solids in the feed,

$$Q_2 = S_1 * C_p * [T_{p2} - T_{p1}] \quad (4.32)$$

Let Q_3 be the amount of heat required to heat the remaining water in the product,

$$Q_3 = W_2 * 4.2 * [T_{P2} - T_{P1}] \quad (4.33)$$

The total heat requirement in kJ is given by,

$$Q_t = Q_1 + Q_2 + Q_3 \quad (4.34)$$

Here, the heat required for heating the air from ambient temperature has to be considered, hence the Q_{net} in kJ is given by considering heat loss and other factors.

$$Q_{net} = 1.25 * Q_t * \left[\frac{T_1 - T_{air}}{T_1 - T_2} \right] \quad (4.35)$$

The amount of energy in kWh/kg of water is given by,

$$E = \frac{Q_{net}}{Ev} \quad (4.36)$$

4.6 Calculation models for vacuum freeze-drying

In freeze-drying, the sublimation of the product occurs at -20 °C inside the freezing chamber maintained at ~1.0 mbar. The vacuum pump maintains sufficient lower pressure inside the chamber.

The following data were initialized for calculation involving freeze-drying.

Table 10: Parameters initialization for vacuum freeze-drying

Parameters	Value	Parameters	Value
Initial mass flow rate	Depends on the previous process	Feed initial temperature	Storage temperature (0 or -1°C)
Desired Concentration	~98 %	Operating pressure	at 1.0 mbar or lower
Chamber temperature	-20 °C	Amount of water in the product	< 2 percent

The energy required to evaporate the water is divided into the following stages,

1. The product is frozen from initial feed temperature to chamber temperature maintained at -20 °C.

Let Q_0 be the initial heat energy that is to be removed from the product at this stage. It is the difference in enthalpy from inlet product temperature to the final freezing temperature.

It is calculated as similar to models described in freeze concentration above and below freezing point since the freezing point of the substance is lower than zero. The c_p values are calculated as a function of temperature and composition.

2. After this sublimation of ice occurs, which results in the direct phase change of ice into vapor without liquid phase since the operating conditions take place at low temperature and low pressure. The heat energy required will be the difference in enthalpy between the saturated solid state to the saturated gas state at $-20\text{ }^\circ\text{C}$ and 1 mbar.
3. Finally, the cooling energy is provided by the refrigeration capacity to transform vapor to ice on the evaporating surface. It is given by the difference in enthalpy of saturated gas at $-20\text{ }^\circ\text{C}$ to the solid at $-40\text{ }^\circ\text{C}$ at the same pressure. Here $-40\text{ }^\circ\text{C}$ is the evaporator surface temperature.

Other additional energy which is to be considered in the vacuum freeze-drying is the work input to the compressor to provide the necessary cooling capacity at sufficient temperature and the work input of the vacuum pump to maintain relatively low pressure during the entire drying process. The work input to the cycle is calculated based on the refrigeration capacity as shown below.

Refrigeration capacity, Q_o

The refrigeration capacity is provided by the product of the amount of ice formed and the difference in enthalpy of saturated gas at $-20\text{ }^\circ\text{C}$ to the solid at $-40\text{ }^\circ\text{C}$ at 1 mbar.

$$Q_o = M_i \Delta h \quad (4.37)$$

Carnot COP of the refrigeration capacity operating at $T_h = 30\text{ }^\circ\text{C}$ and $T_l = -50\text{ }^\circ\text{C}$

$$COP = \frac{T_L}{T_H - T_L} \quad (4.38)$$

Carnot's work is given as below,

$$W_{car} = Q_o * \frac{T_c - T_e}{T_e} \quad (4.39)$$

Vacuum Pump work:

In vacuum pump operation, it compresses the air from atmospheric pressure of 1 bar to the lower pressure of 1mbar. Here, T_1 is the initial room temperature of 293 kelvin, and m is the mass flow rate of the air in kg/s. Hence, the work consumed by the vacuum pump in kW is given below,

$$W = -\frac{m * nRT_1}{n - 1} \left[\left(\frac{P_2}{P_1} \right)^{\frac{n-1}{n}} - 1 \right] \quad (4.40)$$

4.7 Calculation equations for rotary drum drying

The following data were initialized for energy calculation involving rotary drum drying.

Table 11: Parameters initialization for rotary drum drying

Parameters	Value	Parameters	Value
Initial mass flow rate	Depends on each process	Product initial temperature	-1 or 0 °C
Desired concentration	~98 %	Amount of water in the feed	Depends on the previous process
Inlet steam (air) temperature	300 °C	Amount of water in the product	< 2 percent

In the rotary dryer, various factors lead to high energy demands. The heat energy is provided by the exchange between the hot air and the product. The following are the various parts to be considered,

1. Heat to raise the temperature of the feedstock solid, where M_{s1} is the amount of the solids at the inlet feed. T_h is the water boiling temperature at 100 °C and T_i is the feed inlet temperature.

$$Q_1 = M_{s1} * C_p * (T_h - T_i) \quad (4.41)$$

2. Heat lost in residual moisture, is given by the heat carried away by the amount of moisture present in the exit feed. Where h_1 is the corresponding enthalpy at T_i , $h_{sat liq}$ is the saturated liquid at 100 °C.

$$Q_2 = M_{w2} * (h_{sat liq} - h_1) \quad (4.42)$$

3. The heat required to raise water temperature to saturated temperature, where M_v is the amount of moisture removed.

$$Q_3 = M_v * (h_{sat liq} - h_1) \quad (4.43)$$

-
4. The heat required to raise the temperature of the water to vapor temperature is given by the product of the mass of vapor to the latent energy.

$$Q_4 = M_v * (\Delta h) \quad (4.44)$$

5. Hence, the total heat load Q_{tot} in kW is given below,

$$Q_{tot} = Q_1 + Q_2 + Q_3 + Q_4 \quad (4.45)$$

6. Considering heat loss and additional energy required for heating the air:

$$Q_{final} = 1.25 * \frac{300 - T_{a1}}{300 - T_{a2}} * Q_{tot} \quad (4.46)$$

Where T_{a1} and T_{a2} are the inlet air and exit air temperature which are 10 °C and 92 °C respectively and 300 represents the temperature of the hot air in °C. The amount of energy in kWh/kg of water is given by dividing the amount of evaporated water in kg/s to the Q_{final} ,

$$E = \frac{Q_{final}}{Ev} \quad (4.47)$$

4.8 Softwares used

4.8.1 Engineering Equation Solver (EES)

Engineering Equation Solver (EES) is a program which is used to solve nonlinear systems of equations. It is extremely useful owing to its variety of different functions and equations for thermodynamic and heat transfer problems. The transcritical CO₂ system and the HTHP model has been designed and analysed in the EES. EES has a comprehensive database of the properties of several refrigerants used in refrigeration systems.

4.8.2 Dymola

Dymola is a modelling and simulation program that uses the open Modelica modelling language. It is capable of handling quite complicated systems and is utilized in aerospace, automotive, robotics, process, and other industries.

For dynamic simulations, TLK-Thermo GmbH's Dymola software was used, along with TLK-Thermo GmbH's components and refrigerant libraries. TIL 3.5.0 libraries were utilized to simulate heat exchangers, compressors, and valves, as well as TIL Media 3.5.0 for refrigerants and secondary fluids. The transcritical CO₂ system has been simulated in Dymola and the results were

compared with EES. For visualizing and plotting the results, software DaVE was used. The PH and TS diagram can be visualized in TLK DaVE.

4.8.3 SOLIDWORKS

SolidWorks is basically a computer aided design (CAD) and computer-aided engineering (CAE) tool used for solid modelling. It creates models and assemblies using the parametric feature-based method. In SolidWorks, creating a model normally begins with a 2D drawing, which is then transformed into the appropriate 3D model. The software includes a number of tools that may be used to create and construct the model in a more complete manner.

The complete process involved in the production of the final hydrolysates is modelled and assembled step by step to visualize the actual process in an industrial scale. The system with different combinations of the concentrations and drying equipment are modelled. After the final modelling is completed the modelled files in parts are then assembled with respective component in the assembly environment. Finally, rendering are done on the assembled parts and drawings can be created either from parts or assemblies if necessary.

4.8.4 MATLAB

MATLAB is a computer language that engineers and scientists use to address complicated engineering issues. The MATLAB language is included in the software, which is a matrix-based language to perform computational mathematics.

Matrix operations, function and data visualization, algorithm implementation, user interface and interfacing with programs written in other languages are all possible with MATLAB. The software has been used in the thesis to perform the analytical calculations involved in each process. It helps to save time when performing complex iterative calculations.

4.9 Energy recovery solutions

The methods and the procedure utilized in the design and development of the simulation models are described in this section. The simulation models are modelled and validated by comparing the results in EES and Dymola. The key objective of the validation is to study and analyse the system behaviour for FPH production applications. The obtained percentage of error is less when comparing the results from Dymola and EES. The single-stage system using CO₂ (natural refrigerants) was studied during project work, as an improvement in thesis work, efforts have been made in designing a more effective and better two-stage system.

mixture is performed to recover the waste heat in the heat recovery heat exchanger. The heat source for the process is taken from the waste heat, which is exchanged with heat recovery HX, the outflow FPH has a temperature of around 55 °C. This is cooled to 4 °C by the evaporator. The heating of hydrolysates and energy recovery are simulated using Dymola software to study the system behaviour in a dynamic environment.

In the simulation, a two-stage CO₂ cycle consisting of compressors, gas cooler, expansion valves, intermediate pressure receiver, and evaporator was modelled. The system is operated at three pressure levels low-pressure level at 25 bar, medium pressure level at 40 bar and high-pressure level at 100 bar which is represented in the system as blue, yellow, and red lines respectively.

From the *Figure 24*, process 1 represents the refrigerant which is drawn from the evaporator and is compressed to a medium pressure range of 40 bar. The pressure ratio is not so high and hence less work is consumed by the first compressor. The exit of the gas is flown into the intermediate receiver where it is separated into liquid and vapor, the vapor is recompressed by the second compressor and the refrigerant flows through the gas cooler and sub-cooler heat exchanger. It is allowed to expand into the intermediate pressure receiver through the first expansion valve. Inside the receiver, the lower pressure fluid is combined with the liquid from process 2 and it is allowed to expand through the second expansion valve and flows into the evaporator and the cycle repeats.

A superior level of control on the boundary conditions and the input parameters is possible in the software. The expansion valves are controlled using a PI controller through the setpoint method. CO₂ was selected as a working fluid due to its better thermodynamic properties as follows,

Table 12: CO₂ properties

<i>-Heat rejection at constant pressure and gliding temperature.</i>	<i>-Higher compressor efficiency, high volumetric refrigeration capacity, hence small compressor.</i>
<i>- Excellent temperature fit is achieved between the working fluid and the water.</i>	<i>- Less superheat loss, higher energy savings, high COP.</i>
<i>-Superior heat transfer in the heat exchanger.</i>	<i>- Low change in temperature with respect to pressure drop.</i>

Initially, the hydrolysates properties are similar to water since the hydrolysates have less solid content and hence water has been used as a medium in the modelling. Tube and tube heat exchangers with the same heat transfer coefficients are utilized in both evaporator and gas coolers.

Heat exchanger area, size and the number of tubes are calculated and are provided as an input to the system. The heat transfer coefficients are given in the table below.

Table 13: Heat exchanger heat transfer coefficients

Heat Exchanger	Heat transfer Coefficient (W/m ² K)
Evaporator	2000
Gas cooler	2000
HX Ice Melter	2000

The evaporator capacity was calculated to be $Q_o = 107$ kW by considering the mass flow rate of 1841 kg/h of hydrolysates mixture, specific heat capacity and the temperature difference after the heat recovery heat exchanger 55 °C to the final temperature of 4 °C. In the simulation, at the evaporator, the hydrolysates are cooled, and the released heat were absorbed by the working fluid. The effective compressor from the software was used in the simulation, and the volumetric efficiency and isentropic efficiency were fixed to 0.7. The speed of the compressor was fixed to 50 Hz.

4.9.2 Thermo-dynamic process and the state points

Process 1-2 & 3-4: Isentropic compression

In the process, the compressor compresses the refrigerant to higher temperatures and pressure. The isentropic process is assumed during the compression process in an ideal cycle. During the compression process, the efficiency of the compressor is not 100%, also compressor losses should be considered. A value of 0.7 was assumed as the compressor efficiency, and it is represented as,

$$\eta_{comp} = \frac{h_{2s} - h_1}{h_2 - h_1} \quad (4.48)$$

Here, h_1 and h_2 represent the enthalpy before and after compression, and h_{2s} represent the isentropic enthalpy. The ideal work performed by the first compressor is given by, $W_{is} = m_R * (h_{2s} - h_1)$. The equation can be stated as if the isentropic efficiency is taken into account.

$$W = \frac{W_{is}}{\eta_{is}} [kW] \quad (4.49)$$

Process 4-6: Isobaric rejection

Hot gas rejects the heat in the gas cooler, which is used for heating the hydrolysates, in our simulation the mixture is heated to 50 °C from 10 °C. CO₂ heats the water to a higher temperature at constant pressure and gliding temperature. Superior heat exchange inside the heat exchanger occurs. Further, subcooling is provided by the sub-cooler to recover a portion of recoverable heat to melt the ice. The sum of condensing heat is provided as:

$$Q_c = m_R (h_4 - h_6) = Q_e + W \quad [kW] \quad (4.50)$$

Process 6-7 & 8-9: Isenthalpic expansion

After heat rejection at constant pressure, expansion occurs at constant enthalpy. The expansion valve lowers the temperature and pressure of the refrigerant, $h_6 = h_7$ & $h_8 = h_9$.

Process 9-1: Isobaric heat absorption

The refrigerant absorbs heat from the heat source and evaporates inside the evaporator. The heat load is provided by the heat source by cooling the hydrolysates to 4 °C. This can be calculated by the equation:

$$Q_0 = m_R (h_1 - h_9) \quad [kW] \quad (4.51)$$

The mass flow rate of the CO₂ refrigerant at the top stage is given below.

$$m_{R,high} = m_{R,low} \left(\frac{h_2 - h_8}{h_3 - h_7} \right) \quad (4.52)$$

Net work done by both compressors,

$$W_{net} = W_1 + W_2 \quad (4.53)$$

The COP of the heat pump system is given below,

$$COP_{HP} = \frac{Q_c}{W_{net}} \quad (4.54)$$

4.10 High-temperature heat pump (HTHP) system design

Generally, the production of fish protein hydrolysates requires excessive high temperatures above 100 °C for applications like evaporations and drying to remove the moisture from the product. The high-temperature heat pump system (HTHPs) using butane and propane cascade cycle was studied as an alternation for evaporation or drying techniques.

Conventionally, drying can be performed using several methods. Different techniques consume a high amount of energy based on their working principle, operating capacity, and system design. HTHP on the other hand operates more effectively with reduced energy demands and delivers the necessary heat output. HTHP integrated evaporation methods can be used to preheat the hydrolysate mixture during the evaporation process. The traditional heat pump system suffers heat delivery at the higher temperature, but technological advancements in compressor technology, working fluid selection and system modification makes high-temperature application feasible.

The following propane-butane system design (*Figure 25*) has been studied in EES software to study the system behaviour and application of HTHP in the production process of fish protein hydrolysates. Butane working fluid at the top stage is best suited for high-temperature heat delivery due to its higher critical temperature, which can be used to heat the fluid up to 120 °C.

In the propane cycle, the evaporation pressure was designed at 6.3 bar, the pressure after the first compressor was about 22 bar. 5k temperature difference is kept in the evaporator and the cascade heat exchanger. For the HTHP system, the heat source should be higher. This can be achieved from waste process heat or a similar available heat source. The cascade heat exchanger performs as an evaporator for the butane cycle and a condenser for the propane cycle. Propane condenses and delivery the heat, which acts as a heat source for the butane refrigerant ([Opeyemi et al., 2017](#)).

The propane evaporates in the evaporator at constant pressure at process 1 and it is passed into the internal heat exchanger (IHX). The propane is then compressed to a higher temperature and pressure at process 3. It is then condensed in the cascade HX and allowed to pass through the IHX to heat the incoming refrigerant from processes 1 to 2. After rejecting the heat at process 5 it is allowed to expand in the expansion valve (control valve) and the propane cycle continues.

In the butane cycle, the refrigerant evaporates at constant pressure at 5.5 bar and reaches process 7. From there, it is passed through IHX and gains heat and then compressed to the higher temperature and pressure of 135°C and 26 bar respectively. It is then condensed in the condenser. The refrigerant then passes through the IHX and expands in the second expansion valve and the butane cycle repeats.

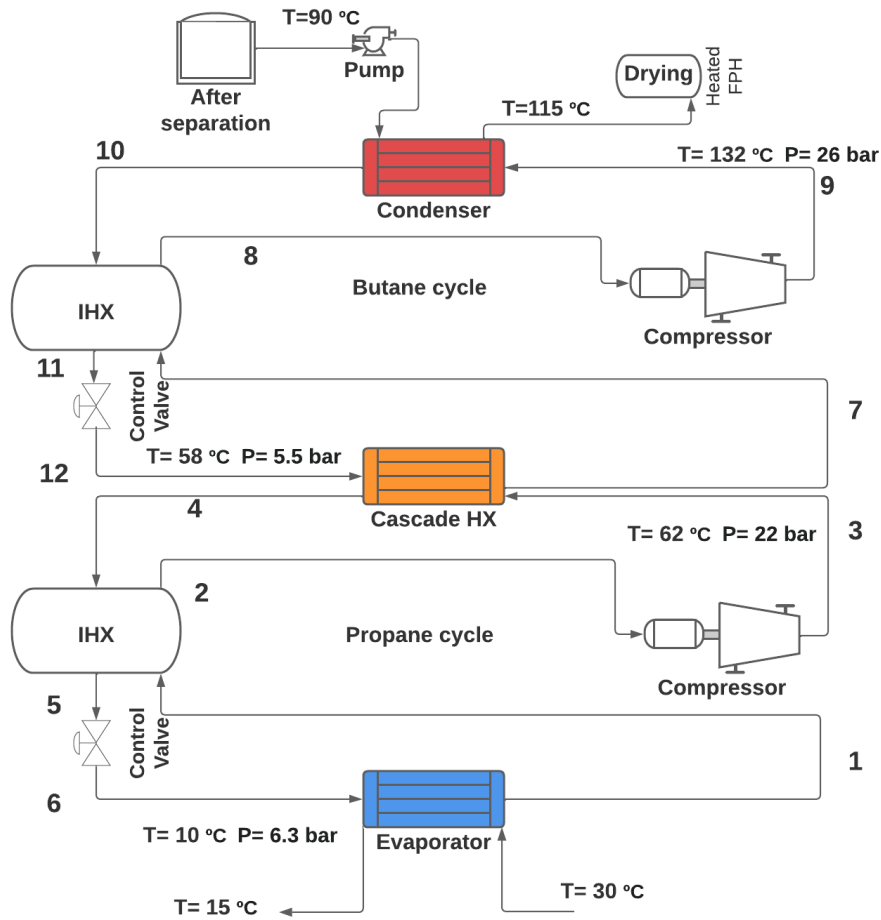


Figure 25: HTHP system: Propane-Butane cycle

4.11 Economic analysis

Economic investigation determines the total capital cost, plant operating, maintenance cost, profitability evaluation, sensitivity analysis, feasibility study, and analyses of the uncertainties associated with the project. For the industrial project, it is highly necessary in determining the overall project cost and to find whether the project is profitable or not. Economic analysis is used to evaluate it more effectively. All the approaches given below are from relevant chapters from process engineering economics topics, (Couper, 2007; Hillestad, 2022). The profitability analysis is performed in accordance with investment analysis chapters (Georges, 2020).

4.11.1 Capital costs estimating methods

Generally, the accuracy of the project estimate depends on the number of detailed design details available, time spend on preparing the estimation and the accuracy of the available cost data. At the initial stages of the project plan, only an approximation can be made, accuracy depends on the amount of information available. The following are the methods used for estimating the cost of the project.

1. Rapid cost estimates

In this approach, the cost of the project is estimated based on the cost of the early project which has the same technology process. It is a quick method of estimating the costs. Only the data of plant production capacity is necessary and not the design data. The capital costs of the plant based on the capacity are provided in the following equation,

$$C_2 = C_1 \left(\frac{S_2}{S_1} \right)^n \quad (4.55)$$

Where, C_1 = Capital cost ISBL of the plant with production capacity S_1

C_2 = Capital cost ISBL of the plant with production capacity S_2

The value for the exponent factor n is usually taken from 0.6 to 0.8.

2. Cost estimation based on the factorial method

The factorial method of cost estimation is used to predict the capital cost of the process plants based on the purchase cost of the collective equipment in the plant. The capital cost accuracy will depend on the stage of design data available, and the reliability of the equipment cost. The following are the reliable approaches which are considered in the factorial method.

Hand method

Hand developed certain approximation methods for quick estimating of capital investment cost. He has gathered reliable information based on different processing plants with various sizes and production types. He multiplied the purchase equipment cost with a factor value (*Table 14*) based on the processing plant type to achieve the fixed capital investment. His mentioned factors will cover the additional cost of instrumentation, piping, insulation, and electrical cost along with the equipment cost but the contingency factor is not included. The Hand method has a tendency to produce high results.

Table 14: Hand factor for cost estimation

Equipment type	Factor
Fractionating columns	4
Pressure vessels	4
Compressors	2.5
Heat exchangers	3.5
Pumps	4
Fired heaters	2
Instruments	4
Miscellaneous equipment	2.5

Wroth method

Wroth provided his approximation factor for more detailed cost estimation. His factor covers the additional cost which is not mentioned by the Hand approach. It includes painting, foundations, structures, overhead and supervision, and engineering.

Table 15: Wroth Factor for cost estimation

Equipment type	Factor
Blender	2
Compressors	2
Blowers and fans	2.5
Centrifuge (process)	2
Ejectors	2.5
Furnaces	2
Heat exchangers	4.8
Instruments	4.1
Motors, electric	3.5
Pumps (Positive displacement)	5
Refrigeration	2.5
Process Tank	4.1
Storage Tank	3.5
Towers	4

Equipment cost

The equipment cost information in the production of FPH is given below, the equipment cost is taken from reliable product manufacturing sites based on our production capacity. Important equipment costs in concentration and drying stages are validated with relevant literatures who had performed study on economic analysis and are agreed with the supervisors.

Table 16: Equipment cost details

Equipment Name	Initial value (USD)	Hand & Wroth Factors	Final Equipment Cost (USD)	Final Equipment Cost (NOK)
Crusher	120000	2.5	300000	2700000
Tricantor	180000	2.5	450000	4050000
Hydrolysis, Sterilization & other tanks	456000	4	1824000	16416000
Heat exchangers	200000	3.5	700000	6300000
Membrane filter setup unit	90000	2.5	225000	2025000
Pumps and Motors	100000	4	400000	3600000
Miscellaneous equipment	200000	2.5	500000	4500000
Sensors, and other control devices (Multiplied by Factor 1.25 times)				
Spray dryer	280000	2.5	700000	6300000
Drum dryer	220000	2.5	550000	4950000
Vaccum freeze dryer	480000	2.5	1200000	10800000
Freeze concentrator	650000	2.5	1625000	14625000
Three stage evaporators	500000	2.5	1250000	11250000
Mechanical vapor recompression	400000	2.5	1000000	9000000
Engineering cost (Considered 10%)				
Final contingency cost (8%)				

The GEA economic analysis calculation has freeze concentration unit price of 1 million Euros for a dewatering capacity of 400 kg/h, (Beek et al., 2018). These values are taken as a reference for freeze concentration and amplified based on our production capacity.

Also, efforts have been taken to contact directly with the sales manager of Sulzer industry in knowing the updated equipment price for freeze concentration. Contact was made with NUAS Technology AS, in determining the hydrolysates production facility cost and our estimated values were very close. The cost estimated above is based on the available initial data, however, it can vary based on various considerations. Factors like location are a major influencing factor, for example, the same equipment that can cost 4 to 5 times cheaper if it is manufactured in China or India than in Germany or Switzerland. However, reliability, automation and service requirement are important factors which can vary the cost of the same equipment. Investors should select carefully and decide on a balance between cost and quality.

4.11.2 Depreciation cost

It is defined as the decrease or reduction in the value of a property over its period of use in a specified time. The fixed assets like buildings, equipment, structures, machinery etc will lose their value over a period. Hence, the depreciation cost of a property or an asset is used to find its value after a certain period 'n'.

Salvage value

The salvage value is defined as the total value of a property which is left at its end of life. After the end of the life of equipment, the assets will be sold for a lower value which is considered as salvage or remaining value.

Depreciation methods

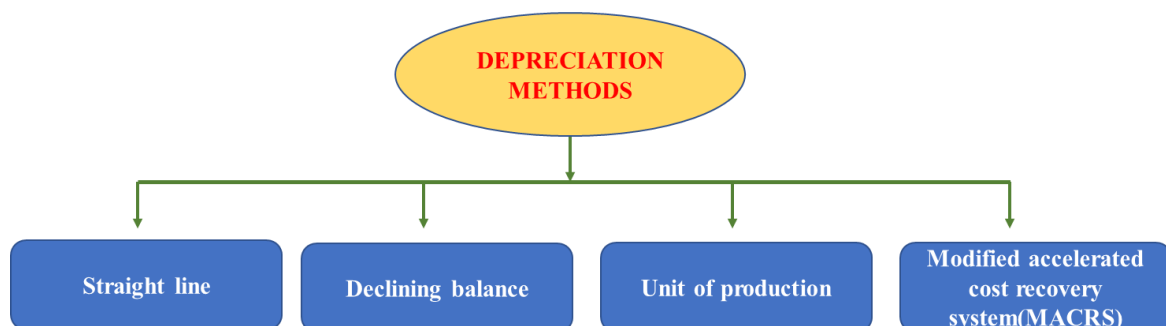


Figure 26: Types of depreciation

Straight line method

It is one of the most widely used approaches in the industry. In this method, the cost of the property is divided and distributed uniformly over its period lifespan.

The annual depreciation cost is given as below,

$$D = \frac{I - S}{n} \quad (4.56)$$

Where D represents the depreciation value, I is the investment cost, S is the salvage value and n is the number of years of a lifetime.

If the salvage value of the asset is not known, it is usually not considered in determining the depreciation of a property. Then the equation becomes,

$$D = \frac{I}{n} \quad (4.57)$$

For our estimation, we have taken the salvage value equal to 5% of the capital cost of the assets.

4.11.3 Profitability analysis

Pay-Back time determination

In this method, the net initial capital amount is divided by the annual average cash flow.

$$\text{Pay - back time} = \frac{\text{Total investment}}{\text{Annual average cash flow}} \quad (4.58)$$

Return on investment

Another method of determining the profitability analysis is to determine the return on investment.

It is given as below,

$$ROI = \frac{\text{Annual net profit}}{\text{Total investment}} * 100\% \quad (4.59)$$

There are other methods also available in calculating the profitability analysis. They are the Time value of money and the Net present method. In our analysis, we have used the most common method of payback time determination to estimate the profitability analysis between the process alternatives having concentrated and drying equipment.

Pay-Back time determination equations

Annual costs are calculated as,

$$AC = (IC * AF) + (Energy\ Value * EP) + MC \quad (4.60)$$

Where, AC represents the Annual Costs, IC- Investment Cost, AF- Annuity Factor, EP- Energy Price, MC- Maintenance Costs

Annuity factor (a)

$$a = \frac{r}{(1 - (1 + r)^{-n})} \quad (4.61)$$

Where, r – rate of interest, n- number of years.

Net annual savings (B)

$$B = \{(E_1 * EP) - (E_2 * EP)\} + (MC_1 - MC_2) \quad (4.62)$$

Where, E₁ represents the energy value in kWh of process 1, E₂ represents the energy value in kWh of process 2 alternatives. MC₁ represents the maintenance cost of process 1 and MC₂ represents the maintenance cost of alternative process 2.

Additional investment costs: (I_o)

$$I_o = (I_2 - I_1) \quad (4.63)$$

Where, I₂ represents the total investment cost of alternative process 2 and I₁ represents the investment cost of alternative process 2.

Payback time calculation

$$PB = \frac{I_o}{B} \quad (4.64)$$

The initialization parameters used in the calculations are listed below in *Table 17*,

Table 17: Parameters for economic analysis

Parameters	Values
Rate of Interest (R)	5 %
Number of years (n)	20
Operating hours	5000
Energy Price for the Manufacturing industry	0.36 NOK/kWh

4.11.4 Sensitivity analysis

The sensitivity analysis is used to analyse the influence of different parameters and their effect on the project. It is a simple tool used to identify the important parameters which are having a significant influence. The influence of technical and economic parameters in determining the profitability of the system is studied. Sensitivity analysis is used to predict, how some important values are getting altered when different parameters in the system are modified. In the sensitivity analysis, parameters like investment cost, operating hours, and energy prices are changed, and the payback time is determined.

The cost model's various parameters are adjusted, assuming a certain range of error for each factor in turn. This will indicate how vulnerable the errors of cash flows and economic criteria are in the forecast figures. A sensitivity analysis provides some insight into the degree of risk involved in creating projections about the project's performance.

Statistical techniques for risk analysis

Each parameter is changed individually in a simple evaluation, and the outcome is a qualitative insight into which variables have the greatest effect on project effectiveness. Statistical methods are used in more formal risk analysis to examine the effect of modification of parameters and thus quantitatively determine the range of fluctuation in the economic criteria. This enables the design engineer to estimate the level of certainty with which the selected economic standard can be said to surpass a given threshold.

Projecting the maximum project cost when investment cost changes +25 % to -25 %

The following statistical approach is used to find the maximum project estimation when the variation occurs. The estimation values are expressed in the upper value (H), the lower value (L) and the mean value (HL). From the ranges of estimation, the upper and lower values are found. By knowing the estimated cost of ISBL, the mean value and standard deviation are calculated. It is then adjusted for the engineering cost. Finally, the contingency cost is calculated from the above-computed values.

Mean value, x

$$X = \frac{(H + 2ML + L)}{4} \quad (4.65)$$

Standard deviation, S_x

$$S_x = \frac{(H - L)}{2.65} \quad (4.66)$$

Considering engineering cost,

$$X_{Total} = 1.1 * X \quad (4.67)$$

$$S_{x,Total} = \sqrt{(1.1 * S_x)^2} \quad (4.68)$$

Accounting contingency charges, the final cost of the project when 98% confidence level is taken it will be less than,

$$X_{Total} + 2.05 * S_{x,Total} \quad (4.69)$$

Chapter 5: Results

Energy analysis in the entire process chain in the production of the FPH was briefly explained and presented. First, the results of freeze concentration, two-stage process TWICE, and freezing into blocks were presented with the different drying processes. Then, the other concentration process MSE, and MVR are provided with drying combinations. Finally, the results from system modelling and economic analysis are presented in different subchapters.

5.1 Concentration using freeze concentration

The freeze concentration method reduces the overall energy demands in the process chain and has a significant energy reduction. The heat load to be removed from the hydrolysates to concentrate 30% of hydrolysates with a mass flow rate of 1841 kg/h from the initial feed temperature of +4 °C to the final freezing temperature of -3° C is equivalent to 135.5 kW (~135 kW). The energy required to freeze 1 kg of water is found to be 265 kJ/kg. The results are in accordance with studies stated by [Miyawaki et al., \(2005\)](#). Using numerical models as described in the methods, the initial temperature at which nucleation of ice occurs was calculated to be -0.6 °C.

During the concentration process, water in the hydrolysates freezes and forms ice, which is removed in the wash column by providing sufficient heat to melt the ice. The fraction of ice removed from the feed hydrolysates was equivalent to 76.7%. The heat load to melt 1411 kg/h of ice formed was calculated to be 137 kW, by considering sensible heat above and below freezing point and latent heat when the phase change occurs. The amount of ice to be melted determines the necessary heat load. For energy calculation, 178 kW is taken by considering some additional heat load. Before freeze concentration the hydrolysates mixture is cooled to 4 °C from 90 °C and the heat to be removed is shown in the scheme. Here, the specific heat capacity is calculated as a function of temperature.

In freeze concentration, apart from the energy required for freezing the hydrolysates and melting the ice, the refrigeration work must be considered. The refrigeration work was calculated to be 30.4 kW with an evaporation temperature of -40 °C and a condenser temperature of 0 °C. The Carnot COP is 5.8. In the scheme presented below in *Figure 27*, the heat load for thawing the product, heating to hydrolysis temperature and then to sterilization temperature is provided.

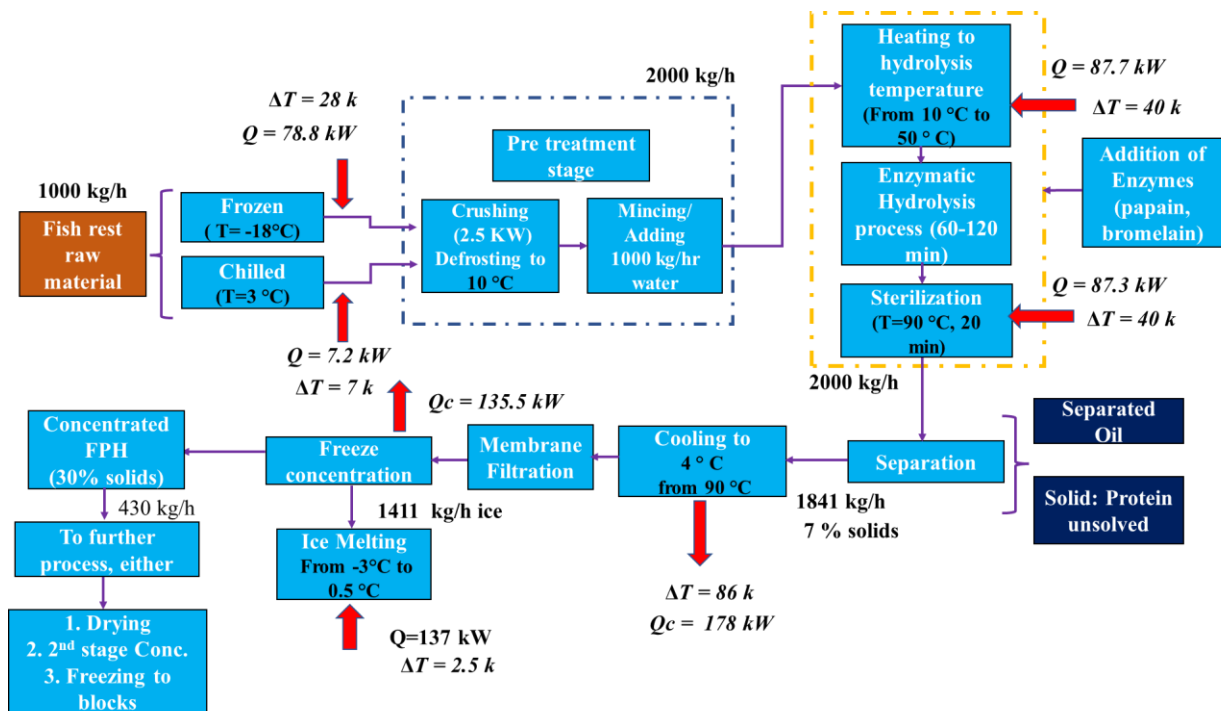


Figure 27: Process flow diagram with freeze concentrator

The freeze concentration method leads to reduced energy demands, here the main principle is the crystallization of liquids. Generally, the energy required to crystallize the liquids is lower when comparing the energy for vaporizing the liquid, as the latent energy to change from liquid to gas phase is higher than the latent energy to phase change from liquid to solid. The high-temperature operation can damage the heat-sensitive products. Hence, such products can be dehydrated using this method without compromising the quality.

The influence of concentration level in the freezing point depression was calculated and is given below in *Table 18*. It is observed from the results (*Figure 28*), that higher the concentration level of solids higher the freezing point of the solutions, this is due to the presence of reduced water content. Generally, the freezing temperature of solids such as proteins, fats etc is much lower than water and hence the freezing point gets decreases with increased concentration.

Table 18: Concentration vs Freezing point

Concentrations (%)	Freezing point (°C)	Concentrations (%)	Freezing point (°C)
5	-0.4	35	-4.2
10	-0.8	40	-5.2
15	-1.3	45	-6.5
20	-1.9	50	-8.0
25	-2.6	55	-10.0
30	-3.3	60	-12.4

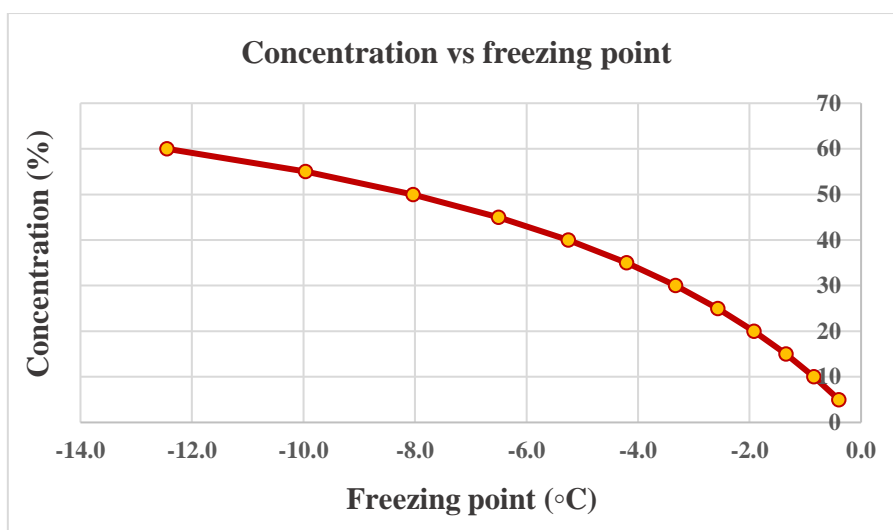


Figure 28: Concentration vs Freezing point plot

5.1.1 Two-stage freeze concentration process and block freezing

The conventional freeze concentration technology with the suspension method can concentrate the hydrolysates up to 30% solids. This is due to the limitation that at higher concentrations the viscosity increases with the freezing point which is experimented at NTNU laboratory ([viscosity results](#)). Also, the removal of ice from the wash column is difficult. The engineers from Sulzer industry investigated TWICE technology by combining the static layer method to concentrate juices to 60% and coffee extract up to 40% conc, ([Dett et al., 2020](#)), and observed that at low temperature processing the color, aroma, and nutritional values have remained. TWICE is a two-stage freeze concentration process to concentrate the liquid to higher concentration. The process works by combining the principle of suspension crystallization and static layer crystallization. The basic scheme is given below in *Figure 29*,

The working principle of TWICE technology is that in the layer crystallization method, a homogeneous crystalline layer forms gently on a chilled heat-transfer surface. Vertical plates are utilized internally, which are chilled or heated by circulating the refrigerant. The temperature gradient between the liquid and solid phases is the primary driver for crystallization. Slow cooling results, ice crystal structure forming uniformly on the plates' outer surface. The concentrated liquid is removed from the crystallizer when the necessary fraction has been crystallized. A single-stage represents the feeding of hydrolysates into the crystallizer, crystallization to occur, pumping the concentrate and finally melting and discharging of ice.

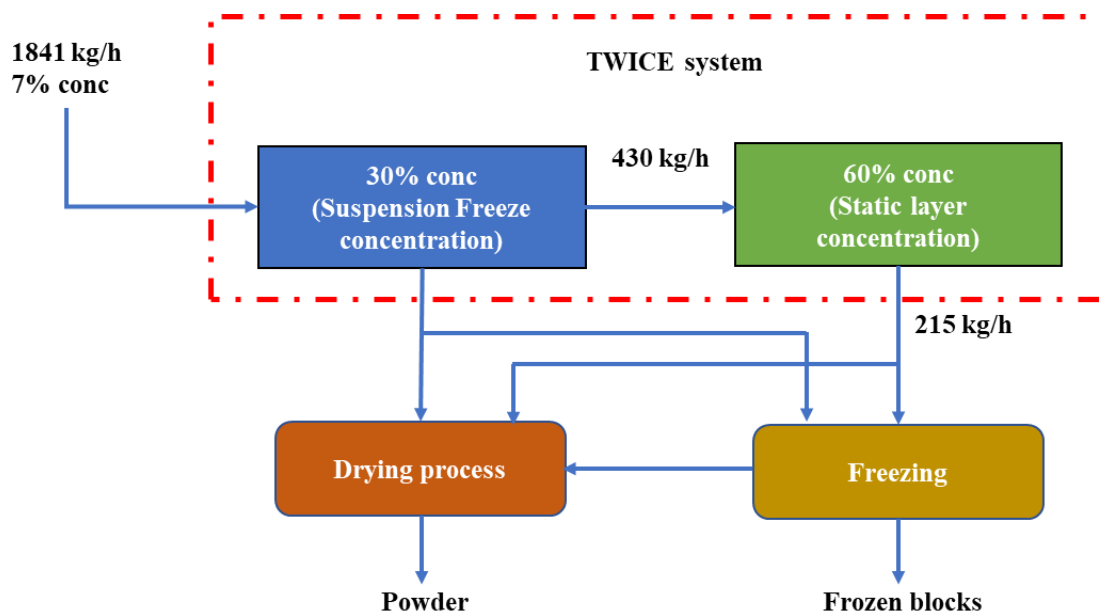


Figure 29: Processes after freeze concentration

The outlet mass flow rate from 1st stage of freeze concentration (FC) was calculated to be 430 kg/h which is processed in the 2nd stage of FC. The solution inlet temperature was -1 °C. The water content X_w is 70% since the solids concentration from 1st stage process was 30%. The corresponding freezing point and freezing point depression were computed. During the process, the hydrolysates mixtures are concentrated to maximum concentration assuming 60%, and the solution temperature is maintained at a final freezing temperature of -5 °C. The freezing load is calculated at around 9.4 kW; the water removed during the process is estimated at the rate of 215 kg/h. The heat load required during the melting of the ice in the wash column is estimated to be ~21 kW. The refrigeration load and Carnot work can also be calculated similarly to the earlier method. The results are as follows,

Table 19: TWICE- Two stages FC process data

Inlet mass flow rate (kg/h)	X_w Initial	Freezing point (°C)	Freezing load (kW)	Amount of ice removed (kg/h)	Melting load of ice (kW)
430	0.7	-3.3	9.4	215.3	20.8

The feasibility of concentrating up to 60% of the hydrolysates mixture is not validated with the freeze concentration process, but the reference has been taken with the Sulzer industry in concentrating the juice products to 60%. Hence, the present study has been performed, to identify the possible energy demands if the two-stage process was involved. Developments are still ongoing in improving the concentration level during the freeze concentration process to 60%. The TWICE technology is suitable for highly viscous products and non-aqueous substances. The organoleptic properties and nutritional value of the products are preserved even at higher concentrations in the freeze concentration process, unlike the evaporation techniques.

Freezing by plate freezers

Concentrated hydrolysates are further frozen into frozen blocks, or they can also be dried using driers based on application and requirements. The advantages of concentrates are, that they can be reconstituted easily when adding water. Hence, the frozen form of hydrolysate blocks can be processed again based on application requirements with no difficulties. Other advantages are that it can be shipped and stored for the long term since the frozen concentrate is more stable. Hence in this study, the block freezing of hydrolysates was also investigated and the energy requirement was calculated.

In onboard vessels, the concentration step using freeze concentration (FC) techniques can be installed and fish protein hydrolysates can be processed. After the freeze concentration process, the conc. hydrolysates can be frozen into blocks using plate freezers. The corresponding freezing load is calculated in the below table. Two cases were studied. If the two-stage concentration was not performed, the concentration of 30% solids after 1st stage FC can be directly frozen into blocks. Next, the increased concentration of 60%, when processed at a two-stage FC process and then frozen into blocks was also studied. The final freezing temperature was set at 20 °C. The freezing load was calculated by calculating the sensible heat-enthalpy difference above the freezing temperature of the solution to the initial temperature and enthalpy below the freezing point to the final freezing temperature and the latent heat of phase change.

It is observed that the freezing load when freezing 30% concentrated hydrolysates is higher than the 60% concentrated solution. This is because the mass flow rate is an important factor along with the enthalpy change in freezing load estimation. Most of the water is removed when the hydrolysates are concentrated to the maximum level, hence the freezing load when processing 60% conc. hydrolysates are lower. The number of plate freezers requirements in an onboard fishing vessel is determined by the plate freezers capacity installed. For an average freezing capacity of 250 kg/h one or two plate freezers can be needed when freezing the hydrolysates mixture. The

plank equation is used to determine the freezing time of the blocks by knowing the desired block sizes and its thermal properties. Downstream of the concentration process, an accumulator tank can be installed before the plate freezers for providing temporary storage owing to match the loading and unloading of the hydrolysates from the freezers. The freezing load requirements for the freeze concentration process at different concentration levels is given below (*Table 20*),

Table 20: Freezing load requirements for FC process with different conc,

Initial concentration (%)	Intel temperature (°C)	Inlet mass flow (kg/h)	X_w_Initial	Freezing point (°C)	Freezing load (kW)
30	-1	430	0.7	-3.3	25.2
60	-3	214.7	0.4	-12.5	4

Followed this, the FPH can be further dried using any of the drying methods and the energy values must be included when determining the overall energy demands,

5.1.2 Freeze concentration (30%) with different drying methods

Generally, after the freeze concentration (FC) process, the water in the hydrolysates is removed using different drying processes. Drying consumes more energy and the energy requirement for each drying is given below in *Table 21*. The flow rate of FPH after the freeze concentrator was ~ 430 kg/h with a concentration of 30% and was further dried to 131.5 kg/h with 98% solids by drying methods. The amount of water evaporated was 298 kg/h. The inlet temperature of hydrolysates during the drying process was around -1°C. The energy values and heat load requirements are shown below in *Figure 30*,

The 3D modelled image of the process with freeze concentration and spray drying process is provided in [subchapter at 5.8](#) in *Figure 40*,

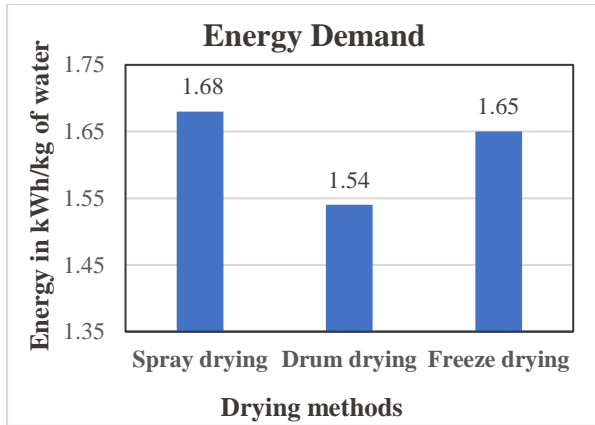


Figure 30: a) Energy demands for different process

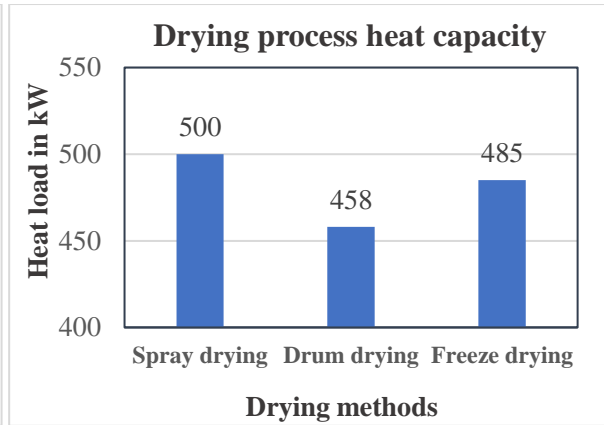


Figure 30: b) Drying process heat capacity requirement

Figure 30: Energy demands & Heating capacity in process with freeze concentrator

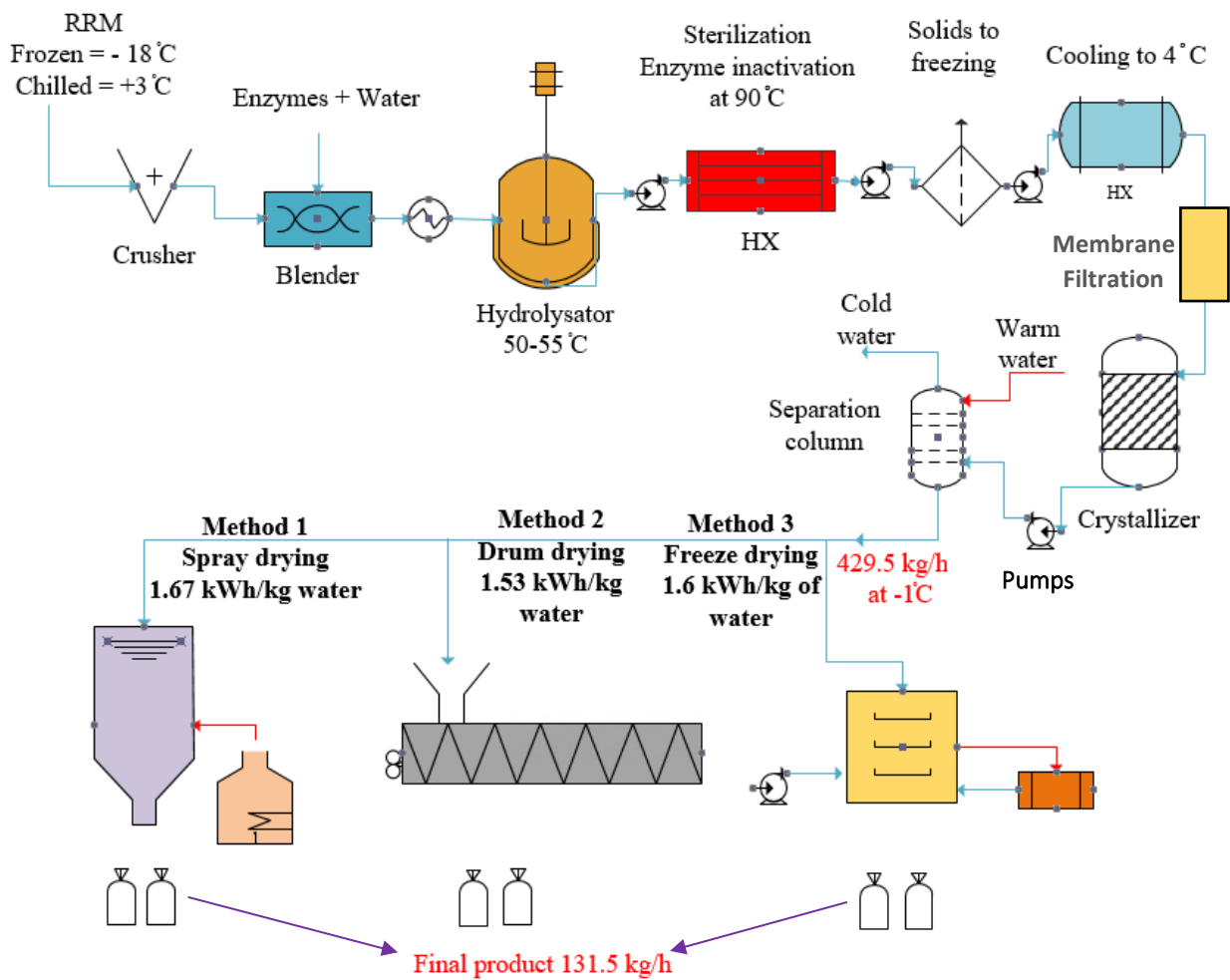


Figure 31: Process flow diagram of freeze concentrator with drying methods

From the above results, it is observed that the drying process consumes high energy between 1.5-1.67 kWh/kg of water removal. The obtained result during the calculation is well in the range when compared with Baker and McKenzie (2005), calculated 0.8 to 5.5 kWh/kg of water removal. The high energy required is due to the energy needed in raising the feed temperature to the boiling point temperature and the latent energy for changing the liquid phase to the vapor phase. The latent energy part was the major energy demand during the drying process. In freeze-drying, the sublimation process takes a significant amount of energy to change the solid to vapor phase without the liquid phase. Process calculation is given in [Appendix-2](#).

This energy is the heating energy that transforms the ice which is at low temperature inside the vacuum chamber into vapor. The cooling load is provided by the refrigeration capacity. Additionally, the feed absorbs 213 kJ/kg ~ 0.06 kWh/kg of energy when freezing to -20°C. The corresponding refrigeration work and Carnot COP of the cycle are calculated and given in the table below.

Table 21: Energy and work requirement in freeze concentration with drying methods.

TYPE OF PROCESS		ENERGY REQUIRED		ADDITIONAL WORK
		HEATING LOAD	COOLING/ FREEZING LOADS	
Concentration by freeze concentration method		$Q_h = 137 \text{ kW}$	$Q_c = 135.5 \text{ kW}$	$W_{car} = 30.4 \text{ kW}$
				$COP = 5.8$
Drying	Method 1: Spray drying	$E = 1.68 \text{ kWh/Kg}$ of H_2O		
		$Q = 500 \text{ kW}$		
	Method 2: Drum drying	$E = 1.54 \text{ kWh/Kg}$ of H_2O		
		$Q = 458 \text{ kW}$		
	Method 3: Freeze drying	$E_h = 0.79$ kWh/kg of H_2O	$E_c = 0.8 \text{ kWh/kg}$ of H_2O	$W_{car} = 85.41 \text{ kW}$, $COP = 2.78$
		$Q = 232.73 \text{ kW}$	$Q_c = 235.8 \text{ kW}$	Vacuum pump, $W_p = 85.4 \text{ kW}$

Freeze concentration energy requirement,

The overall energy demands for different process with freeze concentration is given below in *Table 22*. As discussed earlier, based on the type of final requirement and application, the different processes can be carried out after freeze concentration (FC). The concentrate can be directly dried into powders in **case 1** or can be frozen into blocks if it is an onboard processing unit and then dried into a powder in **case 2**.

TWICE represents the two-stage FC process used to concentrate the hydrolysates to 60%. The results are also given below, as **case 3** illustrates the production process with two-stage FC followed by spray drying and **case 4** represents the same process but when freezing and thawing was included. If the freezing blocks do not require a drying procedure after 30 % or 60 % and may be used in blocks, the energy for drying is removed from the *Table 22*. The volume flow rate is a greater factor which largely influences the energy demands in cases 3 and 4. Since the concentration after freeze concentration is higher (60%) more moisture is removed during the process itself in the form of ice and reduced volume of hydrolysates are dried in a spray dryer. Hence the energy demands in the spray drying process are relatively lower.

Table 22: Energy demands for different cases with the freeze concentration process

Case-1 (kWh)	Case-2 (kWh)	Case-3 (kWh)	Case-4 (kWh)
1245.3	1320	968	996

Case-1: Energy requirement for production process with 30% conc with FC and spray drying

Case-2: Energy requirement for production process with 30% conc with FC then freezing and spray drying

Case-3: Energy requirement for production process with 60% conc with FC and spray drying

Case-4: Energy requirement for production process with 60% conc with FC then freezing and spray drying

5.2 Concentration by multistage evaporation (three effects).

In the next alternative in the concentration step, the multistage evaporation results were presented. Hydrolysates are concentrated at each stage and flows out of the final stage with a concentration of 50%. Initially, the hydrolysates after the separation process flow at the rate of 1841 kg/h into the

multistage evaporator with three effects. The concentrated hydrolysates then flow at the rate of 257.7 kg/h and the amount of vapor removed is calculated using mass balance at 1583 kg/h.

In the multistage evaporation process, the calculation was performed for two cases.

Case 1: The hydrolysates flow into the evaporator has a temperature of 90°C.

Case 2: The hydrolysates are stored to storage temperature (~ 0 °C) and then concentrated further by three-stage evaporation.

The heat load and the energy demand during the process are given below in *Table 23*. During the process, the cooling load for condensing the vapor at the last effect should be taken into consideration. It is estimated that the vapor evaporated at the last stage was 527.6 kg/h, calculated from the total evaporating vapor with the concentrating level at each stage. The condenser is maintained at a lower temperature of 30 °C with a pressure of 0.2 bar.

Table 23: Three-stage evaporator energy requirement

	Heat load (kW)	Energy required to remove one kg of water (kJ/kg of water)	Cooling load for condensing the vapor at the last stage (kW)
Case 1	338	768 (0.21 kWh/kg)	364
Case 2	399	906 (0.25 kWh/kg)	

5.2.1 Three stage evaporation drying combinations

The hydrolysates are further dried using any one of the drying methods like spray drying, drum drying and vacuum freeze-drying, and the results are tabulated below in *Table 24*. The hydrolysate after three-stage evaporation flows at the rate of ~ 258 kg/h. Generally, the hydrolysates are cooled to storage temperature. The calculation for the drying process was taken with the initial storage temperature (0°C). The amount of vapor evaporated when concentrating to 98% was 126.2 kg/h. The heat requirement for evaporating 126.2 kg/h of vapor is given in below *Figure 32*. The 3D modelled image of the process with three stage evaporator and spray drying process is provided in [subchapter 5.8](#) in *Figure 38*. The calculation part is provided in [Appendix-3](#).

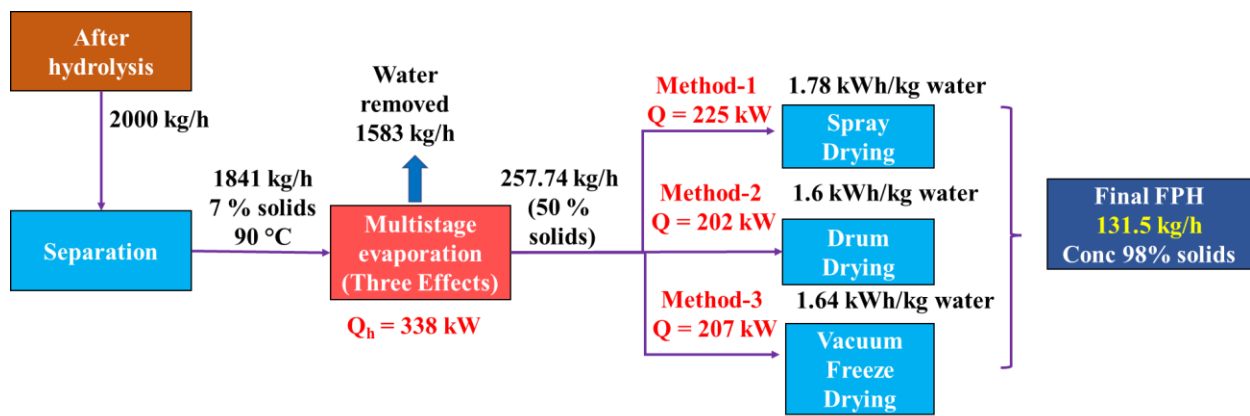


Figure 32: Process flow diagram in Three-stage evaporator

The thermodynamic principle of the multi-effect evaporator is that it consists of a series of reboilers that operates at different pressures; the water evaporated from the previous effect is condensed and used as a heat source in the next stage. When the water present in the hydrolysate is evaporated, the substances is concentrated. The heat absorption of the hydrolysates depends mainly on the heating temperature of vapor from previous stages and the heat capacity value of the solids. The energy demands and the heating capacity requirements during the process scheme with three effect evaporator is provided in below table,

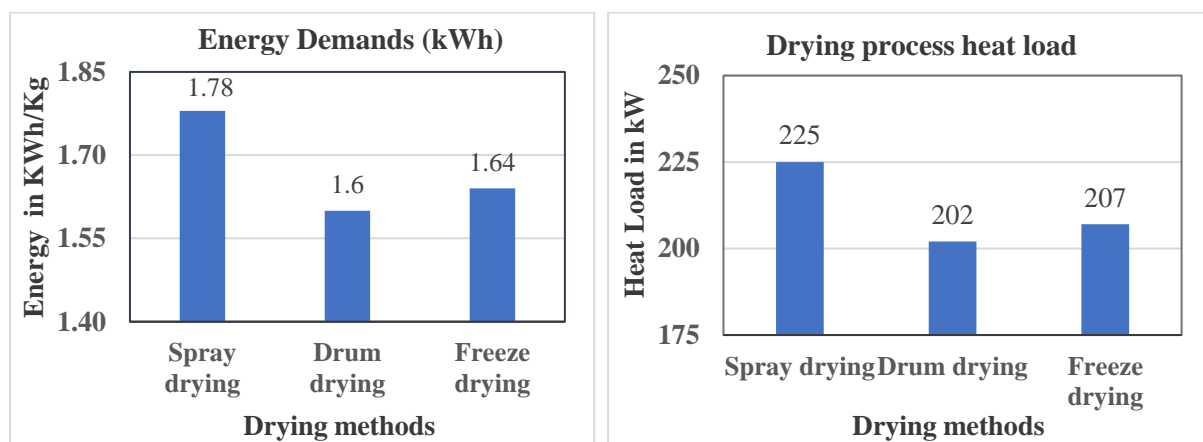


Figure 33: a) Energy demands for different drying process

Figure 33: b) Drying process heat capacity requirement

Figure 33: Energy demands and heating capacity required in process with MSE

The three-effect evaporator operates by decreasing pressure levels along with the flow of vapor. Generally, the condensate at each stage is not utilized if is at a lower temperature. However, the condensate has a sufficient amount of sensible heat when leaving the vapor chest of the evaporator and this can be utilized.

Table 24: Energy and work requirement in three-stage evaporators with drying methods.

PROCESS		ENERGY REQUIRED		ADDITIONAL WORK
		HEAT LOAD	COOLING/ FREEZING LOAD	
Drying Alternatives	Method 1: Spray drying	E = 2 kWh/kg of H ₂ O		
		Q= 252.4 kW		
	Method 2: Drum drying	E = 1.6 kWh/kg of H ₂ O		
		Q= 202 kW		
	Method 3: Freeze drying	E _h = 0.79 kWh/kg of H ₂ O	E _c = 0.8 kWh/Kg of water	W _{car} = 36.3 kW, COP= 2.78
		Q= 99.5 kW	Q= 101 kW	Vacuum pump, W _p = 50.6 kW

In the MSE system, when the stream passes from a higher temperature stage to a lower temperature stage, it generates vapor inside the effect owing to the flashing. By flashing, the sensible heat can be extracted and utilized which produces the low-pressure vapor. Hence, the vapor can be reused as a heating source in the next effect and the steam economy is improved. In the energy reduction scheme (ERS), the condensate from the evaporator is utilized to preheat the incoming liquid with the use of a counter-current heat exchanger.

During the process, parameters like boiling point rise, heat losses, product physical property, overall heat transfer coefficient (U), heat transfer area, composition and feed flow rate are important. To increase the temperature, vapor re-heaters are provided outside each effect. In the flow process, the concentrations are fixed to a final concentration of up to 50%. The vapor in the last effect enters the condenser.

When comparing the spray drying process and drum drying process between freeze concentration and multistage evaporation, the energy required to evaporate one kg of water is slightly higher in the process where evaporation is used. This is due to, the solids content in the hydrolysates after

multistage evaporation being concentrated to 50 % than in freeze concentrator (30%). Hence, the additional heat is absorbed by the increased solids in the drying process.

5.3 Mechanical vapor recompression evaporation (MVR)

The energy demand during the MVR process is the amount of work input that is provided to increase the pressure of the vapor for sufficient heat transfer. The heat energy from the evaporated vapor is reutilized and this method offers significant energy savings. In this process, the hydrolysates are concentrated at 50% and the amount of vapor evaporated is 1583 kg/h.

The work input of the cycle operating at a higher pressure of 1.5 bar from lower pressure of 1 bar was calculated to be 103.1 kJ/kg. The heating capacity of the system Q_c is 2310.7 kJ/kg. According to experiments, the compression work input in the MVR regeneration system is estimated at 130.7 kJ/kg of water removal (Zhang et al., 2021), and our obtained results are in accordance with it.

The compressor removes the vapor from the evaporator and increases the pressure. Energy for evaporation is returned to the system. The pressure difference of the compressor is small resulting in low energy input. Hence the COP of the system is relatively very high around 22. Neave et al., (2002), also mentioned, that in an MVR system a COP of 10–30 may usually be reached.

The process can be operated at varying pressure, this can be seen as a reference in the Ph diagram of the water phase diagram. Higher the pressure, higher the heating capacity but the energy or the work input to the system is also higher which overall decreases the COP of the system which is represented below in *Figure 35*.

Table 25: Energy requirement in mechanical vapor recompression (MVR)

Operating High Pressure (P_c)	Cycle COP	Heating capacity Q_c in kJ/kg	Minimum energy requirement in kJ/kg of water	Heat load in kW
1.5 bar	22.4	2310.7	103	45.3
2 bar	12.9	2352.8	182.6	80.3

In the MVR process, the heat energy is added to the low-pressure vapor by providing the work input. This increases the vapor temperature; pressure and it can be used to do useful work. The compressed vapor can be used to heat the feed to produce the low-pressure vapor. In this process only during starting, steam was consumed and further, no external steam input was required.

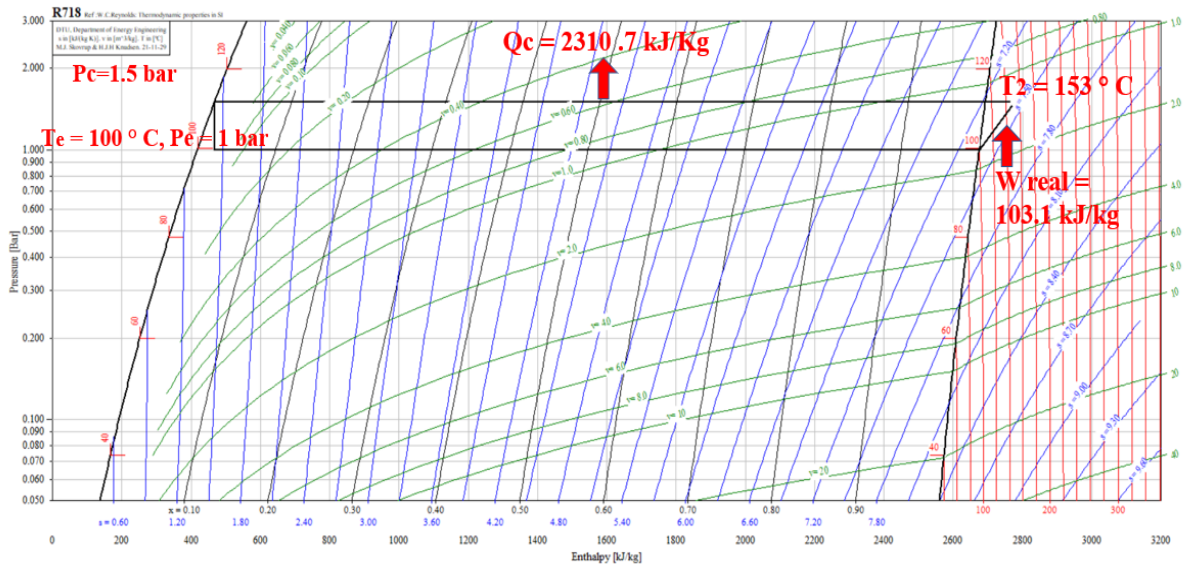


Figure 34: Ph diagram of water with condensing pressure 1.5 bar

The regeneration efficiency of the MVR system is less than one. This is due to the fact for an ideal isothermal compression process it is difficult to recover the heat energy since it results in exergy destruction. Instead of compressors, the heavy-duty fan was designed and also used since the pressure lift was not so high.

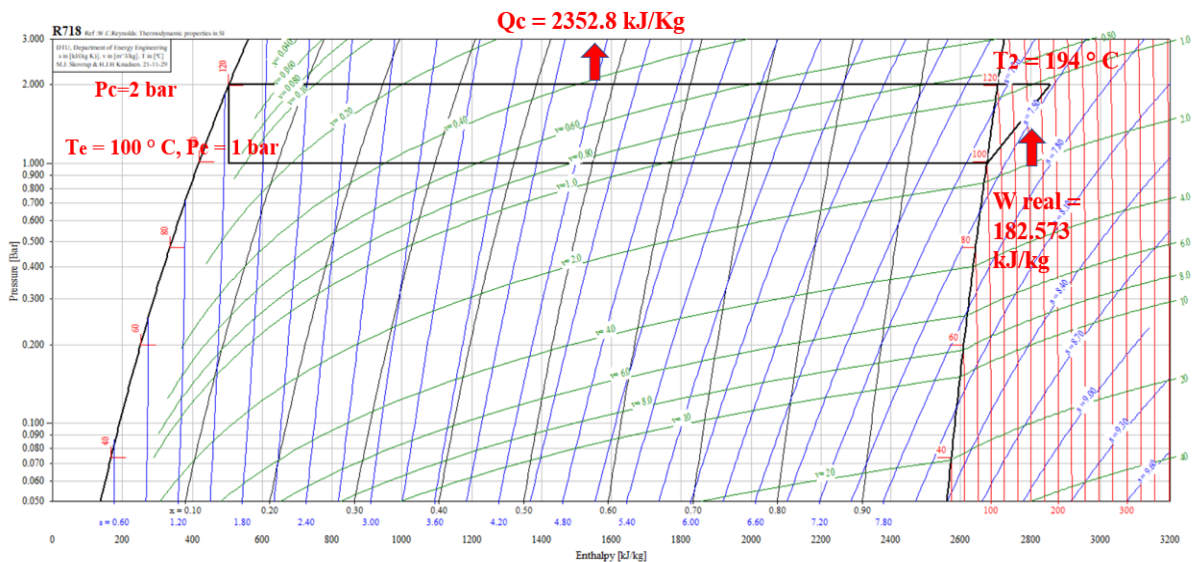


Figure 35: Ph diagram of water with condensing pressure 2 bar

The energy demands during the drying process after MVR process remain the same as similar in MSE process, because the concentration level, and exit mass flow rate are the same. The 3D modelled image of the process with MVR and rotary drum drying process is provided in [subchapter 5.8](#) in [Figure 39](#).

5.4 Process scheme with direct drying

The study was also extended to investigate the energy demands when direct drying was performed. Although, it is well known that energy demands in direct drying will be very high. This analysis was performed to have a comparative study with other processes. After separation, the hydrolysates flow of 1841 kg/h was cooled to a storage temperature of 0°C from 90°C. The heat load to be removed during the process was considered to be 186.4 kW. Further, the drying process calculation has been performed and the results are given below in [Table 26](#),

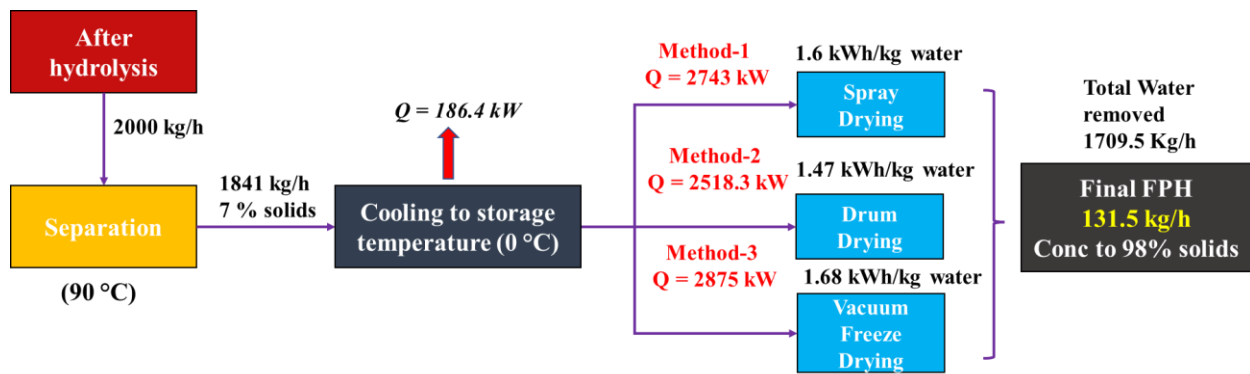


Figure 36: Schematic process flow in direct drying method

From the table, it is observed that 1.6 kWh is essential to remove per kg of water in the spray drying process, and drum drying consumes a slightly lower value when compared with the vacuum freeze-drying and spray drying. However, the value presented is the minimum energy requirement, the actual energy requirement can be higher, and it depends on the process design. In the freeze-drying, apart from the values presented in the table, the energy required to freeze the product from storage temperature to -20°C is also accounted and is equivalent to 338 kJ/kg (0.09 kWh/kg). Since the initial freezing point of the feed is lower than zero, the calculation was performed considering sensible heat and latent heat.

Table 26: Energy requirement in the direct drying process.

PROCESS		ENERGY REQUIRED		ADDITIONAL WORK
		HEATING ENERGY	COOLING/FREEZING ENERGY	
Drying Alternatives	Method 1: Spray drying	E = 1.6 kWh/kg of H ₂ O		
		Q= 2743 kW		
	Method 2: Drum drying	E = 1.47 kWh/kg of H ₂ O		
		Q= 2518.3 kW		
	Method 3: Freeze drying	E _h = 0.79 kWh/kg of H ₂ O	E _c = 0.8 kWh/kg of H ₂ O	W _{car} = 490 kW, COP= 2.78
				Vacuum pump, W _p = 367.5 kW

The above *Figure 36* represents the heat requirement in kW when evaporating 1709.5 kg/h of water. Due to the high mass flow rate to evaporate, the Carnot work and vacuum pump work also increased. This data is very clear, as direct drying after separation results in higher energy demands and hence concentrating stages before drying should be done to reduce the overall energy needs.

5.5 Heat pump assisted drying

When high-temperature heat pumps are integrated into the drying process, it increases the energy efficiency of the process. In the spray dryer, the exhaust air has sufficient heat energy, which is usually not used, however, it can be used as a source of heat for the heat pump. The air is heated at the condenser side, hence lowering the amount of energy that the heaters in the driers are using. The high temperatures heat pumps are used to heat the air to a temperature up to ~120°C. Using a high-temperature heat pump, with natural refrigerants like ammonia or CO₂, the energy recovery can be achieved to sufficiently heat the air to a higher temperature, this reduces the energy needs for heating the air.

In spray and drum drying, a significant amount of the energy was consumed by heating the drying air to the desired high temperature. Hence, the calculation was performed to understand the

influence of inlet air temperature on the energy demands in the spray dryer. The heat transfer is very inefficient by heating the air from 15°C to 200°C, hence the temperature lift must be reduced.

The energy variation with respect to the inlet air temperature for the spray dryer is given below. It is observed in *Figure 37*. The inlet air temperature plays a significant role in energy demands. When the temperature of the air was increased from 10°C to 110°C, the energy required to evaporate per kg of water is reduced to 0.84 kWh/kg ~ 3020 kJ/kg, which is a 50% reduction in energy demands in the spray drying process. Few researchers even observed energy savings upto 60%. By using a heat pump, the energy recovery can be achieved to sufficiently heat the air to a higher temperature, this reduces the energy needed for heating the air. Waste heat recovery can be an efficient option to heat the drying air which reduces the overall energy demands.

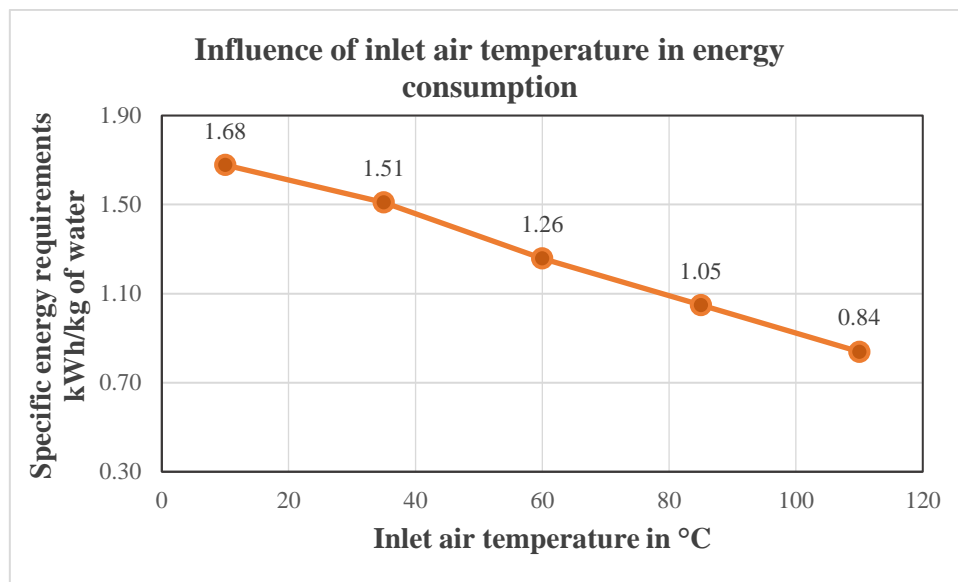


Figure 37: Spray dryer energy demands against inlet air temperature

Heat pump assisted drying consumes less energy, since the heat pump cycle has higher COP, the coefficient of performance of the heat pump system is described as the ratio of condenser capacity to the work input of the cycle. If the COP of the system is 3 it means for every 1 kW of work input 3 kW of heat output is generated.

The open-loop drying cycle is less efficient as the heat from exit air after drying has been rejected into the atmosphere. Heat recovery provides a more efficient way of utilizing the excess waste heat and this improves the system performance. The work input to the cycle is reduced. Hence, the closed-loop drying cycle is an efficient system that can be used more efficiently for drying the products at the higher temperature. *Table 27* shows the SMER value between hot air drying and

heat pump assisted drying. The value remains higher for heat pump (HP) drying as the exit air heat is reused which overall increases the system effectiveness.

Table 27: SMER values for Heat pump drying and other methods

	Direct hot air drying	Vacuum freeze-drying	Heat pump Drying
Specific Moisture Extraction Rate (SMER - kg H₂O/kWh)	0.12-1.28	0.72-1.2	1-4
Investment cost	Lower	Higher	Moderate
Operating cost	Higher	Very high	Lower

5.6: Summary of overall energy demands

This subchapter summarizes the total energy requirement when concentrating 1000 kg/h of the rest raw material to 131.5 kg/h (98% solids). The energy requirement for each process was calculated separately and is provided in [Appendix-4](#). and the final results are provided below (*Table 28*). The results are based on the summary of concentrating process and drying process. Individual process energy demands are explained in respective chapters.

Table 28: Summary of overall energy demands when processing 1 ton RRM (kWh)

Drying method used	Freeze concentration	Three effect evaporators	Mechanical vapor recompression	Direct drying
Spray drying	1245.3	1182	629	3183
Drum drying	1124.3	1158	606	2958
Vacuum freeze-drying	1230	1163	611	3315

From the results above, it is seen that when drying using direct drying methods the process consumes a high amount of energy around 2900-3300 kWh when processing 1000 kg/h of RRM. In direct drying, the energy used for rotary drum dryer is slightly lower than other processes, however, the drying process requires higher energy. Hence, concentrating techniques before the final drying process should be implemented to reduce the energy demands.

When concentrating 30% by freeze concentration and then final drying with drying methods, results in lower energy demands around 1120-1245 kWh which is 60 % energy savings when compared with direct drying methods. 30% concentration level was studied with freeze concentration, when comparing with three effect evaporator (MSE) the FPH was concentrated to 50% and the rest was dried by the drying process, which makes the process fewer energy demands of around 1200 kWh.

Comparing all the above processes, when concentrating using the mechanical vapor recompression (MVR) method and drying using any of the drying processes results in very low energy requirements of 605-630 kWh, when compared with the direct drying this is almost 80% energy saving. Since MVR works on the energy recovery principle. For heat sensitive products, the freeze concentrating process can be widely used, as the process operates at lower temperatures and removes the water. Lower temperature operating process leads to improved process efficiency. Scaling, and corrosion issues are reduced also, the product quality is enhanced.

5.7 Carbon footprints of main electricity generation technologies

Efforts have also been made to identify the process-wise environmental impact category of Global Warming Potential (GWP) based on CO₂ emissions. Energy can be generated from the different processes; the source and process requirements can vary from one technique to another. The electricity generation from most of the common processes and their corresponding CO₂ emission per kWh production is given below in *Table 29*.

The life cycle study includes all the foreground and background processes that are the contributors to environmental impacts. For any production, there are both direct and indirect emissions associated with the process. The life cycle assessment calculates the complete impacts and emissions generated from the process. The industries should follow the government policies and laws in reducing CO₂ emissions. In Norway, since the electricity generation is from hydropower it results in less emission of ~ 6 g CO₂ eq/kWh. However, for the same electricity production, if its source is varied, the corresponding emissions will change. Hydropower based electricity production has the lowest emissions while coal-based electricity production has higher emissions.

Table 29: Carbon footprints of different electricity production technologies

Process	CO ₂ emission (g/CO ₂ eq/kWh)
Wind power	20-35
Solar power	10-80
Hydropower	6
Coal power	930
Natural gas	530
Coal with Carbon Capture & Storage (CCS)	200-240
Gas power with CCS	250
Nuclear power	15-30

Source: TEP4223 Life Cycle Assessment ([Strømman, 2020](#))

From the data, it is understood, that for every kWh reduction in energy utilization, environmental impacts equivalent to 6 g CO₂ can be avoided which reduces the global warming potential. (Detailed explanation is provided in discussion chapter). Hence, in our process in the production of fish protein hydrolysates, concentrating using either freeze concentration method or multistage evaporator process or mechanical vapor recompression method, with combinations with drying process results in significant energy savings and can reduce environmental impacts significantly.

5.8 Process schemes represented in 3D models.

The detailed hydrolysates production process is modelled in SOLIDWORKS software to represent the production on an industrial scale. The concentration process like freeze concentration, three-stage evaporation, and mechanical vapor recompression process was modelled with combinations with drying process like spray dryer or with rotary drum dryer.

Table 30: Equipment details in 3D Modelled images

1. Crusher	6. Tricantor	11. FPH accumulator tank	16. Spray dryer
2. Heat exchanger 1	7. Centrifuge for oil	12. Pump	17. Mechanical vapor recompression
3. Hydrolysis tank	8. Storage tank	13. Buffer tank	18. Rotary drum drying
4. Heat exchanger 2	9. Centrifuge for solids	14. Storage water tank	19. Membrane filtration
5. Sterilization tank	10. Freezer box	15. Three-stage evaporator	20. Freeze concentration unit

It is seen from the 3D images that all equipment before concentrating stages remains the same, the change in equipment is represented in the images. The detailed equipment list of the modelled images are given in the above table. Detailed modelled images are provided in [Appendix-5](#).

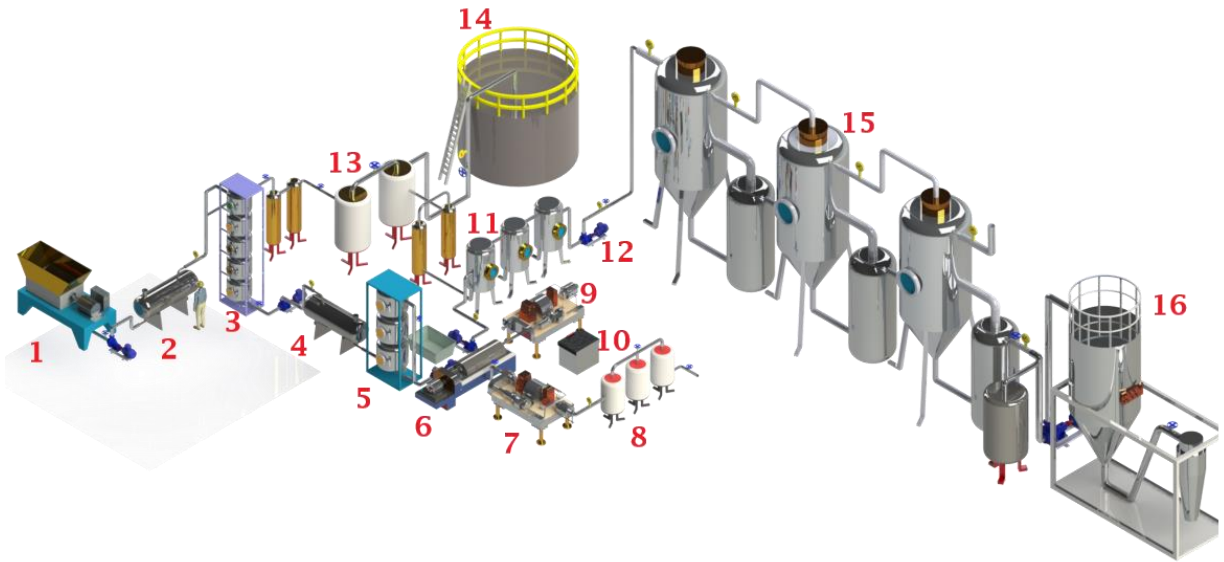


Figure 38: Process with three stage evaporator and spray drying

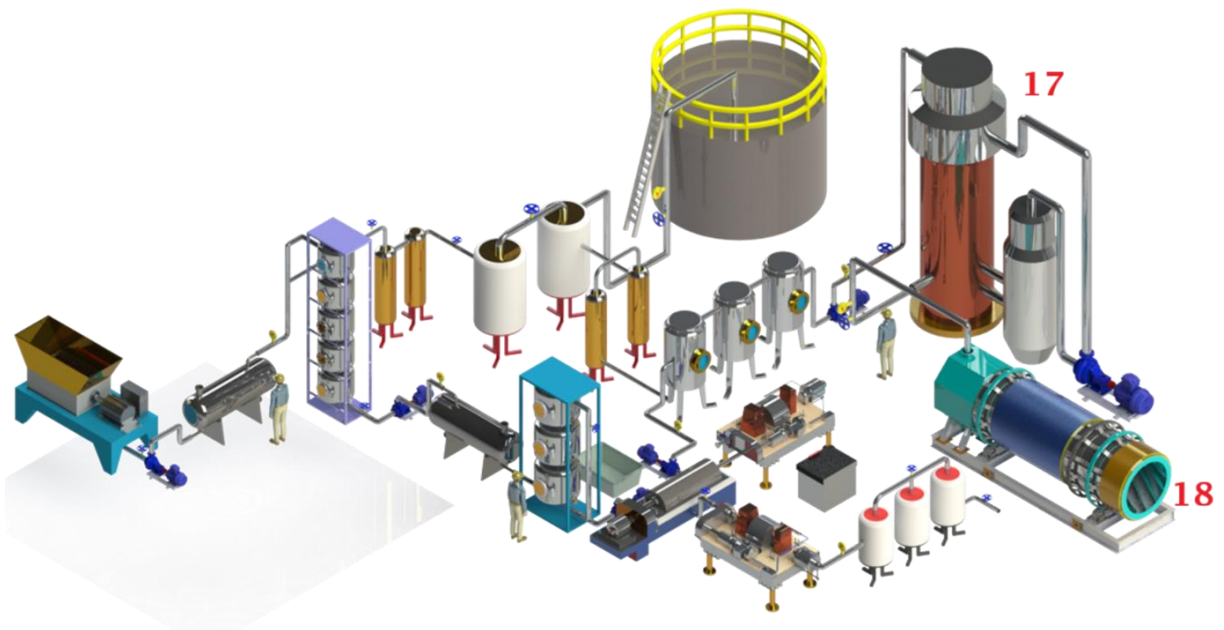


Figure 39: Process with mechanical vapor recompressor and rotary drum drying

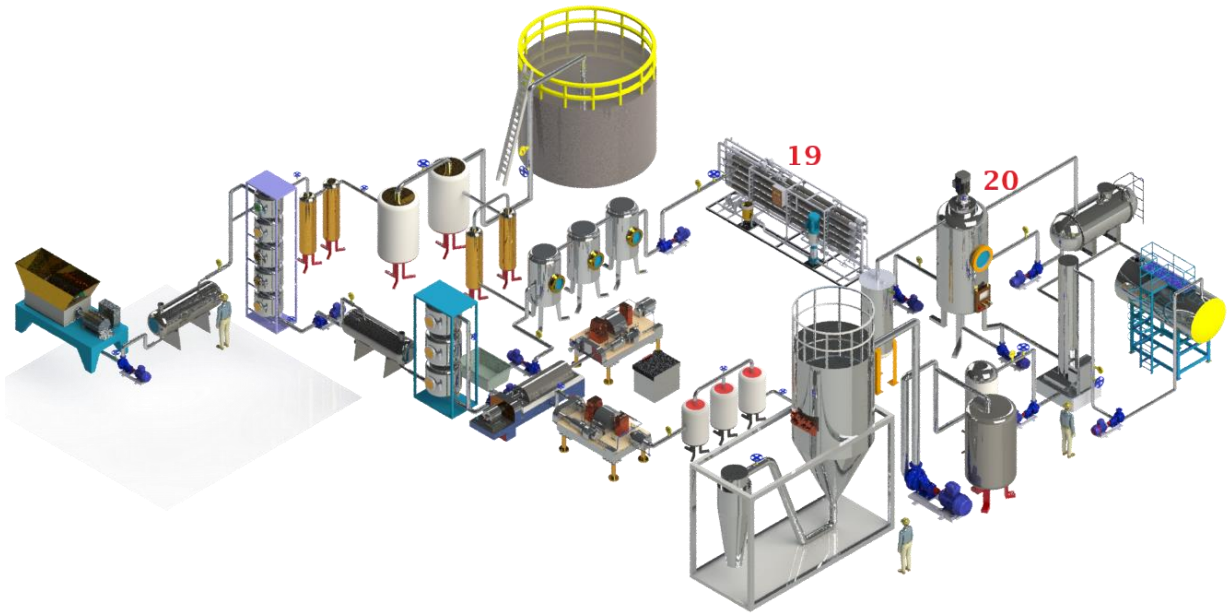


Figure 40: Process with Freeze concentration and spray drying

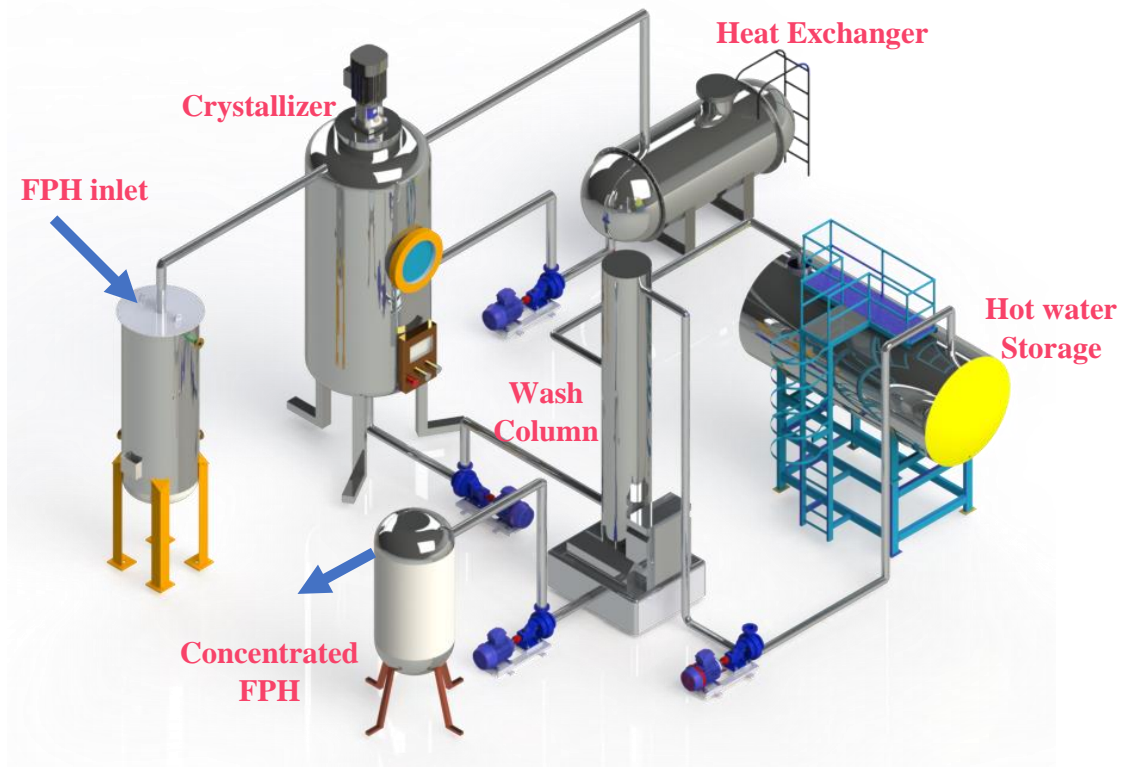


Figure 41: Freeze concentration plant

5.9 Simulation results

This subchapter describes the results of the simulation model performed in Dymola software. The results from the EES code are compared with Dymola and discussed. The heating of hydrolysates and heat recovery options are discussed. The COP of the heat pump and refrigeration is calculated. The COP of the heat pump is defined as the ratio of condenser capacity (Gas cooler and sub-cooler) to the net compressor work. Several assumptions and simplifications are considered during the simulation model. During the simulation process, the power input to pumps is negligible and hence neglected.

The compressor efficiencies were kept constant during the simulation period, which reflects some deviation from actual compressor work. The frequency of the compressor is also fixed. Initially, the frequency control was provided by the PI controller to the compressor based on the suction side pressure which is maintained at 25 bar. The frequency of the compressor was controlled effectively using a PI controller. The mass flow into the compressor is regulated by the evaporator heat load.

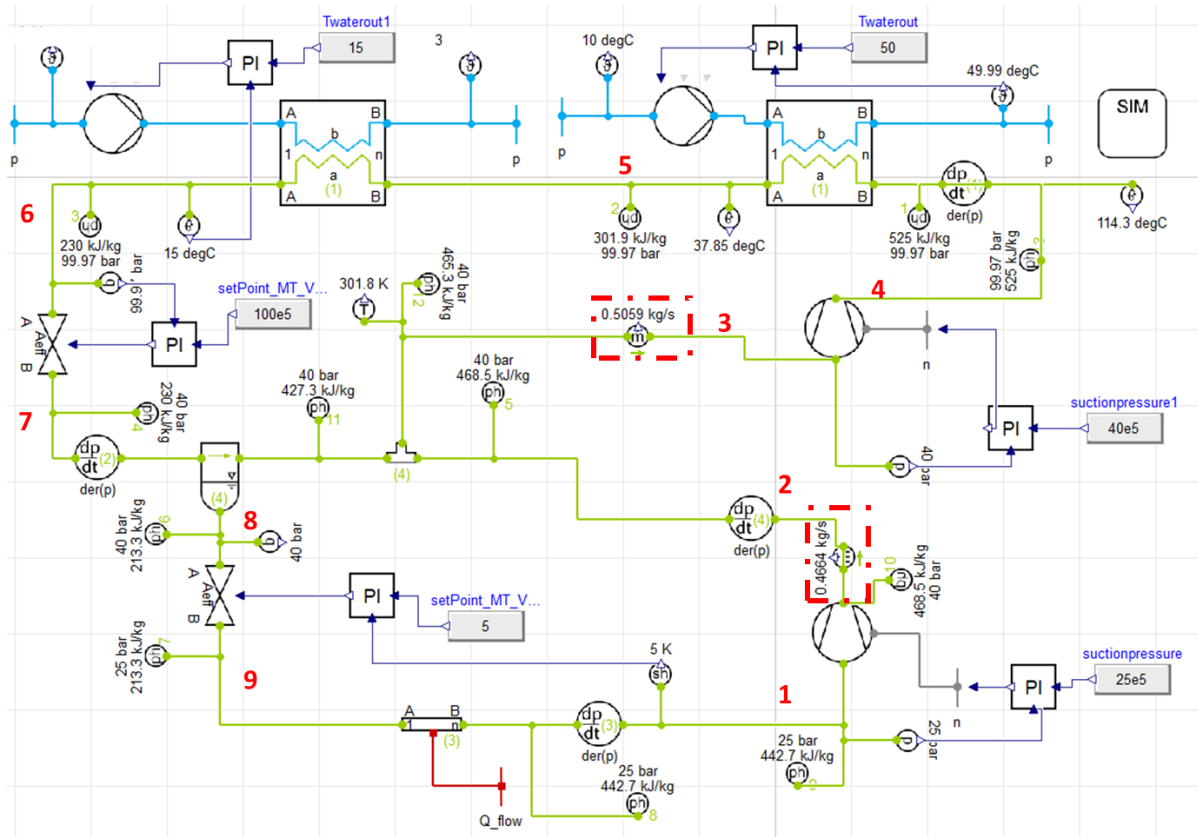


Figure 42: Simulation model of Two-stage CO₂ Transcritical cycle

In the Ph diagram (*Figure 43*) at process 1-2, the refrigerant is compressed to a higher temperature of 114.3 °C. The top side pressure was set to 100 bar. The enthalpy at state point 2 is 525 kJ/kg, the high-temperature refrigerant rejects the heat in the gas cooler and further subcooled to a small temperature difference and the enthalpy at state 6 is 230 kJ/kg. The working fluid (WF) is further expanded and enthalpy at state point 7 is the same as 6. Then, the refrigerant absorbs heat from the heat source and evaporates and reaches state 1 with enthalpy 443 kJ/kg. In the transcritical cycle, heat rejection occurs in the gas cooler with a temperature glide, but in the subcritical cycle, condensation occurs at a constant temperature. After state point 6, the working fluid expands into the subcritical area and is shown in the Ph diagram.

From the calculated evaporation capacity, the refrigerant mass flow rate at the lower cycle is 0.47 kg/s and the mass flow at the top cycle is 0.5 kg/s. The design is made in such a way as to reduce the charge by lowering the condensation pressure (*Figure 42*). The work input to both the compressors was calculated to be 45 kW. And the total heating capacity was calculated as the product of mass flow rate at the top stage and the difference in enthalpy between state points 4 and 6 was found to be 148.8 kW and the COP of the heat pump was 3.3.

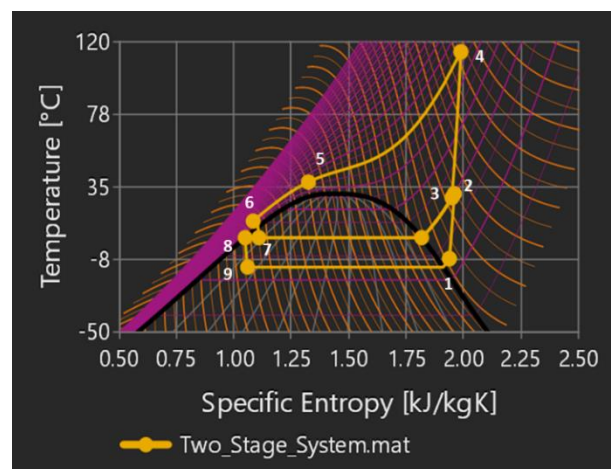
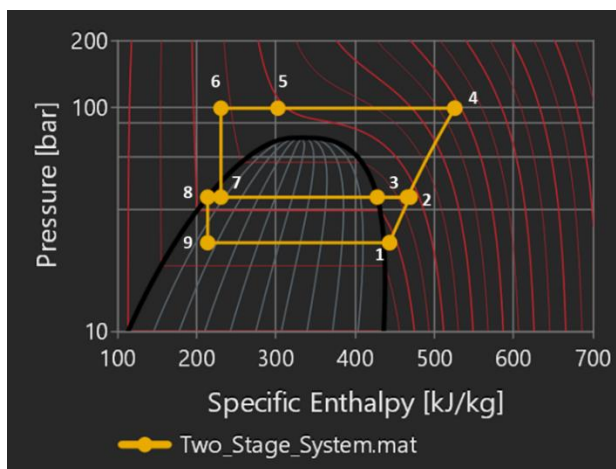


Figure 43: a) Ph diagram of CO₂ Transcritical system **Figure 43:** b) TS diagram of the system

Figure 43: Ph diagram and TS diagram of CO₂ Transcritical model

Operating the system at a constant steady load makes the system efficient, The COP of the transcritical system is enhanced due to the pressure lift in the compressor being maintained low. The PI controller effectively controls the system over time. Initially, the system has deviated from set values and the results diverged this can be seen below in *Figure 44*, the variation of COP as a function of the simulation time is represented. At the start of the simulation, the results show an

oscillation of COP, however during the simulation period, most of the fluctuations are damped by the increasing sensitivity of the PI controller.

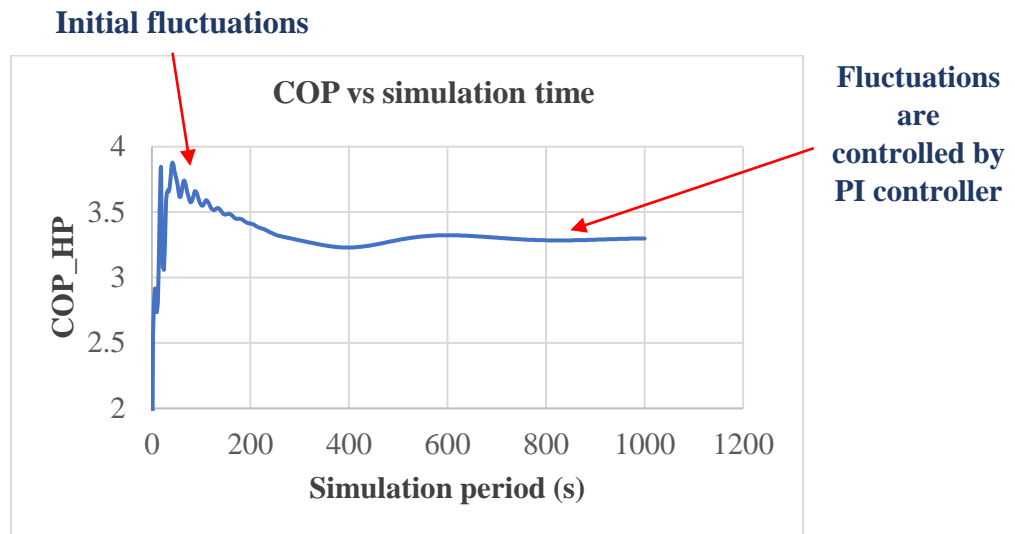


Figure 44: Effectiveness of PI controller (COP vs Time)

At the evaporator side, the mass flow rate of 1841 kg/h of water is initialized and flows into the evaporator. The hydrolysates which are water in our simulation are cooled to -3 from +4 °C. The corresponding heat load is calculated and is given as an input and is represented in “Q_Flow”. In the gas cooler heat exchanger, the mass flow rate of 1841 kg/h was heated to 50 °C from 10 °C. The heat exchanger area was increased, and the compressor was controlled using the PI controller to regulate the mass flow. Hence, a lower mass flow rate of the refrigerant is regulated at the top stage. For higher efficiency, the transcritical CO₂ system should operate at near optimum pressure level.

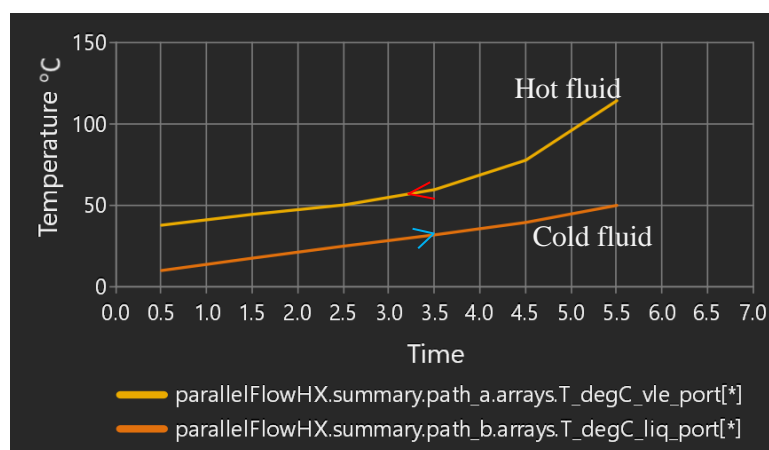


Figure 45: Counterflow of hot & cold fluids inside HX

At the gas cooler, the refrigerant heats the hydrolysates temperature from 10 °C to 50 °C. The CO₂ refrigerant was cooled from 114°C to 37°C. The counter flow behaviour of both the fluid temperatures is represented above in *Figure 45*,

The simulation study performed here was to understand the actual working process of the system for heating and cooling with the possible heat recovery. The investigation also studied how to control the frequency of the compressors using the PI controller. The following are the detailed observations which are made from the simulation results,

- The COP of the system drops when there is a rise in the discharge pressure. This is seen in the below graph (*Figure 46*). Running the system at optimum parameters will lead to higher system performance, otherwise the COP will decrease. The gas cooler heating capacity with a constant pressure decreases when the refrigerant pressure rises. The rise in COP is due to a drop in the pressure ratio, which results in less compression work. The mass flow rate of the refrigerant is an important factor since both the COP and the heating capacity are dependent on mass flow rates.

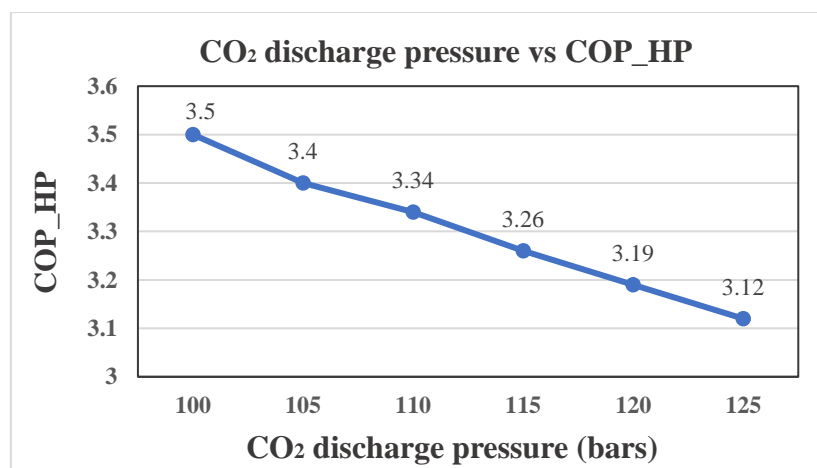


Figure 46: CO₂ discharge pressure vs Heat pump_COP

- The ideal heat rejection pressure for the CO₂ transcritical system has been analysed by several researchers in their publications and they developed a correlation for the ideal discharge pressure. [Liao et al. \(2000\)](#), established a relationship between the evaporating temperature and the gas cooler's outlet temperature, and the correlation between the gas cooler approach temperature and ambient temperature was identified by [Sawalha et al. \(2008\)](#). Both these research findings highlight the significance of isentropic efficiency as an important factor in overall performance.
- When the gas cooler length is increased, the pressure drops with respect to length (dP/dx) increase. The corresponding gas cooler length lowers, as the width increases, and it leads

to a drop in the pressure. On the other hand, to reduce the gas cooler pressures, the heat exchanger length should also be increased to have the same effectiveness in the system. The refrigeration COP against evaporation temperature is given below,

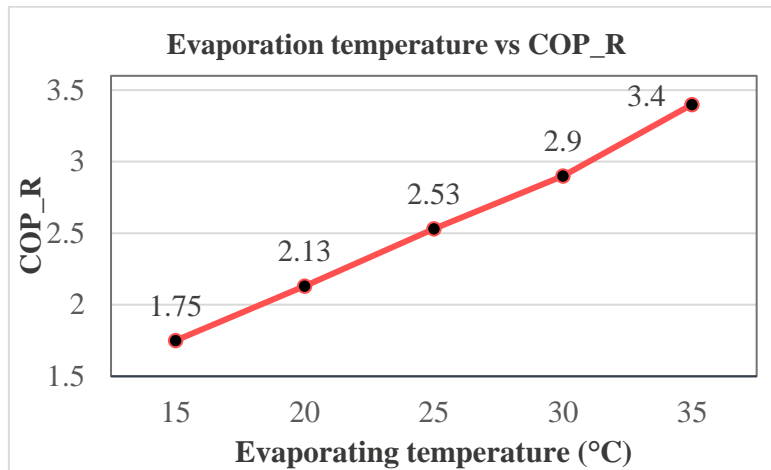


Figure 47: CO₂ evaporating temperature vs refrigeration COP

- By reducing the temperature gradient between the hot and cold fluids, the heat transfer inside the gas cooler is made more effective. There are two approaches in reducing the length of a gas cooler's entrance: the first approach is to increase the number of channel pairs and the next way is to increase the channel width.
- [Liao et al. \(2000\)](#), examined and found that the optimal discharge pressure for a transcritical CO₂ cycle is determined by three factors: the evaporating temperature T_{evap} , the temperature of the gas cooler T_{GC} , and the isentropic efficiency of the compressors. The parallel compressor when operated at a lower pressure ratio improves the compressor's performance ([Angel et al., 2017](#)).
- In the transcritical cycle, the heat rejection occurs in the supercritical region, where the working fluid does not undergo a phase change. When compared to a subcritical cycle, the condensation occurs at a constant temperature, the gas cooler is employed for heat rejection, allowing for temperature glide. CO₂ is one of the most widely used natural refrigerants in commercial transcritical heat pump cycles. It is designed to produce hot water temperatures of about 60 °C. Its critical temperature is 31.1°C and its critical pressure of 7.39 MPa.
- In recent years, the CO₂ refrigeration systems have more widespread applications, particularly in the commercial refrigeration sector ([Kim et al., 2017](#)). Several research has investigated to determine the ideal high pressure. [Baek et al. \(2013\)](#), experimented on the

CO₂ refrigeration system and determined the optimal discharge pressure under specific operating conditions

- Further, higher pressure ratios would be required to attain the temperature levels required for high-temperature systems. This will lead to increase compression and expansion losses in the transcritical CO₂ cycle. To reduce the above-mentioned losses [Yang et al. \(2017\)](#) experimentally studied a cascade model with CO₂ in a transcritical cycle and R152a in a subcritical cycle. The R152a subcritical cycle was used to pre-heat the working fluid hence increasing the evaporation temperature and pressure of CO₂ in the transcritical stage. This reduces the pressure differences in the gas cooler and the evaporator resulting in a higher COP.
- The mechanical efficiency of the compressor increases with compressor speed and pressure rate. Factors like CO₂ mass flow rate and the enthalpy difference directly influence the power utilized in the compressor. The CO₂ mass flow rate decreases when the discharge pressure rises due to the expansion valve when being not fully opened. Also, there is a rise in CO₂ mass flow rate with an increase in the compressor frequency. Since the increase in compressor speed discharges more CO₂.
- The optimal high side pressure and system coefficient of performance was influenced by the gas cooler outlet temperature. As a result of the huge pressure changes in the transcritical CO₂ heat pump system, the control of the high side pressure is one of the most important factors impacting the coefficient of performance. The temperature of the gas cooler T_{gc} increases with respect to an increase in CO₂ mass flow rate. To get a higher COP and a lower discharge pressure of the system, the compressor frequency has been lowered to discharge a lower mass flow of CO₂. The factors which are considered to be important are the evaporation temperature, high pressure, gas cooler outlet temperature, and isentropic efficiency ([Qin et al., 2022](#)).

5.9.1 Performance-enhancing measures

In our simulation the CO₂ heat pump system has a coefficient of performance (COP) of 3.5 in EES, the system can be further improved by changes in system design or by performing several modifications which are presented in this subchapter.

Several researchers have improved the CO₂ heat pump systems using technologies like ejectors and expanders. [Zhu et al. \(2018\)](#), investigated the effects of output water temperature and other parameters on the ejector and the complete system. The results of his experiments indicated that the system with the ejector is more efficient than the previous system. Also, the COP of the system is enhanced by up to 30.3 percent according to his final results.

Few scientists indicated that the expansion work loss of CO₂ systems is excessive and mentioned that to improve the system's performance this expansion work must be recovered effectively. [Hafner et al. \(2021\)](#), studied the use of an ejector in the transcritical cycle and concluded that the system performance was improved with the addition of the ejector technology. [Zheng et al. \(2016\)](#), investigated and found that the performance of a transcritical CO₂ system with two-stage evaporation and the ejector was improved 2.5 times. [Agrawal et al. \(2007\)](#), studied the heating performance of various two-stage transcritical CO₂ heat pump systems and observed that the flash gas bypass system delivered the best performance of the system.

In addition, to change in system design the heat source can also be changed to increase the system performance and to increase the COP of the system. Several researchers studied different heat sources. [Faria et al. \(2016\)](#), studied the transient and steady-state behaviour by choosing solar energy as the evaporator's heat source. [Ill'an-G'omez et al. \(2021\)](#), investigated water as the heat source to improve the functioning of the system, Also, geothermal energy was used as a heat source in a conventional system by [Li et al. \(2018\)](#).

Some researchers studied blend refrigerant (R744/R290) on the performance of a heat pump water heater ([Ju et al., 2018](#)). And the results indicated that the cycle performance improved with the optimum concentration. Also, a new type of heat pump was analysed by [Yu et al. \(2018\)](#), with a CO₂-propane mixture, the results showed that a higher heating capacity is obtained from the system for low ambient conditions.

5.10 HTHP's results

From the EES results, the important results were discussed, when the butane condensing pressure was at 23 bar, a heat pump COP of 2.1 was achieved. This cycle was operated at higher condensing pressure to provide a higher temperature output and hence the COP of 2.1 was obtained. The mass flow rate in the butane cycle and propane cycle is calculated to be 1.45 and 0.85 kg/s respectively and the corresponding network input to the cycle was 171 kW. The important parameters and results are as follows, The EES code is provided in [Appendix 8](#).

Table 31: COP and other data of the HTHP system

P_C_Butane	23 bar
M_H	1.45 kg/s
M_L	0.845 kg/s
W₁	65 kW
W₂	106 kW
P_C_Propane	22 bar
COP	2.1

The increase in butane condensing pressure results in the reduction of the system COP. It is observed from *Figure 48*, that at a lower condensing pressure of 16 bar a COP of 2.45 was achieved. However, at very high pressure the COP drops dramatically to around 2. The temperature of the discharge gas is also an important factor when designing the HTHP system. The corresponding temperatures of the butane refrigerant are plotted against the condensing pressure and are represented below in *Figure 49*,

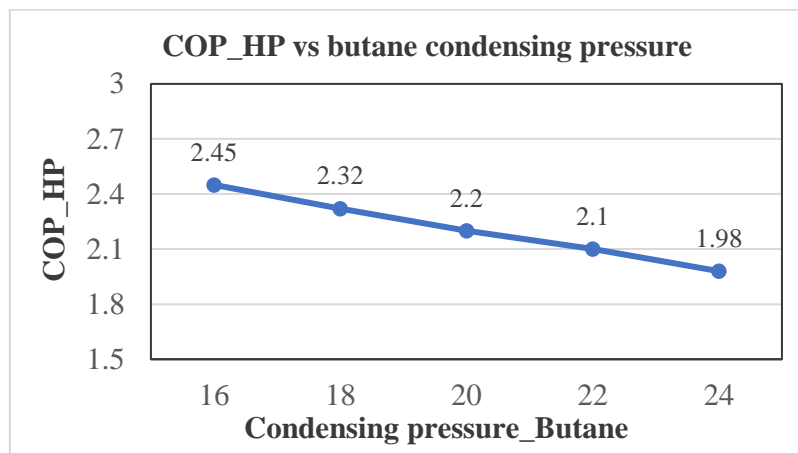


Figure 48: Butane condensing pressure vs Heat pump_COP

Studies indicated that in the HTHP system the working fluids should have a higher critical temperature for high heat output. However, it is understood from our results increasing the temperature beyond the optimum level will increase the system heating capacity, however, it lowers the system COP. Another advantage of butane as a working fluid in HTHP is low operating pressure with high temperature output. Butane's thermodynamic characteristics make it ideal for single-stage compression with heat delivery up to 130 degrees Celsius. Instead of high-speed compressors, a larger compressor is required for increased mass flow capacity.

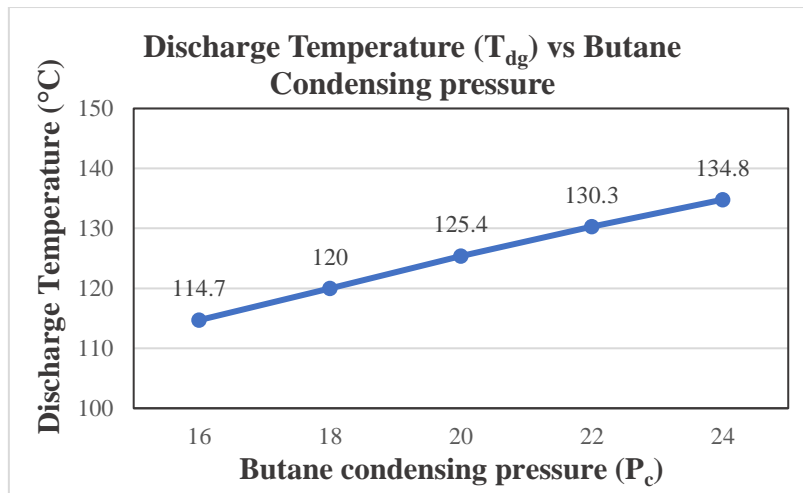


Figure 49: Butane condensing pressure vs Discharge temperature

The superheat value is an important factor to prevent compression into the vapor-liquid dome. When enough superheat is not available at the suction side of the compressor, the butane can be compressed into the dome at higher isentropic efficiency. Since butane has an overhanging vapor-liquid dome. The saturated vapor line bulges when the condensation temperature approaches the critical point. Hence, a high suction superheat is necessary to avoid the compression into the liquid vapor dome, as it leads to compressor damage, [Bamigbetan et al. \(2019\)](#). Hydrocarbon mixtures have the potential to have a higher COP value, however, operational safety is more important due to its flammable behavior.

The natural working fluids can also be favorable working fluids to HTHP; however, the technology has to be mature due to the following reasons. The high discharge temperature of ammonia after the compressor, combined with its high pressure and condensation temperature, limits its use in HTHP. When water is considered a refrigerant, its density is relatively low hence large or compressors running at higher rpm are necessary to shift equal mass flows.

When CO₂ was selected as a refrigerant in HTHP, due to the higher heat sink output temperature, it will demand developments in component technology for the compressors running at higher operating pressure, better heat exchangers, and piping systems. The temperature glide should be closer in the gas cooler for CO₂ trans-critical HTHP. Also, CO₂ has a lower critical temperature of 31°C. To run the system in trans-critical mode, the evaporating temperature must be lower than 31°C, irrespective of the heat source temperature which brings a constraint in HTHP applications.

For HTHP, the main technology restrictions are the operating parameters of the compressors (temperature and pressure). Other constraints which are also included are the stability of the working fluid at the higher temperature, electric motor cooling of the compressor, the thermal

stability of lubricating oil, compressor material strength, and working of electronic expansion valves at high temperatures, [Bamigbetan et al. \(2017\)](#).

The compressor operating constraints can be removed by developing superior compressor designs. [Bamigbetan et al. \(2019\)](#), analyzed the prototype compressor and found that due to butane's favorable thermodynamic features the prototype compressor has an isentropic efficiency of 74 percent and a volumetric efficiency of 83 percent. They also observed that the operational parameters (pressure and temperature) were acceptable, with the potential of having higher temperature heat delivery.

Several studies also mentioned that for HTHP the following measures can be taken, the thermal protection of the compressor electric motor can be improved for high-temperature usage. Also, the motor can be cooled using the suction fluid from the evaporator. For compressors, a low-pressure switch can be an important safety factor for butane as a refrigerant. This will avoid the formation of the explosive mixture during the compressor start-up due to the entry of air. At the compressor discharge end, a sensor switch detecting the higher temperature (160 °C) can be installed.

5.11 Economic analysis results

The results of economic calculation for the different processes are given below. For each process, the net investment cost, operating energy value, its corresponding energy cost, depreciation, and maintenance cost are given. The calculated payback time is also provided for comparison. The cost estimation was based on associated literature review and price information from the industry for related production size and capacity. Hand factor has been considered over the base price of each cost to provide the right approximation over piping, foundations, electrical wiring, and painting. Finally, the engineering cost of 10% and contingency factor (8%) were adjusted to the above values to have the final estimation. Summary table of economic data of drying process with alternatives combination of freeze conc, MVR, MSE are provided in [Appendix 6, a](#).

From the below chart, the **investment cost** for the process chain with all equipment to produce fish protein hydrolysates, with freeze concentration at the concentration step and drying using spray drying was estimated to be 84 million NOK. Also, if the drying process was carried out either rotary drum drying or vacuum freeze dryer it yields 82 and 89 million NOK respectively. In comparing all the drying processes in freeze concentration techniques, the investment cost for the process including vacuum freeze concentrator has a higher value, this was due to the superior equipment required in providing necessary freezing. Although, the cost variation between these alternatives was not so significant.

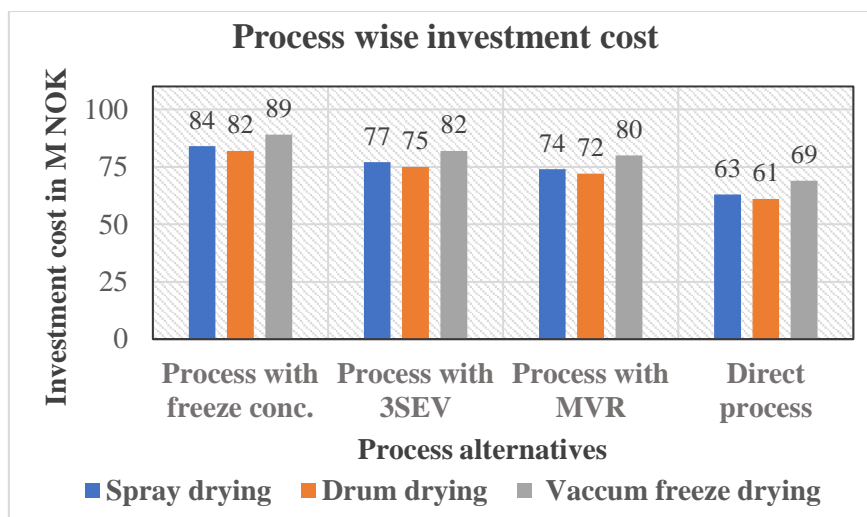


Figure 50: Investment costs of different process

Secondly, in process with a three-stage evaporator (multi-stage/3SEV) was studied, and its combination with a spray dryer yields an estimated amount equivalent to 77 million NOK. This value when compared with the freeze concentrator and spray dryer process scheme is almost 8% lower in price. Also, the process combination with drum drying and vacuum freeze drying with three-stage evaporator results in 75 and 82 million NOK respectively. This is almost 8.5% and 7% lower when compared with the process with a freeze concentrator. Because, in the freeze concentrator process, we need to include the concentrator and wash column cost as primary equipment. The refrigeration unit for freezing the hydrolysates is included in secondary equipment. In addition to this, the whole process in the production of fish protein hydrolysates also includes the cost of membrane separation, since the solids require filtration to remove salts and other big particles before the freeze concentration process to make the concentration process effective.

Finally, the investigation of the mechanical vapor recompression process when combined with a spray dryer yields a total amount of 74 million NOK. When compared to the freeze concentrator and spray dryer production process, it is 12 % less expensive. Furthermore, combining the process with drum drying and vacuum freeze drying with a mechanical vapor recompression process, yields 72 and 80 million NOK, respectively. When compared with the freeze concentrator process it is 12% and 10% lower.

In comparison, when the production of fish protein hydrolysates was performed without a concentration process, the whole process cost with a direct drying process with a spray dryer was calculated to be 63 million NOK and with rotary drum drying and vacuum freeze-drying alternatives yield 61 and 69 million NOK respectively. Generally speaking, the concentration steps with freeze concentration, three-stage evaporator or with mechanical vapor recompression adds almost 20 to 25% addition cost. However, this additional investment cost is compensated by the

lowest operating cost, since the energy value required to remove water is comparatively lower when compared direct drying processes.

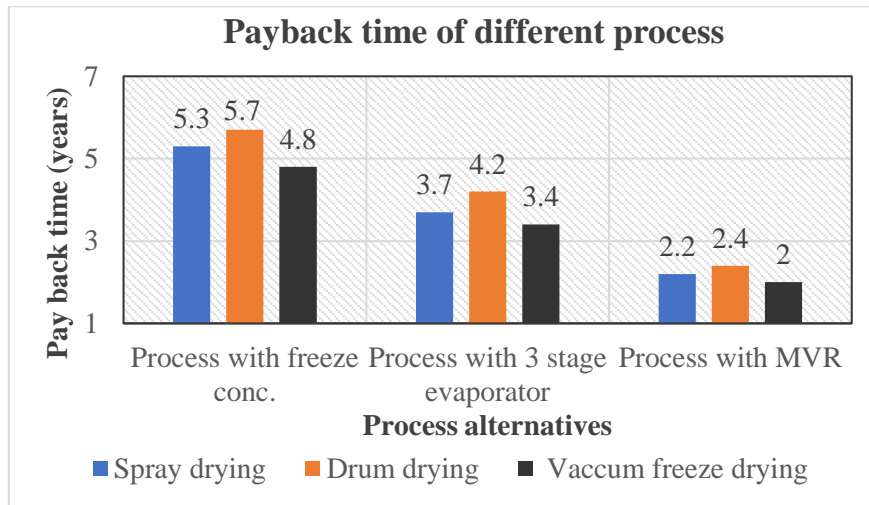


Figure 51: Payback time of different processes

Payback time is an important factor in accessing the profitability of any selected process. When producing the fish protein hydrolysates, direct process schemes of FPH are compared with the process with a concentrating step included. From this data, investors can have an estimation of different available processes and its payback time when producing FPH powders.

In the above plot, (Figure 51) the bar plot with freeze concentration included process provides a payback time of 4.8 – 5.7 years. These results obtained were then compared with the process with direct drying process as an alternative. During the analysis, the investment cost and the operating energy value was an important factor when calculating the payback time. Also, the entire process chain with alternatives in the drying process like spray dryer, rotary drum dryer and vacuum freeze dryer resulted in values around 5 years. In comparison, a process with a rotary drum dryer has the highest payback time among the process with freeze concentration included.

Next, when the process with direct drying was studied with a process with three-stage evaporators (3SEV) as an alternative process it resulted in a lower payback time. 3SEV with spray dryer has a payback time of 3.7 years, also with alternatives in drying techniques with drum drying and vacuum freeze drying resulted in 4.2 and 3.4 years respectively. When comparing these values with the freeze concentrator, the payback time was quite lower. This was mainly due to the lower energy value needed during removing water from FPH. Lower energy value results in lower energy cost and hence the process has a lower payback time.

Finally, in the bar chart, the process with mechanical vapor recompression (MVR) evaporator has the lowest payback time of all the available alternatives. The entire process which has MVR and

with spray dryer has a payback time of 2.2 years, while drum drying and vacuum freeze drying have payback times of 2.4 and 2 years, respectively.

In summary, the process with MVR has the lowest payback time when compared with the one with freeze concentrator and 3SEV. Although, the choices with drying methods like spray dryer, drum dryer or freeze dryer, the payback time does not change so significant in years. Investors can choose a freeze concentrator when the low-temperature water removal process is necessary, also the quality can be retained. The process schemes with mechanical vapor recompression have the lowest payback time. The reason for the lowest payback time is, that the investment cost was similar to three-stage evaporators since in our study we have considered a single-stage mechanical vapor recompression system. It's the operating energy costs which is a determining factor, since the energy value per hour in removing the water is around 600-630 kWh for 1 ton of RRM and is almost 46 % lower. This is a determining factor since the plant operating hours are considered 5000 hours.

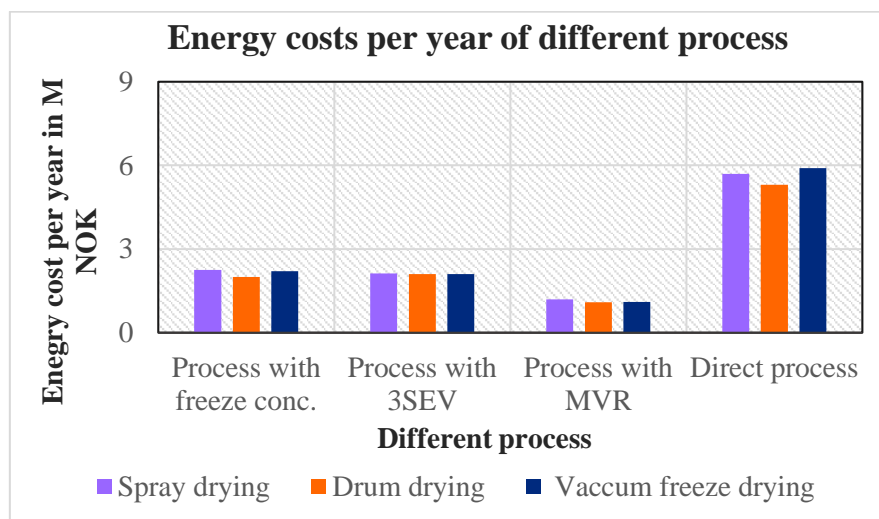


Figure 52: Process wide yearly energy costs

The chart above (Figure 52) depicts the operating energy value per year involved in the production of powdered FPH from different process. It is seen from the chart, that for process with freeze concentration with the drying process alternatives resulted in an energy cost value of 2 to 2.2 million NOK per year. The energy value of a spray dryer per hour is 1245 kWh, the corresponding energy cost per year is also higher when compared with process alternatives of drum drying or vacuum freeze dryer.

Similarly, the process with three-stage evaporators has almost the same energy cost between 2 to 2.1 million NOK annum. Since the hourly energy cost in processing one ton of rest raw materials has a value between 1150 – 1180 kWh. Almost, all the processes with different drying alternatives

like spray, drum, and vacuum freeze dryers have the same energy values. The process with MVR has the lowest yearly operating costs. This indicates that the concentrating process has a more significant impact on lowering the overall energy costs than the drying process.

On the other hand, the production process with a direct drying process has a very high operating energy cost per year up to 6 million NOK. The process with a rotary drum dryer has a slightly lower operating energy cost. When compared with the process having concentrating steps before final drying has almost 60-70% lower energy cost value per annum. It is evident from *Figure 52* that the direct drying process with any of the drying techniques would result in higher energy value and it leads to higher energy costs. Also, in our calculation energy value of 0.36 NOK/kWh and operating hours of 5000 per year are taken. Changes in these values also lead to variation in the overall energy costs per year.

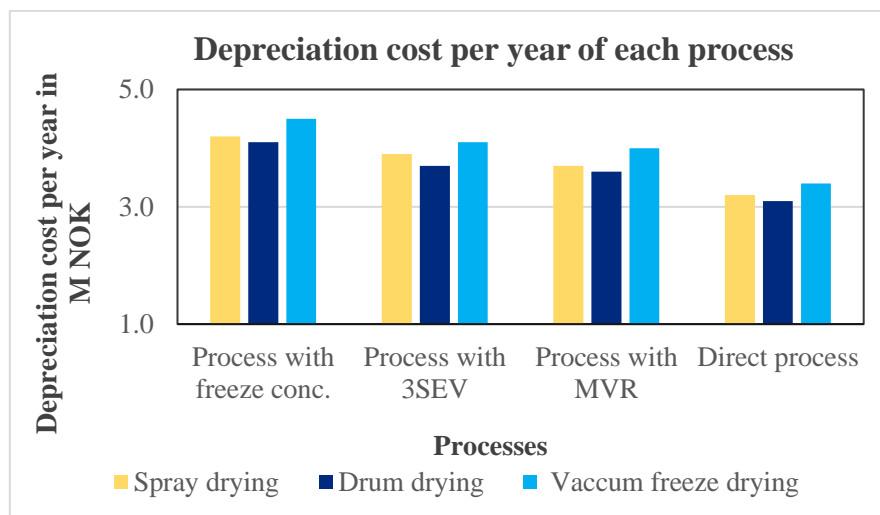


Figure 53: Yearly depreciation cost of each process

The depreciation costs are the reduced value of the plant due to continuous operation over a certain period. Here, the depreciation value was calculated based on the investment cost of the process to that of the plant lifetime considering the salvage value. The salvage value was the remaining value of the asset which was taken 5% of the overall investment cost. For the process with direct drying, the yearly depreciation costs were between 3.1 to 3.4 million NOK, while the process with freeze concentration with the drying methods has a higher depreciation cost per annum of 4.1 to 4.5 million NOK (*Figure 53*). Since the depreciation cost is related to the investment cost of the process, the scheme with freeze concentration has a higher value following the process with a three-stage evaporator and then the process with a mechanical vapor recompression evaporator.

The main production process has been considered and all costs and revenue are studied in a more detailed manner. The results are given below,

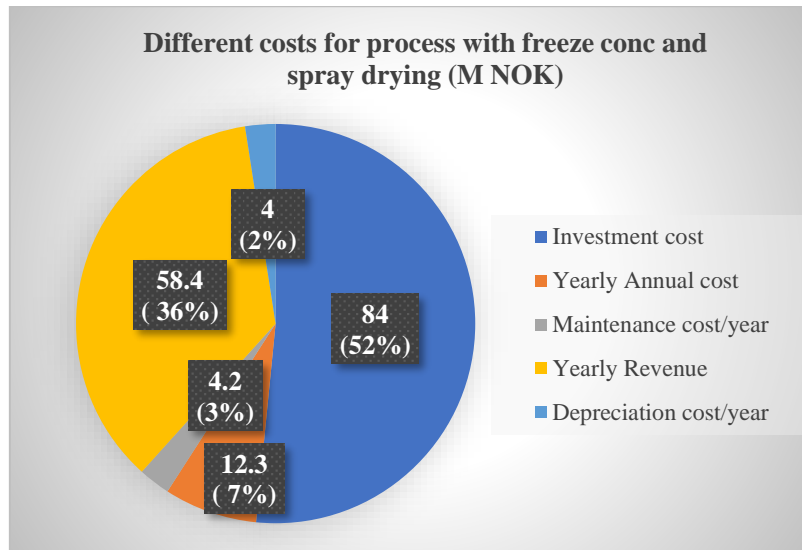


Figure 54: Different costs for process with freeze concentration with spray drying

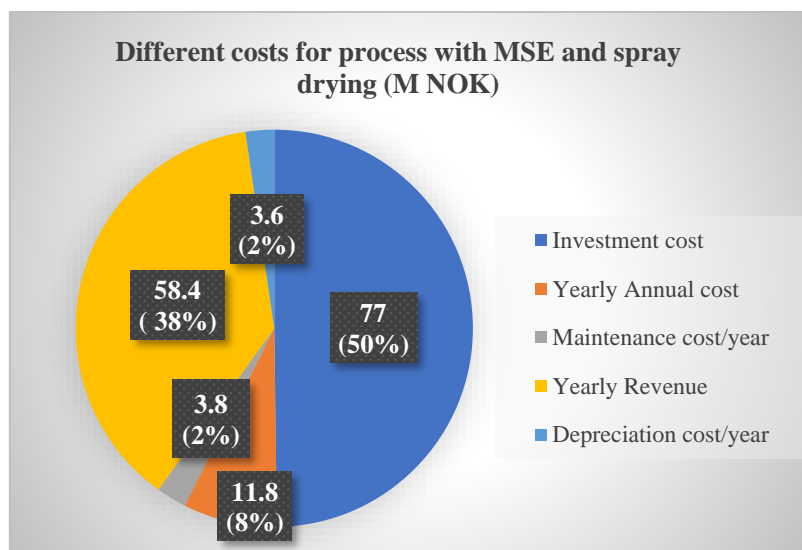


Figure 55: Different costs for process multi-stage evaporator with spray drying

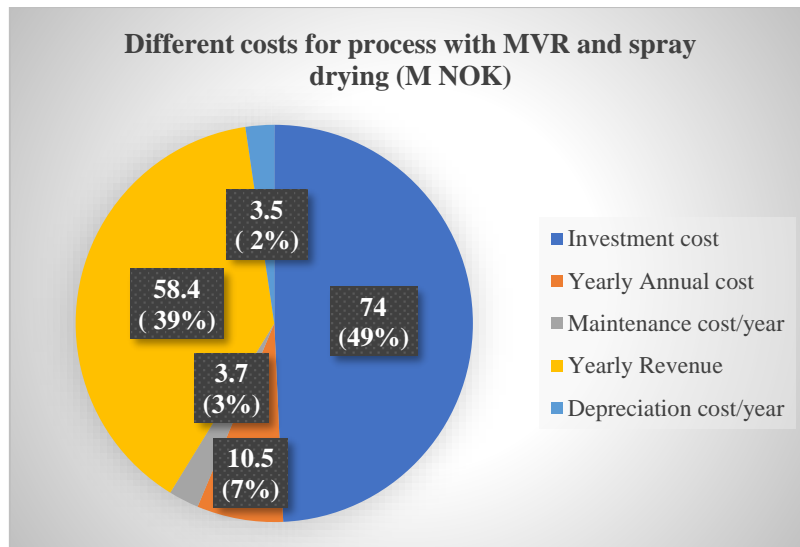


Figure 56: Different costs for process mechanical vapor recompressor with spray drying

The above charts show the different costs of the typical process alternatives of freeze concentrator and multistage evaporator and mechanical vapor recompression evaporator with spray dryer in the drying stage. The different costs include the cost of investment, annual cost, depreciation and maintenance cost and the yearly revenue generated by the plant. The revenue was calculated from the FPH powder output of 130 kg/h and the market value of FPH was considered around 80 NOK/kg and the operating hours of the plant are 5000 hrs. The primary by-products i.e., the final FPH powder are accounted in this calculation. Also, in our calculation the RRM was from white COD fish and hence the amount of oil obtained from the process was not so high and it was not included in calculating the yearly revenue. Additionally, the secondary by-products, the unsolved protein mix after the end of separation nearly have the same value as the primary products. However, the additional energy required to remove the moisture from the secondary products must also be taken.

In the *Figure 54*, the process with freeze concentrator and spray dryer, it is observed that the investment cost accounted for 84 million NOK which is 52% respectively, and the maintenance and depreciation cost each have a value of 4.2 and 4 million NOK which is 3 and 2% respectively. The calculated revenue is around 58 million NOK, and it shares almost 36% of the entire chart. When considering the yearly cost i.e., the yearly operating cost with yearly investment and maintenance cost considering the real rate of interest, the generated revenue is relatively profitable. Note, here the revenue calculated here is not the actual profit, the raw material cost of the RRM also may vary from 2-5 NOK/kg, we should also estimate the actual tax before calculating the real profit.

Beek et al., GEA, (2018), stated that the investment cost of the system with freeze concentration is higher than the process with only spray drying. However, the OPEX- operational expenditure is a driving factor for freeze concentration technology to be considered since it offers greater energy savings. However, when combined with freeze-drying the CAPEX and OPEX seem economically feasible.

When comparing the results with other processes, i.e., the one with MVR and 3SEV(MSE), the revenue generated remains the same value, since the production output capacity and the type of products produced remain the same irrespective of the process chosen. It's the other costs will vary based on the type of process. It has been obtained from the graph, the yearly annual cost for this two-process accounted for 11.8 million and 10.5 million NOK which is around 8 and 7% respectively.

5.11.1 Sensitivity analysis results

For the sensitivity analysis, the results from the process with freeze concentration and spray drying were provided. Parameter like operating hours has a greater influence in determining the payback determination. When the operational hours were 5000 hrs the payback time was calculated to be 5.3 years. In the sensitivity analysis approach, the operational hours are varied from 4000 to 5000 hrs. The graphs show that with an increase in the operational hours, the payback time was reduced. For the lower value of plant operating hours say 4000 a higher payback time was calculated. The reason for these results is as follows,

- Higher operational hours result in higher energy demands, and hence the annual energy cost was increased. Since the annual operating cost or the energy costs are influenced directly by the operating hours. This factor was inversely proportional to contributing to the payback time determination. (*Figure 57*)
- The change in operational hours between the two processes (one with direct spray drying and the second with the inclusion of freeze concentration equipment) was analysed, while the additional investment cost remains the same hence the payback time decreases when the operational hours increased.

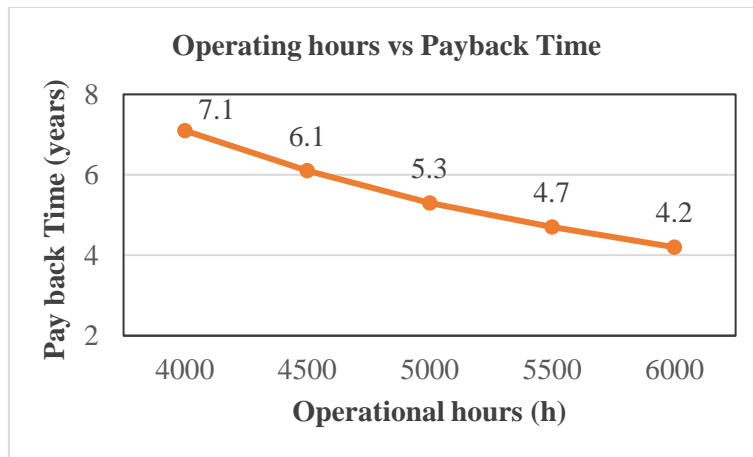


Figure 57: Operating hours vs Payback Time

In the next results, the equipment cost was varied and its outcomes in payback results are investigated while keeping other parameters constant. When the equipment cost of the freeze concentrator was increased from 10 to 25%, the payback time shows an increasing trend, higher the investment cost requires more period to generate the revenue and to compensate for this change in equipment cost. Also, when the investment cost of the freeze concentration was reduced by 10 to 25% the payback time was lowered, (*Figure 58*). Hence, the selection of equipment cost was a very important factor as it directly affects the payback time.

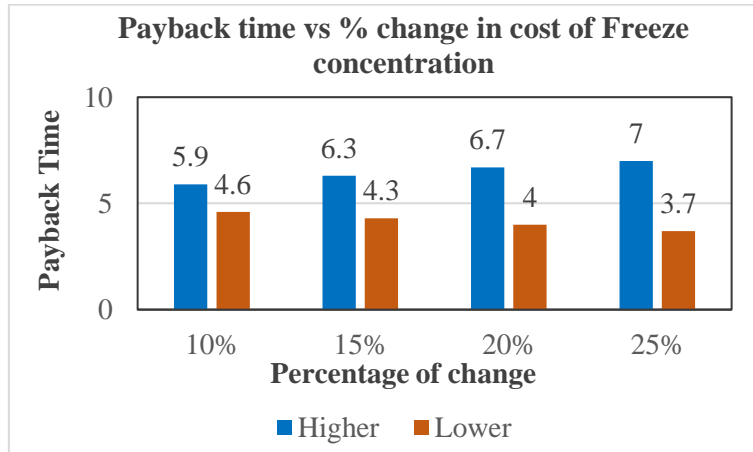


Figure 58: Influence of changes in investment cost in determining the payback time

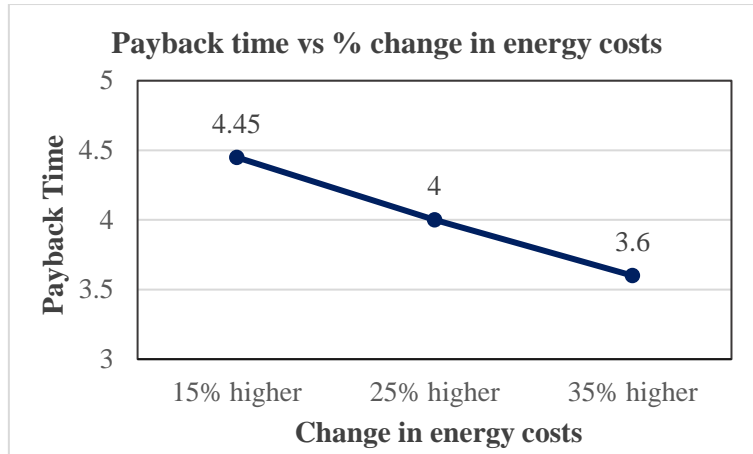


Figure 59: Influence of changes in energy costs in determining the payback time

Finally, the energy cost was analysed with respect to the payback time, while keeping other parameters constant. For calculations, the energy cost value was taken to be 0.36 NOK/kWh, ([Electricity Statistics Norway](#)) the payback time was calculated to be 5.3 years. However, the current electricity price for the energy-intensive manufacturing sectors was revised to 0.46 NOK/KWh (April 2022). Hence, in the sensitivity analysis the electricity prices are increased to 15% (0.41), 25% (0.45) and 35% (0.49). The payback time was inversely proportional to the energy costs, hence with an increase in the energy costs, the payback time is reduced as shown above in *Figure 59*. Increased energy costs increase the annual operating costs but the investment value is the same and hence the payback time is lowered. Since the payback time (PB) was calculated as the ratio of additional investment cost to that of net annual savings.

Statistical method for predicting the maximum project cost for process with freeze concentration and spray drying.

Changes in investment cost +25 to -25%

The calculated ISBL value is 70 million NOK

Higher value: 87.5 M NOK	Lower value 52.5 M NOK	Median value 70 M NOK
--------------------------	------------------------	-----------------------

Mean value, X_{ISBL}

$$X = \frac{(H + 2ML + L)}{4}$$

$$X_{ISBL} = \frac{(87.5 + 2(70) + 52.5)}{4}$$

$$X_{ISBL} = 70 \text{ M NOK}$$

Standard deviation, S_x , ISBL

$$S_x = \frac{(H - L)}{2.65}$$
$$S_x = \frac{(87.5 - 52.5)}{2.65}$$
$$S_{x, ISBL} = 13.21$$

Considering engineering cost, (additional 10%),

$$X_{Total} = 1.1 * X$$
$$X_{Total} = 78$$
$$S_{x,Total} = \sqrt{(1.1 * S_x)^2}$$
$$S_{x,Total} = \sqrt{(1.1 * 13.21)^2}$$
$$S_{x,Total} = 14.53$$

Accounting contingency charges are as follows, the final cost of the project when a 98% confidence level is taken will be less than,

$$X_{Total} + 2.05 * S_{x,Total}$$
$$78 + (2.05 * 14.53)$$
$$\mathbf{107 \text{ Million NOK}}$$

This value represents the maximum estimated value of the project when considering +25 to -25% changes in the investment cost. Also, a 98% confidence level was considered in the study, and the engineering costs and contingency costs are adjusted to the ISBL cost when calculating the results. Using this statistical approach, investors can easily predict the cost of the project before planning the actual budget. Also, when performing the cost estimation, note should be taken that the accuracy of estimation is based on available initial data, and this can be subject to change.

Chapter 6: Discussion

- From the results, it is well determined that when producing the fish protein hydrolysates powder, the energy demands are higher when dryers are utilized. From our calculated results, the process like spray drying, vacuum freeze-drying or rotary drum drying consumes higher energy between 1.5 to 1.9 kWh/kg of water removal for drying the hydrolysates. These results are validated with results from [Baker and McKenzie](#) (1.25-3.2 kWh/kg). The heat pump integrated study with a spray dryer resulted in energy savings of up to 50%. This illustrates how heat pump technology can be integrated for greater energy saving and recovery the waste heat.
- The concentration techniques are investigated in detail in our study to reduce the energy demands significantly and to make the production process most energy efficient. The concentration techniques are installed before the drying techniques and are used to concentrate the hydrolysates with less energy use. Techniques like freeze concentration (FC) and evaporation techniques like three-stage evaporation (3SEV/MSE) and mechanical vapor recompression evaporator (MVR) are efficient technologies and can be used in concentration stages to reduce the energy costs as observed in our results.
- The below graph (*Figure 60*) is derived from the results when processing 1-ton rest raw material per hour, concentrating at 30% in freeze concentration process or concentrated to 50% in the three-stage evaporator and mechanical vapor recompression process, further the hydrolysates are dried using dryers. The energy required in the process with freeze concentration and dryers was around **1120-1250 kWh**, and with three-stage evaporator and spray dryers was around **1160-1180 kWh** and mechanical vapor recompression and dryers was around **600-630 kWh**. The final FPH powders are produced at the rate of 130 kg/h.
- It is understood that the freeze concentration method was found to have greater energy savings and the technique preserves the quality since it processes the hydrolysates at a lower temperature. However, the concentration level achieved using freeze concentration can be 30% and higher the concentration, the removal of ice can be difficult, and some hydrolysates can be washed along with water. To have a maximum concentration (50%) at the concentration stage, the advanced evaporation techniques can be used as an efficient technique.

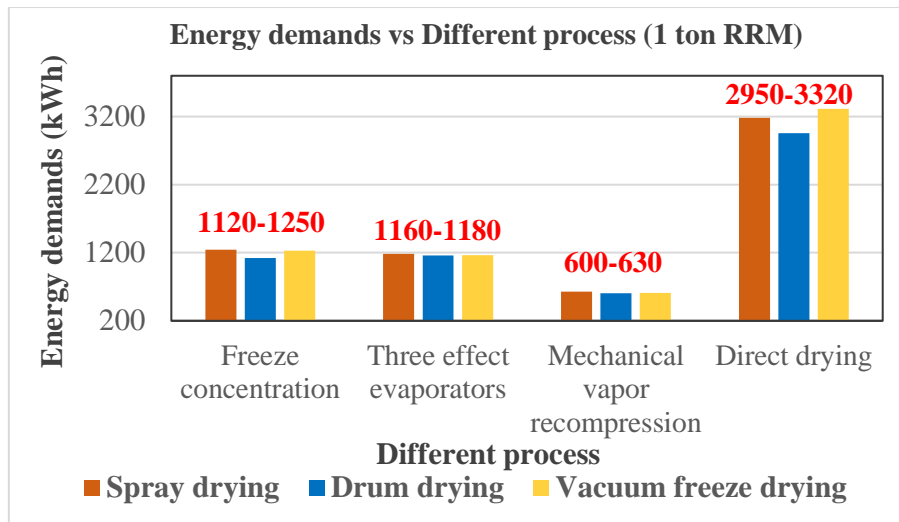


Figure 60: Energy demands vs Different processes for 1-ton RRM

- For a most efficient process, first concentrating to 30% can be performed using freeze concentration (FC) techniques and followed by an evaporation method or two-stage FC process (TWICE) to enhance the concentration to 50-60% and finally, dryers can be used to dry the hydrolysates to produce the final FPH powder. Studies released by the US Department of Agriculture Eastern Regional Research Center stated that when milk was concentrated by freeze concentration process followed by vacuum evaporation can increase the milk solids up to 45 percent with less effect on flavor (Dickey et al., 1995). However, when the additional process is included to reduce the energy costs, it will increase the initial investment cost, and this will question the investment profitability.

- When including the concentrating methods in the technological scheme in the production of final FPH the additional cost required was investigated. **The profitability analysis** was performed in a very detailed approach, and the results are already discussed in the economic analysis chapter, it indicates that the payback time obtained with the process with freeze concentration in combination with dryers was around **4.8-5.7 years**, and the process with the three-stage evaporator in combination with dryers was around **3.4-4.2 years** and process with mechanical vapor recompression in combination with dryers was around **2-2.4 years**.

- [Beek et al., \(2018\)](#), from GEA analyzed a reference freeze concentration plant when concentrating 27% with membrane in pre-concentrating stage and further dried with spray drying, they observed a payback time of **4 years** for a smaller plant capacity. Also, they mentioned the operational cost of a freeze concentration plant was greatly influenced by the size of the facility.

- Communications with the chemical engineer from Sulzer industries pointed out that, a maximum concentration of up to 60% can be achieved using two-stage freeze concentration techniques. Hence, in the thesis work, the energy required for two-stage freeze concentration techniques was also studied with conc. varying from 30 to 60%. It was observed from the results when processing 1-ton RRM in producing the hydrolysates powder with 30% concentration at freeze concentration and spray drying demands an energy value of about 1245 kWh/kg of water removal. However, if the hydrolysates are concentrated to 60% at the freeze concentration stage and spray drying was performed it requires an energy value of 968 kWh/kg of water removal. This is 22% energy savings, since at higher concentrations, more moisture is removed in the freeze concentration process and less amount of moisture is removed in the spray drying process. The energy required for concentrating the hydrolysates is less when compared with the drying process. Overall, when processing 1 ton of RRM, with a 1:1 ratio of RRM and water, around 1710 kg/h of water was removed to produce the final powder at 130 kg/h.
- Few applications demand hydrolysates concentrate in frozen blocks. For onboard processing, techniques like freeze concentration can be installed and the hydrolysates can be concentrated to maximum concentration level. It is then frozen and stored in the onboard fishing vessel and later can be processed to powder at land-based drying facilities. The freezing load and energy required for onboard concentrating are investigated. It is observed at higher concentrations (60%) the process requires less freezing and thawing energy. This additional energy for freezing and thawing when hydrolysates blocks are produced are represented in the below *Figure 61*.

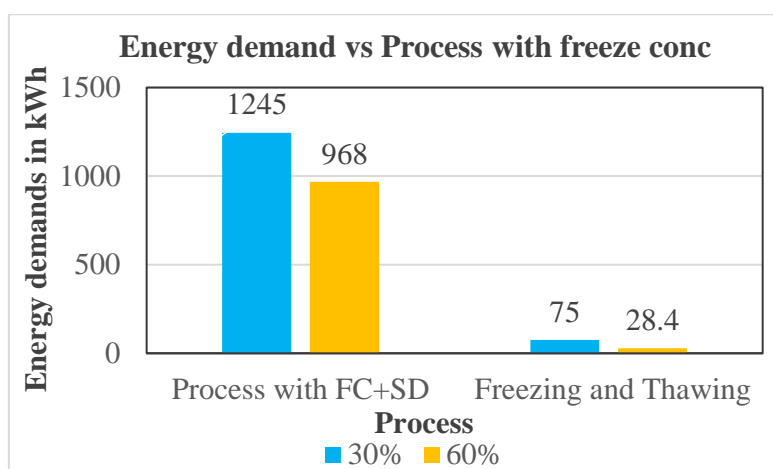


Figure 61: Energy demands in different process with freeze concentration (FC) and spray dryer (SD)

Technological aspects of concentrating techniques:

- The technological aspects of the concentrating methods are analyzed in more detail. From the results, in comparing the spray dryer with rotary drum dryer or vacuum freeze dryer, the drying methods almost all methods have higher energy demands and there was no major reduction in energy value in all drying methods when comparison. Vacuum freeze-drying has the advantage of producing quality dried products suitable for heat sensitive products than other drying processes since the process does not operate at high temperatures. Hence, it is understood the concentration methods are the important determining factor for achieving greater energy savings and studied in broad perspective as follows,
- In the **evaporation process**, advanced techniques like MVR, and MSE are studied in the present work. These are technologically more sophisticated than thermal vapor recompression evaporators or single-effect evaporators. During the evaporation process when concentrating the fish protein hydrolysates, the heat is supplied to the FPH which heats up and evaporated inside the evaporator. As a result, the non-volatile chemicals (solids) content in the hydrolysates increases thus increasing the concentration. At a lower pressure and temperature, the evaporated vapor contains nearly the same thermal energy as the supplied heating steam. The heat source mostly used in the evaporator is steam which condenses on the heating side of the evaporator and provides the heat of condensation at the evaporation side.
- **In the three-stage evaporator**, inside each effect, the heat load from the steam is equivalent to the thermal energy possessed in the vapor rising from each effect. With 1 kg/h of supplied steam, almost 1 kg/h of vapor can be evaporated from the FPH mixture, because the specific evaporation heat on the heating side is nearly the same on the product side. The economy of an evaporator is defined as the amount of steam supplied to evaporate per kg of vapor from the hydrolysates, it varies usually 0.8. The vapor from the first effect is used as a heating medium for the second stage/effect thus lowering the energy value, with two stages the energy need is halved (GEA).
- The advantages of MSE are it offers better heat transfer inside the evaporator, the downtimes are reduced with quick startup, low energy demands during the operating stage, condensing cooling load is reduced, the continuous operation mode is possible, the process is economic and allows good control. However, the challenges are: it requires a larger heat exchanger area for effective evaporation which increases the column height. Fouling reduces the overall heat transfer. Pressure drop is also possible in a falling film evaporator. (Shu et al., 2013).

-
- In **mechanical vapor recompression (MVR)**, the evaporated vapor from a lower evaporation pressure and the temperature level is compressed by a blower or compressor to the heating pressure, the heat energy is thus recycled to heat the arriving hydrolysates. The power input in the mechanical vapor recompression is almost proportionate to the desired increased pressure and temperature level. The installed heat exchanger area is also important in our study. The steam costs should be considered in the evaporation process, In the MVR process, the steam is only consumed during starting stage as a heating medium. When compared with three-stage evaporators, the MVR process consumes less steam than the 3SEV process. The steam costs are increasing over years thus it leads to increased operating costs in the future in the multistage evaporator, thus increasing the number of stages in the multi-stage evaporator is not feasible in the long run when compared with MVR (GEA).

 - MVR technology is thus more energy-efficient in the evaporation method when considered to concentrate fish protein hydrolysates. Reduced energy cost is achieved due to the efficient operating of the process. Also, it requires no additional steam at steady-state operation. Falling film evaporators, and forced circulation evaporators both are compatible with MVR. A larger initial capital cost is compensated by the reduced energy costs. The coefficient of performance of MVR system is superior. The workload of cooling towers is reduced. The evaporation process is simplified thus the plant operation is made simpler. The thermal energy requirement is lower when compared with 3SEV. During the MVR process, the saturation temperature of the vapor rises with compression, increasing its utility as a heat source. Rotating compressors are utilized in MVR because of the high amounts of vapor to be handled. In the MVR system, the challenges are: the presence of water droplets in the vapors increases the wear rate. Also, fouling occurs inside the heat exchanger which reduces the overall heat transfer rate and affects the effectiveness, [Ahirrao et al. \(2014\)](#).

 - In the **freeze concentration process**, it is already mentioned in the results, that better product quality of concentrated fish protein hydrolysates will be obtained than evaporation process. This is due to the following operational benefits: the FPH are **processed at a lower temperature**. The biochemical, and microbiological reactions are not supported at a lower temperature, the product is not damaged by heat. Next, there is an **efficient water separation from the FPH concentrate**: pure ice crystals are separated with no or fewer impurities. The wash column separates the ice crystal efficiently, ensuring the original components stay in the hydrolysates. During the operation of the process, there is **no interaction with air** since the

process takes inside the pressurized system. As a result, all oxygen contact is eliminated, and the risk of oxidation is reduced. The process runs continuously and can be operated for weeks without the need for frequent cleaning; hence **no major intermediate cleaning is required**. When considering the challenges: the investment cost is higher, lower concentration levels than evaporators and some concentrate is lost in the wash away ice (Clark et al., 2011).

- The maximum solid content in freeze concentration is limited by viscosity level. For an effective freeze concentration operation, it requires expertise in operation. The desired feed concentration and flow rate are important. Controlling the feed flow rate with a surge tank is highly necessary. Technology for higher concentration is still maturing in the freeze concentration process, and we can expect it can be used for higher concentration in the future.

Advanced technologies at the concentration and drying stages will benefit the process with greater energy savings in producing the fish protein hydrolysates. The energy savings will directly reduce the yearly CO₂ emission, this will greatly decrease the environmental impacts associated with these emissions. To understand how potentially these technologies can offer the environment in reducing the CO₂ emission levels, the below study was performed with the different energy sources.

As we know that electricity can be produced from different types of sources. In Norway, most of the electricity is produced from a clean source like hydropower. Developing countries on the other hand still use coal sources for producing electricity. In our study, we have considered the electricity source from hydropower and coal-based source and its influence on carbon emissions is studied below,

The FPH was produced at 130 kg/h, when considering the plant operating hours of 5000, the yearly production capacity was around 650 tons of powdered FPH. For hourly production, the process with direct drying process demands an energy value of 3183 kWh, processes with freeze concentrations with spray dryer require 1245 kWh, processes with three-stage with spray dryer require 1182 kWh, and processes with mechanical vapor recompression evaporator with spray dryer requires 629 kWh.

The graph below represents the yearly CO₂ emission levels from the different processes when producing the FPH. The electricity generation was considered from **hydropower-based type**, for every kWh the direct and in-direct emissions account for a CO₂ emission of 6 g. It is seen that when producing the FPH with a process with freeze concentration at the concentration stage and with

spray drying at the drying stage produces a yearly emission of around 37 tons of CO₂ emission, and the process with a multistage evaporator (MSE) with spray dryer produces 35 ton of CO₂ emission.

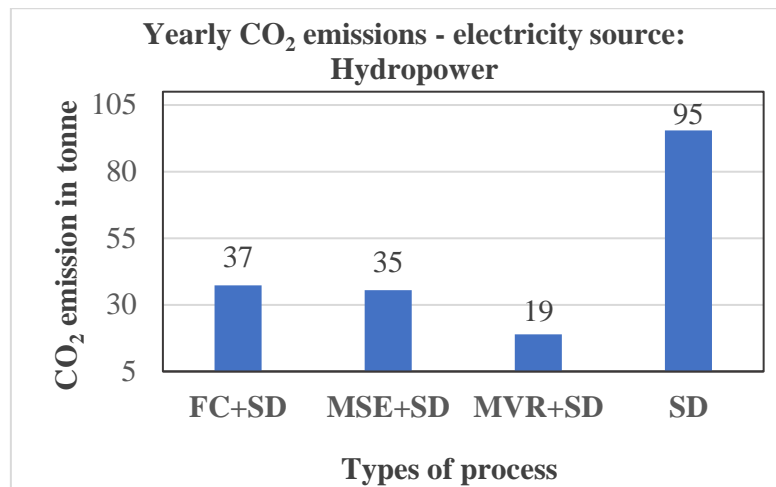


Figure 62: Yearly CO₂ emissions electricity source: Hydropower
 FC: Freeze Concentration, SD: spray dryer, MSE: Multistage evaporator,
 MVR: mechanical vapor recompressor

This is a greater reduction in CO₂ emission levels when a process with direct spray drying was used, which accounts for 95 tons of CO₂ emission. The process with mechanical vapor recompression with spray drying produces yearly 19 tons of CO₂ emission. When compared with other processes this leads to a major reduction in carbon emissions. Electricity source is very important since the production of CO₂ emission is directly related to the type of energy sources like coal, gas, wind, or hydropower. This is represented and the results are given in the graphs.

When the electricity is produced from **coal-based source** with carbon capture and storage technologies, the amount of CO₂ emission is produced at 240 g per kWh. It is observed from the *Figure 63* that with the process with spray dryer produces 3.8 kiloton equivalent of CO₂ emissions, However, when concentrating process when included in the production process, there is a significant reduction in CO₂ emissions.

The process with freeze concentration and three-stage evaporator (MSE) with spray drying produces roughly 1.4-kilo tons of carbon emissions. When comparing this data with hydropower-based electricity production the carbon emissions are lowered to 40 times when electricity is produced from a clean source like hydropower. Finally, the process with mechanical vapor recompressor and spray dryer results in 0.8-kilo tons of CO₂ emission which is 42 times higher for the same process when compared with a hydropower source.

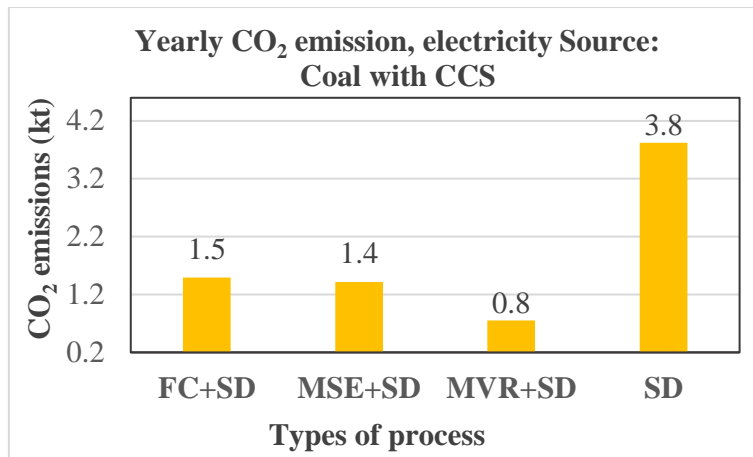


Figure 63: Yearly CO₂ emission, electricity Source: Coal with CCS

From this information, it is very clear how the source of electricity and the energy efficient process plays a significant role in controlling emissions and reducing the environmental impacts. Although, developments in the energy efficient technology are constantly increasing, the industries must operate in a sustainable way by adapting these technology in-order to reduce emissions and to preserve the environment!

Chapter 7: Conclusion

- Production of fish protein hydrolysates using conventional methods is generally an energy-intensive process. In this thesis work, the energy demands in the production of fish protein hydrolysates are investigated in detail using advanced technologies to find the most efficient process. Concentrating and drying technologies are studied together to find an effective combination.
- This investigation was performed with 1-ton RRM processed with 1:1 ratio of water, the hydrolysates are concentrated to 30% with a freeze concentration process, 50% in the three-stage evaporator and mechanical vapor recompression process and further dried using dryers. The energy required with the process with freeze concentration process was around **1120-1250 kWh**. The energy value for the process with three-stage evaporators was around **1160-1180 kWh** and the process with mechanical vapor recompression was around **600-630 kWh**. When compared with the direct drying process, greater energy savings was achieved. The final FPH powders are produced at the rate of 130 kg/h.
- Energy use in the concentration process like freeze concentration, MSE, and mechanical vapor recompression results in lower energy demands. Freeze concentration consumes energy of **273 kJ/kg of water** to freeze and the mechanical vapor recompression evaporator (MVR) has the lowest energy demands value of around **~150 kJ/kg of water** when compared with other processes and provides significant energy savings. The three-stage evaporator is also one of the most energy-efficient ways of evaporating the water from the feed solution. Since the energy or heat possessed in the vapor is reutilized to heat the inlet feed, in this way the energy supplied to the system is reduced significantly. In mechanical vapor recompression, a large amount of heat is transferred with little work and hence energy is recovered in the process.
- Freeze concentration can be used as an effective process in combination with drying to produce the final FPH powder. The freeze concentration method decreases water content, increases shelf-life, stabilizes the quality of food, reduces further energy costs and is suited for heat sensitive products. The two-stage freeze concentration process TWICE can be used to produce a higher concentrated product.
- It is identified that the major consumption of energy occurs in the drying stage. At the drying stage, when analysing the alternative process with freeze drying, spray drying and drum drying, all dryers consume a significant amount of energy between **1.5 to 1.88 kWh/kg of water removed**. Other additional work like Carnot work, vacuum pump work and Carnot COP are calculated. The calculated energy value was well in range as investigated by Baker

and McKenzie for spray drying. Hence, concentrating before final drying reduces the overall energy demands in the production of fish protein hydrolysates.

- Heat pump cycle assisted drying process with spray dryer has significant **energy-saving about 50%**. The simulation results of the transcritical two-stage CO₂ system in Dymola & EES resulted the **heat pump COP of 3.5**. It can be used as an energy recovery solution in the production process of FPH. HTHP can be used as an alternative for evaporation techniques to reduce the energy demand. Finally, the investment analysis resulted a payback time of **4.8 to 5.7 years** for processes with freeze concentration and different dryers, **3.4 to 4.2 years** for processes with three-stage evaporators and dryers and **2 to 2.2 years** for processes with MVR and dryer's combinations.

Chapter 8: Further work

This chapter highlights the suggestions for improvements and further work. Most of the points listed below are related to the extension of the work.

- The concentrating process will be studied in more detail for increasing the concentration level. Technologies like membrane filtration can be studied with the freeze concentrations process.
- Two-stage freeze concentration process: TWICE can be validated for FPH samples to understand the behavior of hydrolysates at higher concentration levels.
- The Transcritical two-stage simulation model performed here is used to analyse the heating applications with the possibility of heat recovery. The system design can be enhanced using ejectors and other configurations in future.
- Simulation models in Modelica/Dymola for different applications will be modelled and analysed. More details on compressor design and parameters can be studied to enhance the performance.
- The absorption ammonia-water cycle will be studied for high temperatures applications.
- The reliability of the system for the different process can be studied and will be validated using Markov analysis.

Bibliography

Petrova, I., Tolstorebrov, I. and Eikevik, T.M., 2018. Production of fish protein hydrolysates step by step: technological aspects, equipment used, major energy costs and methods of their minimizing. *International Aquatic Research*, 10(3), pp.223-241.

Himaya, S.W.A., Ngo, D.H., Ryu, B. and Kim, S.K., 2012. An active peptide purified from gastrointestinal enzyme hydrolysate of Pacific cod skin gelatin attenuates angiotensin-1 converting enzyme (ACE) activity and cellular oxidative stress. *Food Chemistry*, 132(4), pp.1872-1882.

Mujumdar, A.S., 2006. Principles, classification, and selection of dryers. *Handbook of industrial drying*, 3, pp.3-32.

Al-Mansour, H.E., Al-Busairi, B.H. and Baker, C.G.J., 2011. Energy consumption of a pilot-scale spray dryer. *Drying Technology*, 29(16), pp.1901–1910.

Miyawaki, O., Liu, L., Shirai, Y., Sakashita, S. and Kagitani, K., 2005. Tubular ice system for scale-up of progressive freeze-concentration. *Journal of Food Engineering*, 69(1), pp.107-113.

Han, D., Chen, J., Zhou, T. and Si, Z., 2021. Experimental investigation of a batched mechanical vapor recompression evaporation system. *Applied Thermal Engineering*, 192, p.116940.

Schuck, P., Jeantet, R., Tanguy, G., Méjean, S., Gac, A., Lefebvre, T., Labussière, E. and Martineau, C., 2015. Energy consumption in the processing of dairy and feed powders by evaporation and drying. *Drying Technology*, 33(2), pp. 176–184.

Wang, Z., Gong, Y., Wu, X.H., Zhang, W.H. and Lu, Y.L., 2013. Thermodynamic analysis and experimental research of transcritical CO₂ cycle with internal heat exchanger and dual expansion. *International Journal of Air-Conditioning and Refrigeration*, 21(01), p.1350005.

Denisley Bassoli, Starbucks Coffee Company, Chapters in Freeze concentration: Coffee product and economic analysis compared freeze concentration with drying and evaporation techniques, 1989.

Šližytė, R., Carvajal, A.K., Mozuraityte, R., Aursand, M. and Storrø, I., 2014. Nutritionally rich marine proteins from fresh herring by-products for human consumption. *Process Biochemistry*, 49(7), pp.1205–1215

He S., Franco, C. Zhang, W., 2013. Functions, applications and production of protein hydrolysates from fish processing co-products (FPCP). *Food Research International*, 50(1), pp.289–297.

-
- Abejo'n, R., Belleville, M.P., Sanchez-Marcano, J., Garea, A. and Irabien, A., 2018. Optimal design of industrial scale continuous process for fractionation by membrane technologies of protein hydrolysate derived from fish wastes. *Separation and Purification Technology*, 197, pp.137–146.
- Pasupuleti, V.K. and Braun, S., 2008. State of the art manufacturing of protein hydrolysates. *Protein hydrolysates in biotechnology*, pp.11–32.
- Yun, H., Wang, M., Feng, W and Tan, T., 2013. Process simulation and energy optimization of the enzyme-catalyzed biodiesel production. *Energy*, 54, pp. 84–96.
- Kern, D.Q. and Kern, D.Q., 1950. *Process heat transfer (Vol. 5)*. New York: McGraw-Hill.
- Han, D., Si, Z. and Chen, J., 2021. Analysis of an intermittent mechanical vapor recompression evaporation system. *Applied Thermal Engineering*, 193, p.116996
- Ettouney, H., El-Dessouky, H. and Al-Roumi, Y., 1999. Analysis of mechanical vapour compression desalination process. *International journal of energy research*, 23(5), pp. 431–451.
- Darwish, M.A., 1988. Thermal analysis of vapor compression desalination system. *Desalination*, 69(3), pp. 275–295.
- Al-Juwayhel, F., El-Dessouky, H. and Ettouney, H., 1997. Analysis of single-effect evaporator desalination systems combined with vapor compression heat pumps. *Desalination*, 114(3), pp. 253–275.
- Auleda, J.M., Raventós, M., Sánchez, J. and Hernández, E., 2011. Estimation of the freezing point of concentrated fruit juices for application in freeze concentration. *Journal of Food Engineering*, 105(2), pp. 289-294.
- P.J. Fellows, 23 - Freeze drying and freeze concentration, *Food Processing Technology*, Woodhead Publishing Series in Food Science, Technology and Nutrition 2017, Pages 929-945
- Madaeni, S.S. and Zereshki, S., 2008. Reverse osmosis alternative: Energy implication for sugar industry. *Chemical Engineering and Processing: Process Intensification*, 47(7), pp.1075–1080.
- Madaeni, S.S. and Zereshki, S., 2010. Energy consumption for sugar manufacturing. Part I: Evaporation versus reverse osmosis. *Energy Conversion and Management*, 51(6), pp.1270–1276.
- Patel, S. K. and Bade M.H., 2020. Energy targeting and process integration of spray dryer with heat recovery systems. *Energy Conversion and Management*, 221, p.113148

Fröhlich, J. A., Ruprecht, N.A., Hinrichs, J. and Kohlus, R., 2020. Nozzle zone agglomeration in spray dryers: Effect of powder addition on particle coalescence. *Powder Technology*, 374, pp 223–232

Stratta, L., Capozzi, L.C., Franzino, S. and Pisano, R., 2020. Economic analysis of a freeze-drying cycle. *Processes*, 8(11), p.1399.

Almena, A., Goode, K.R., Bakalis, S., Fryer, P.J. and Lopez-Quiroga, E., 2019. Optimising food dehydration processes: energy-efficient drum-dryer operation. *Energy Procedia*, 161, pp.174 -181

Hafner, A., 2019. Compendium master course, Heat pumping processes and systems, TEP 4255, NTNU.

Eikevik, T.M., 2019. Compendium master's course, Heat pumping processes and systems.

Dai, B., Zhao, P., Liu, S., Su, M., Zhong, D., Qian, J., Hu, X. and Hao, Y., 2020. Assessment of heat pump with carbon dioxide/low-global warming potential working fluid mixture for drying process: Energy and emissions saving potential. *Energy Conversion and Management*, 222, p.113225

Bantle, M., Käfer, T. and Eikevik, T.M., 2013. Model and process simulation of microwave assisted convective drying of clipfish. *Applied Thermal Engineering*, 59(1-2), pp.675-682

Angelino, G. and Invernizzi, C., 1995. Prospects for real-gas reversed Brayton cycle heat pumps. *International journal of refrigeration*, 18(4), pp. 272-280

Zühlsdorf, B., Bühler, F., Bantle, M. and Elmegaard, B., 2019. Analysis of technologies and potentials for heat pump-based process heat supply above 150 C. *Energy Conversion and Management: X*, 2, p.100011.

Arpagaus, C., Bless, F., Uhlmann, M., Schiffmann, J. and Bertsch, S.S., 2018. High temperature heat pumps: Market overview, state of the art, research status, refrigerants, and application potentials. *Energy*, 152, pp. 985-1010

De Boer, R., Marina, A., Zühlsdorf, B., Arpagaus, C., Bantle, M., Wik, V., Elmegaard, B., Corberan, J.M. and Benson, J., 2020. Strengthening Industrial Heat Pump Innovation: Decarbonizing Industrial Heat.

van Beek, T., Budde, M. and van Esch, J., 2018. Membrane-Freeze Concentration Hybrid for Temperature-Sensitive Biomolecules. Investigation, Application, and Techno-Economic Benefits. *Chemical engineering & technology*, 41(12), pp.2385-2392.

-
- Bae, S. and Nam, Y., 2022. Economic and environmental analysis of ground source heat pump system according to operation methods. *Geothermics*, 101, p. 102373
- Stratta, L., Capozzi, L.C., Franzino, S. and Pisano, R., 2020. Economic analysis of a freeze-drying cycle. *Processes*, 8(11), p.1399.
- Severine Dett, Lucas Maetz, TWICE, An ice-cold process for highest food concentration, white paper, Sulzer Chemtech, 2020
- Baker, C.G.J, and McKenzie, K.A., 2005, Energy consumption of industrial spray dryers. *Drying Technology*, 23(1-2), pp.365-386.
- Neave, A., 2002. Heat pumps and their applications. In *Plant Engineer's Reference Book* (pp. 41-1). Butterworth-Heinemann.
- Zhang, Q., Liu, X. and Zhang, T., 2021. Exergy investigation of three ideal regeneration methods for liquid desiccant: Thermal air, mechanical vapor recompression and electro dialysis regeneration. *Energy and Buildings*, 249, p. 111258
- Strømman, 2020. TEP4223 Life Cycle Assessment compendium, Master course, NTNU.
- Liao, S.M., Zhao, T.S. and Jakobsen, A., 2000. A correlation of optimal heat rejection pressures in transcritical carbon dioxide cycles. *Applied Thermal Engineering*, 20(9), pp.831-841.
- Sawalha, S., 2008. Theoretical evaluation of trans-critical CO₂ systems in supermarket refrigeration. Part I: Modeling, simulation and optimization of two system solutions. *international journal of refrigeration*, 31(3), pp.516-524.
- Pardinas, A. A., Hafner, A. and Banasiak, K., 2018. Novel integrated CO₂ vapour compression racks for supermarkets. Thermodynamic analysis of possible system configurations and influence of operational conditions. *Applied Thermal Engineering*, 131, pp.1008-1025.
- Kim, M. S., Kang, D.H., Kim, M.S. and Kim, M., 2017. Investigation on the optimal control of gas cooler pressure for a CO₂ refrigeration system with an internal heat exchanger. *International Journal of Refrigeration*, 77, pp.48-59.
- Baek, C., Heo, J., Jung, J., Cho, H. and Kim, Y., 2013. Optimal control of the gas-cooler pressure of a CO₂ heat pump using EEV opening and outdoor fan speed in the cooling mode. *International journal of refrigeration*, 36(4), pp.1276-1284.

Yang, W. W., Cao, X.Q., He, Y.L. and Yan, F.Y., 2017. Theoretical study of a high-temperature heat pump system composed of a CO₂ transcritical heat pump cycle and a R152a subcritical heat pump cycle. *Applied thermal engineering*, 120, pp.228-238

Qin, X., Zhang, F., Zhang, D., Gao, Z. and Tang, S., 2022. Experimental and theoretical analysis of the optimal high pressure and peak performance coefficient in transcritical CO₂ heat pump. *Applied Thermal Engineering*, 210, p.118372

Zhu, Y., Huang, Y., Li, C., Zhang, F. and Jiang, P.X., 2018. Experimental investigation on the performance of transcritical CO₂ ejector–expansion heat pump water heater system. *Energy Conversion and Management*, 167, pp.147-155.

Zheng, L., Deng, J. and Zhang, Z., 2016. Dynamic simulation of an improved transcritical CO₂ ejector expansion refrigeration cycle. *Energy Conversion and Management*, 114, pp. 278–289.

Agrawal, N., Bhattacharyya, S. and Sarkar, J., 2007. Optimization of two-stage transcritical carbon dioxide heat pump cycles. *International Journal of Thermal Sciences*, 46(2), pp. 180–187.

Ju, F., Fan, X., Chen, Y., Ouyang, H., Kuang, A., Ma, S. and Wang, F., 2018. Experiment and simulation study on performances of heat pump water heater using blend of R744/R290. *Energy and Buildings*, 169, pp. 148–156.

Ju, F., Fan, X., Chen, Y., Wang, T., Tang, X., Kuang, A. and Ma, S., 2018. Experimental investigation on a heat pump water heater using R744/R290 mixture for domestic hot water. *International Journal of Thermal Sciences*, 132, pp.1–13.

Yu, B., Yang, J., Wang, D., Shi, J. and Chen, J., 2018. Modeling and theoretical analysis of a CO₂-propane autocascade heat pump for electrical vehicle heating. *International Journal of Refrigeration*, 95, pp. 146–155.

Faria R.N., Nunes, R.O., Koury, R.N.N. and Machado, L., 2016. Dynamic modeling study for a solar evaporator with expansion valve assembly of a transcritical CO₂ heat pump. *International Journal of Refrigeration*, 64, pp.203–13.

Ill´an-Gómez, F., Sena-Cuevas, V.F., García-Cascales, J.R. and Velasco, F.J.S., 2021. Experimental and numerical study of a CO₂ water-to-water heat pump for hot water generation. *International Journal of Refrigeration*, 132, pp.30–44.

Li, H., Yang, Y., Cheng, Z., Sang, Y. and Dai, Y., 2018. Study on off-design performance of transcritical CO₂ power cycle for the utilization of geothermal energy. *Geothermics*, 71, pp.369-379.

Bamigbetan, O., Eikevik, T.M., Neksa, P., Bantle, M. and Schlemminger, C., 2019. Experimental investigation of a prototype R-600 compressor for high temperature heat pump. *Energy*, 169, pp. 730-738

Bamigbetan, O., Eikevik, T.M., Neksa, P. and Bantle, M., 2017. Review of vapour compression heat pumps for high temperature heating using natural working fluids. *International Journal of Refrigeration*, 80, pp. 197–211.

<https://www.ssb.no/en/energi-og-industri/energi/statistikk/elektrisitetspriser>

Dickey, L. C., Craig Jr, J.C., Radewonuk, E.R., McAloon, A.J. and Holsinger, V.H., 1995. Low temperature concentration of skim milk by direct freezing and vacuum evaporation. *Journal of dairy science*, 78(6), pp.1369-1376.

GEA Process Engineering, *Evaporation Technology Using Mechanical Vapour Recompression, Technology and Applications*.

Shu, G., Liang, Y., Wei, H., Tian, H., Zhao, J. and Liu, L., 2013. A review of waste heat recovery on two-stroke IC engine aboard ships. *Renewable and Sustainable Energy Reviews*, 19, pp.385-401.

Shrikant Ahirrao, *Zero Liquid Discharge Solutions, Industrial Wastewater Treatment, Recycling and Reuse*, 2014

Peter Clark, J., 2011. *Processing-Getting a Fix on Freeze Concentration*. *Food Technology-Chicago*, 65(12), p.78.

Georges, L., 2020. TEP4260 - Investment analysis, Heat Pumps for Heating and Cooling of Buildings, NTNU.

Elbarghthi, A.F., Hafner, A., Banasiak, K. and Dvorak, V., 2021. An experimental study of an ejector-boosted transcritical R744 refrigeration system including an exergy analysis. *Energy Conversion and Management*, 238, p.114102

Couper, J.R., 2003. *Process engineering economics*. CRC press.

Toledo, R.T., Singh, R.K. and Kong, F., 2007. *Fundamentals of food process engineering (Vol. 297)*. New York: Springer.

Van't Land, C.M., 2011. *Drying in the process industry*. John Wiley & Sons.

Eikevik, T M., 2021. *Compendium in TEP4265 - Sustainable Food Processing*, NTNU.

Hillestad, M., 2022. TKP4171 -Design of sustainable chemical and biochemical processing plants.

Appendix-1

Experimental preparation of Fish Protein Hydrolysates at industry scale

Laboratory-SINTEF Mobile Sealab, Myre.

Duration: 9-11-21 to 11-11-21



1. RRM inspection (data collecting)



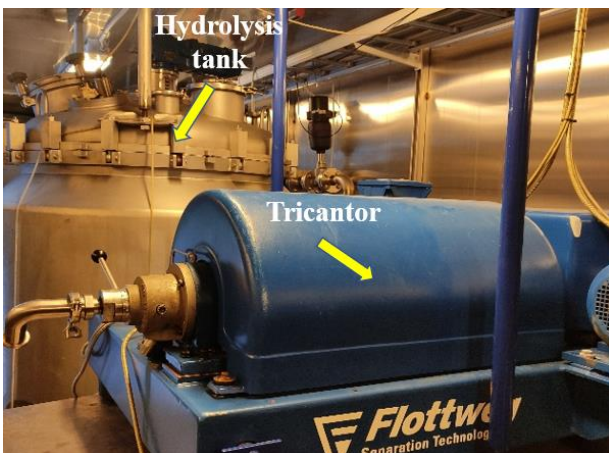
2. Crusher Unit



3. Heat Exchanger



4. Hydrolyses Tank



5. Equipment setup



6. Connecting valves



7. Sample collecting from



8. Container setup



9. Sample collecting



10. Fish protein Hydrolysates



11. Packing



12. Final Sample collection

Appendix 1, a)

**Hydrolysates production, low pressure evaporation analysis and
viscosity measurements at NTNU laboratory**



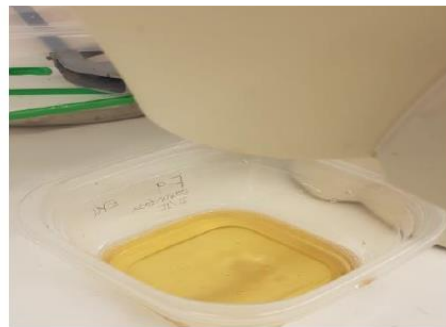
a) Cod Fish heads



b) Hydrolysis process

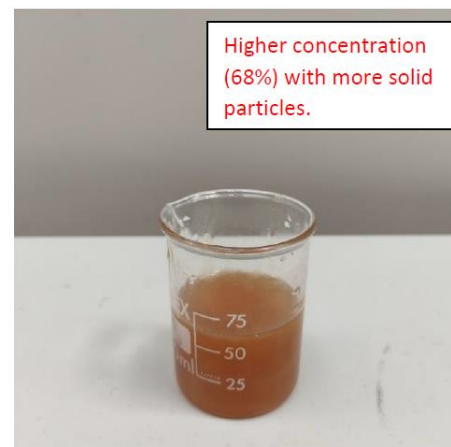


c) Sludge: undissolved proteins

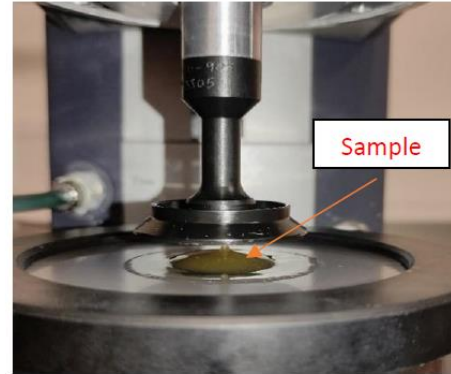
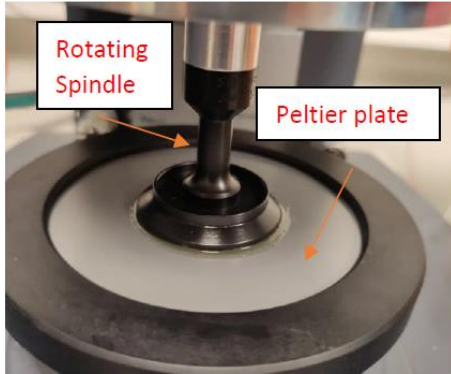


d) Hydrolysates

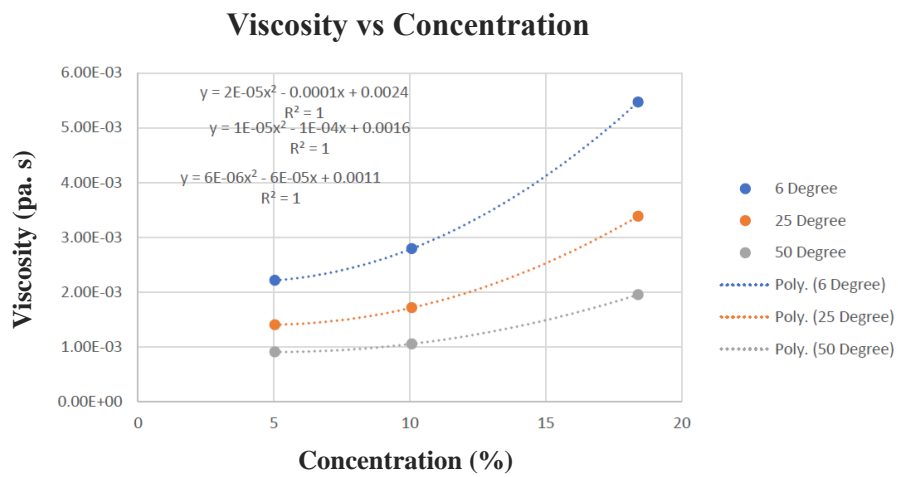
Laboratory production of hydrolysates from white cod fish



Concentrated hydrolysates after low pressure vacuum evaporation process



Rheology measurements of concentrated hydrolysates samples



Viscosity meter results: Concentration vs viscosity



Appendix-2

Freeze concentrator and drying methods calculations



The important process calculation is provided in this chapter, other calculations performed are already described in detail in methods itself.

```
% Calculations of freezing load in Freeze concentration
clc,
clear all;
close all

% Initialization of variables
T=4; % Initial solution temperature
M=1841/3600; %Mass of solution in kg/h

Xw=0.93; %Initial product moisture
Xu=0.0271; % calculated amount of unfreezable water

% Temperature dependent specific heat

CPp1= ((2008+1.2089*(T)+(-0.001)*(T^2))/1000); %specific heat of
protein
CPf1 = ((1984+1.4733*(T)+(-0.0048)*(T^2))/1000);%specific heat of
fat
CPa1 = ((1846+1.8306*(T)+(-0.0465)*(T^2))/1000);%specific heat of
ash
CPw1 = ((4210-1.6297*(T)+(0.0186)*(T^2))/1000);%specific heat of
water

CPnet1=(0.06583*CPp1+0.00217*CPf1+0.002*CPa1+0.93*CPw1);% Net cp,
After seperation

T2=-3; % solution temperature at the end of freezing
L=333.5; % latent heat of ice Kj/kg k

Tf=-0.6; % freezing temperature of solution

CPp2= ((2008+1.2089*(T2)+(-0.001)*(T2^2))/1000);
CPf2 = ((1984+1.4733*(T2)+(-0.0048)*(T2^2))/1000);
CPa2 = ((1846+1.8306*(T2)+(-0.0465)*(T2^2))/1000);
CPw2 = ((4210-1.6297*(T2)+(0.0186)*(T2^2))/1000);
CPi=2.209 %Kj/kgk
%CPice= ((2060+5.6732*(T2)+(-0.0103)*(T2^2))/1000);

CPnet2= (0.0644*CPp2+0.0035*CPf2+0.0021*CPa2+0.93*CPw2);

Delta_H1= (T-Tf)*CPnet1; % sensible heat above freezing point
Delta_H2=(T2-Tf)*(CPnet2-(Xw-Xu)*((L/T2)+(CPw2-CPi))); % sensible
heat below freezing point

H_net= (Delta_H1-Delta_H2)
Q= M*(Delta_H1-Delta_H2)
```

Q=135.5 kW

Spray dryer calculation

```
% From freeze conc.to spray drying (30% solids to 98% solids)

% Initialization of variables
clc,
clear all,

M1=429.5;          % Inlet feed flow rate to the dryer in Kg/h,
S1=0.3*M1;        % Assuming Inlet feed has 30% solids by weight,
W1=M1-S1;
T1=210;           %Heated air temperature
T2=88.39*log10(T1)-112.35; %Exit air temp
TP1=-1;           %Product inlet temp
TP2=T2-TP1;       % product outlet temp
%Mass balance
S2=S1;            % Amount of Solid at inlet equal to amount of solid at
exit feed
M2=S1/.98;        % Mass balance at outlet
W2=M2-S2;         % Water percent by weight at outlet feed
Ev=W1-W2;         %Amount of water to be evaporated

% Heat transfer calculation
Q1 = Ev*(2500+(1.9*T2)-(4.2*TP1)); %Evaporation of water and
heating of watervapor
Q2=S1*4.05*(TP2-TP1);           %The heating of solid, Specific heat
capacity
Q3=W2*4.2*(TP2-TP1);           % heating of remaining water in the
solid,
Qt=Q1+Q2+Q3;                   % Net heat to be supplied.

Qnet=1.25*Qt*((T1-10)/(T1-T2));
y =(Qnet/Ev) % kJ per Kg of water evaporated;
Energy= (y/3600)% Energy demands in kWh/kg of water
```

E=1.65 kWh/kg of water

Rotary Drum drying calculation:

1. Heat to raise the temperature of the feedstock solid,

$$Q_1 = M_{s1} * C_p * (T_h - T_i)$$

M_{s1} = mass of solids in hydrolysates

$$Q_1 = \frac{128.86}{3600} * 3.526 * (100 - (-1))$$

$$Q_1 = 12.8 \text{ kW}$$

2. Heat lost in residual moisture,

$$Q_2 = M_{W2} * (h_{sat liq} - h_1)$$

M_{W2} = mass of water in the exit stream

$$Q_2 = \frac{2.629}{3600} * (419 - (-335.68))$$

$$Q_2 = 0.5 kW$$

3. Heat required to raise water temperature to saturated temperature,

$$Q_3 = M_v * (h_{sat liq} - h_1)$$

M_v = mass of evaporated vapor

$$Q_3 = \frac{298.066}{3600} * (419 - (-335.68))$$

$$Q_3 = 62.5 kW$$

4. Heat required to raise temperature of the water to vapor temperature

$$Q_4 = M_v * (\Delta h)$$

$$Q_4 = \frac{298.066}{3600} * (2256.68)$$

$$Q_4 = 186.84 kW$$

5. Q total

$$Q_{net} = 262.75 kW$$

$$E_{net} = 3173.45 kJ/kg \text{ of water } (262.75 * 3600 / \text{mass of water evaporated})$$

Considering heat loss and energy required for heating the air:

$$Q_{new} = 1.25 * \frac{300 - 10}{300 - 92} * Q_{net}$$

$$Q_{net} = 457.9 \text{ kW}$$

$$E_{net} = 5521.8 \text{ kJ/kg of H}_2\text{O}$$

Energy required during the process in kWh/kg = $Q_{net}/3600$

$$= 1.54 \text{ kWh/kg of water}$$

Vacuum freeze-drying calculation:

1. Freezing energy absorbed by the hydrolysates from -1 °C to -20 °C, (Q_0)

Mass flow in = 430 kg/h (Since the calculated freezing temperature of the hydrolysates is lower than zero, calculation is performed considering above and below sensible heat and latent heat. (Several studies have neglected this part, as is it not so significant))

% After Freeze conc, freezing load absorbed by the feed in vacuum freeze drying.

% From -1 to -20 deg C

% Initialization of variables

T=-1; % final temperature

M=429.566/3600; %Mass of solution in kg/s

Xw=0.7; %Initial product moisture in percent

Xu=0.116; % calculated amount of unfreezable water

%Xu= 0.4*(Xp+Xcc+Xash)

% Temperature dependent specific heat

CPp1= ((2008+1.2089*(T)+(-0.001)*(T^2))/1000); %specific heat of protein

CPf1 = ((1984+1.4733*(T)+(-0.0048)*(T^2))/1000); %specific heat of fat

CPa1 = ((1846+1.8306*(T)+(-0.0465)*(T^2))/1000); %specific heat of ash

CPw1 = ((4210-1.6297*(T)+(0.0186)*(T^2))/1000); %specific heat of water

CPnet1= (0.282*CPp1+0.0093*CPf1+0.00856*CPa1+0.7*CPw1); %Net spe.heat

T2=-20; % initial freezing temp

L=333.5; % latent heat of ice Kj/kg k

Delta_T= ((Xw-1)/(0.0072-(0.140*Xw)));

Tf =0-Delta_T;

```

% Tf=-1; % freezing temperature of solution

CPp2= ((2008+1.2089*(T2)+(-0.001)*(T2^2))/1000);
CPf2 = ((1984+1.4733*(T2)+(-0.0048)*(T2^2))/1000);
CPa2 = ((1846+1.8306*(T2)+(-0.0465)*(T2^2))/1000);
CPw2 = ((4210-1.6297*(T2)+(0.0186)*(T2^2))/1000);
CPi=2.209; %Kj/kgk
%CPice= ((2060+5.6732*(T2)+(-0.0103)*(T2^2))/1000);

CPnet2= (0.282*CPp2+0.0093*CPf2+0.00856*CPa2+0.7*CPw2);

Delta_H1= (T-Tf)*CPnet1; % sensible heat above freezing point
Delta_H2=(T2-Tf)*(CPnet2-(Xw-Xu)*(L/T2)+(CPw2-CPi)); % sensible
heat below freezing point

H_net= (Delta_H1-Delta_H2)
Q= M*(Delta_H1-Delta_H2)

```

$$Q_0 = 213 \text{ kJ/kg}$$

2. Heating Energy for transforming water molecules from solid state to vapor,

$$Q_1 = 2464.024 - (-374.2)$$

Enthalpy values taken from cool pack

$$Q_1 = 2838.2 \text{ kJ/kg}$$

3. Energy for converting vapor to ice in evaporator surface

$$Q_2 = (2838 + (-374.2 - (-411)))$$

$$Q_2 = 2838 + (37.379)$$

$$Q_2 = 2875.6 \text{ kJ/kg}$$

Net Energy requirement,

$$Q_{net} = 5926.14 \text{ kJ/Kg}$$

$$\text{Energy} = Q_{net}/3600$$

$$= 1.65 \text{ kWh/kg of water}$$

Total load capacity,

$$Q_{net} = 0.082 * 5926.14 \text{ kW} \quad (298.066/3600=0.082)$$

$$Q_{net} = 485 \text{ kW}$$

Refrigeration capacity, Q_o

$$Q_o = m \Delta h$$

$$Q_o = 0.082 * 2875.631 \quad (\Delta h = Q_2)$$

$$Q_o = 238 \text{ kW}$$

Carnot COP

Taking $T_c = 30 \text{ }^\circ\text{C}$ and $T_e = -50 \text{ }^\circ\text{C}$

$$COP = \frac{T_L}{T_H - T_L}$$

$$COP = \frac{223}{80}$$

$$COP = 2.78$$

Carnot work:

$$\begin{aligned} W_{car} &= Q_o * \frac{T_c - T_e}{T_e} \\ &= 238.09 * \frac{80}{223} \end{aligned}$$

$$W_{car} = 85.4 \text{ KW}$$

Pump work:

$$\begin{aligned} W &= - \frac{m * nRT_1}{n-1} \left[\left(\frac{P_2}{P_1} \right)^{\frac{n-1}{n}} - 1 \right] \\ W &= - \frac{0.337 * 1.4 * 0.287 * 293}{1.4-1} \left[\left(\frac{0.1}{100} \right)^{\frac{1.4-1}{1.4}} - 1 \right] \end{aligned}$$

$$W = 85.403 \text{ kW}$$

Reference Mass flow of air for 15 kg hydrolysates = 0.0118 kg/s

Hence, air mass flow is calculated based on hydrolysates Mass flow: 298 kg/h

Appendix-3
Three effect Evaporator Calculation

Mass balance:

Mass_1= 1841; % Inlet mass flow into evaporator

X_feed = 0.07; % Percent of solids in the feed

X_product = 0.5; % Percent of solids in the product (50% conc)

Product_M2= Mass_1*(X_feed/X_product)

Vapor_V= Mass_1*(1-(X_feed/X_product)) % Kg/h

Vapor_V1 = Vapor_V/3600 % Kg/s

X_Fraction_percent = (Vapor_V/Mass_1) * 100 % vapor removal in %

Calculation for case 1: 90°C

Heat energy to evaporate 1583 kg/h in kW is given by

$$Q_{net} = M * C_p * \Delta T + M_v * \Delta H$$
$$= \frac{1841}{3600} * 4.05 * (100 - 90) + \frac{1583}{3600} * 2256$$

C_p value is calculated as a function of temperature and composition basis

$$Q_{net} = 1012.7 \text{ kW}$$

Q_{net} in kJ/kg is given by Q_{net} divided by mass of evaporated water in kg/s

$$= 1012.7 / \left(\frac{1583}{3600} \right)$$

$$Q_{net} = 2301.8 \text{ kJ/kg}$$

For three effect evaporator,

$$\mathbf{Q_{net} = 768 \text{ kJ/kg or 338 kW}}$$

Energy required in three effect evaporator is therefore given by

$$Q_{net}/3600$$

$$\mathbf{E=0.21 \text{ kWh/kg of water (i.e 768/3600)}}$$

Cooling load for condensing the vapor,

$$Q_c = M_v(h_3 - h_{liq})$$

Where h₃ is the enthalpy of vapor at third effect (T=60 °C, P=0.2 bar) and h_{liq} is the enthalpy of the liquid at condensing temperature and pressure (0.2 bar and 30 °C)

$$Q_c = 0.15 (2611 - 125.2)$$

$$\mathbf{Q_c = 374 kW}$$

Appendix-4

Summary of energy demands in different processes

(Temperature levels and state initialization is already described in methods).

1. Calculation of overall energy demands in **direct drying process**.

Energy required to concentrate 1 ton/h of RRM				
		Process with direct drying		
	Thawing	78.8		
	Heating to hydrolysis Temp	87.7		
	Sterilization	87.3		
	Cooling to storage temp (0°C)	186.4		
Spray Drying		2743	-	-
Drum drying		-	2518	-
Vacuum freeze drying		-	-	2875
	Net energy required (kWh)	3183	2958	3315

2. Overall energy demands in **freeze conc. process with drying methods**.

Energy required to concentrate 1 ton/hr of RRM				
	Process with Freeze concentrator	Energy requirement		
	Thawing	78.8		
	Heating to hydrolysis Temp	87.7		
	Sterilization	87.3		
	Cooling to 4°C	178		
Freeze Conc. process	Freezing hydrolysates	135.5		
	Melting ice and other requirement	178		
Spray Drying		500	-	-
Drum drying		-	458	-
Vacuum freeze drying		-	-	485
	Net energy required (kWh)	1245.3	1124.5	1230

3. Overall energy demands in **three effect evap. with drying methods**.

Energy required to concentrate 1 ton/h of RRM				
	Process with Three stage evaporator	Energy requirement		
	Thawing	78.8		
	Heating to hydrolysis Temp	87.7		
	Sterilization	87.3		
MSE (60%)	Heat energy	338		
	Condensing vapor	364		
Spray Drying		225	-	-
Drum drying		-	202	-
Vacuum freeze drying		-	-	207
	Net energy required (kWh)	1182	1158	1163

4. Overall energy demands in **MVR process with drying methods.**

Energy required to concentrate 1 ton/h of RRM				
		Process with MVR		
	Thawing	78.8		
	Heating to hydrolysis Temp	87.7		
	Sterilization	87.3		
MVR (50%)	Minimum energy requirement	150		
Spray Drying		225	-	-
Drum drying		-	202	-
Vacuum freeze drying		-	-	207
	Net energy required (kWh)	629	606	611

Appendix-5

Process components modelled in 3D Images

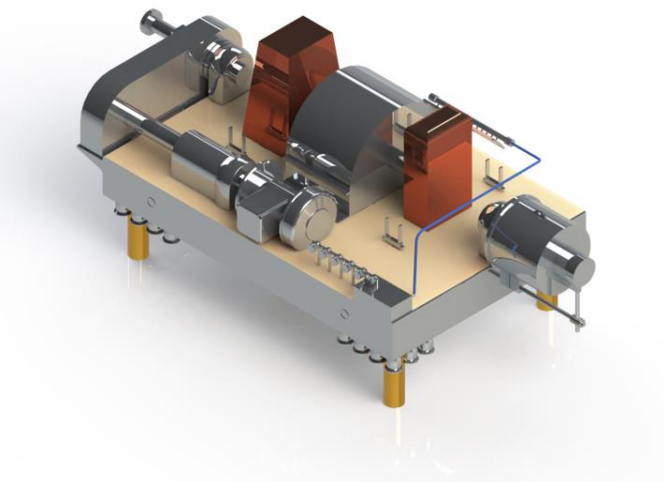
Three stage evaporator



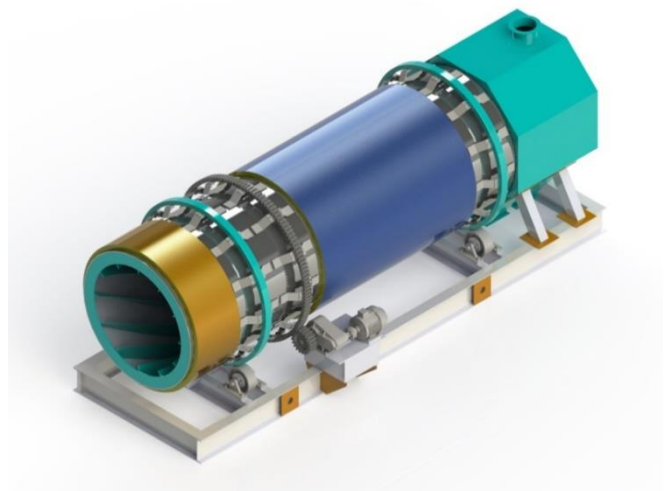
Mechanical vapor recompressor



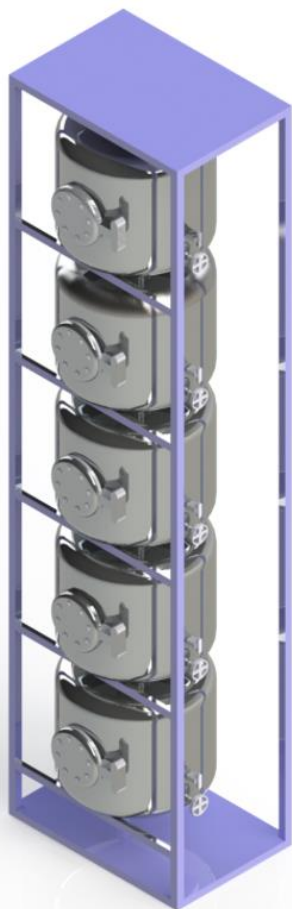
Centrifuge Polisher



Rotary Drum drying



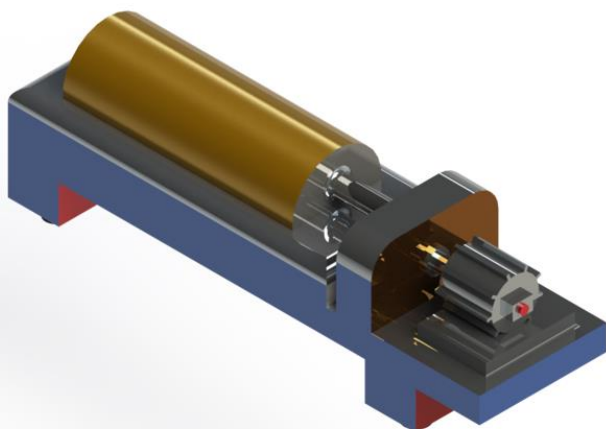
Hydrolysis Tank



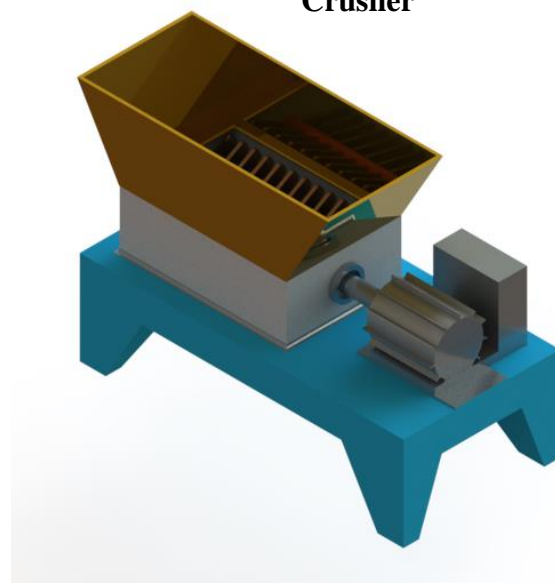
Spray dryer



Tricantor



Crusher



Appendix-6

Economic analysis MATLAB script:

```

clear all
close all

% Process with Freeze conc.and with spray Drying

r=5/100;           % Rate of interest taken 5 %
n=20;             % Number of years
a=(r/(1-(1+r)^-n)); % Annuity factor
E=3183*5000;      % Operating Energy demand per year
energy_p=0.36;    % Energy price in NOK

I=63269910;       % Process 1 investment cost
MC_s=I*(5/100);   % Maintenance cost 5 percent

AC_s=(I*a)+(E*energy_p)+(MC_s); % Net Annual costs

%Additional equipment investment

If=14625000;      % Investment cost of freeze concentrator
in NOK
Is=63269910;

Et=1245.3*5000;  % Operating Energy demand with combined
equipment

MC_t=(If+Is)*(5/100); % Maintenance cost 5 percent

AC_t=(If*a)+(Is*a)+(Et*energy_p) +(MC_t); % Net Annual costs

B=(E*energy_p-Et*energy_p)+(MC_s-MC_t); % Net annual savings
(annual cost reduction plus maintenance)
Io=(If+Is)-I;    %Additional investment costs

% Payback time determination
PB_FC_SD=Io/B

%FC with Drum Drying

r=5/100;           % Rate of interest taken 5 %
n=20;             % Number of years
a=(r/(1-(1+r)^-n)); % Annuity factor
E=2958*5000;      % Operating Energy demand per year
energy_p=0.36;    % Energy price in NOK

I=61666110;       % process with Drum dryer investment
cost
MC_s=I*(5/100);   % Maintenance cost 5 percent of
investment cost

AC_s=(I*a)+(E*energy_p)+(MC_s); % Net Annual costs

%Additional equipment investment

```

```

If=14625000;           % Investment cost of freeze concentrator
in USD
Is=61666110;

Et=1124.3*5000;       % Operating Energy demand with combined
equipment

MC_t=(If+Is)*(5/100); % Maintenance cost 5 percent

AC_t=(If*a)+(Is*a)+(Et*energy_p) +(MC_t); % Net Annual costs

B=(E*energy_p-Et*energy_p)+(MC_s-MC_t); % Net annual savings
(annual cost reduction plus maintenance)
Io=(If+Is)-I;         %Additional investment costs

%Payback time determination
PB_FC_DD=Io/B

% FC with Vacuum freeze Drying

r=5/100;               % Rate of interest taken 5 %
n=20;                 % Number of years
a=(r/(1-(1+r)^-n));   % Annuity factor
E=3315*5000;          % Operating Energy demand per year
energy_p=0.36;        % Energy price in dollar

I=68615910;           % Vacuum freeze dryer investment cost
MC_s=I*(5/100);       % Maintenance cost 5 percent of
investment cost

AC_s=(I*a)+(E*energy_p)+(MC_s); % Net Annual costs

% Additional equipment investment

If=14625000;           % Investment cost of freeze concentrator
in NOK
Is=68615910;

Et=1230*5000;         % Operating Energy demand with combined
equipment

MC_t=(If+Is)*(5/100); % Maintenance cost 5 percent

AC_t=(If*a)+(Is*a)+(Et*energy_p) +(MC_t); % Net Annual costs

B=(E*energy_p-Et*energy_p)+(MC_s-MC_t); % Net annual savings
(annual cost reduction plus maintenance)
Io=(If+Is)-I;         %Additional investment costs

% Payback time determination
PB_FC_FD=Io/B

```

```

%Process with 3 stage evaporator and spray Drying

r=5/100;           % Rate of interest taken 5 %
n=20;             % Number of years
a=(r/(1-(1+r)^-n)); % Annuity factor
E=3183*5000;      % Operating Energy demand per year
energy_p=0.36;    % Energy price in NOK

I=63269910;       % spray dryer investment cost
MC_s=I*(5/100);   % Maintenance cost 5 percent of
investment cost

AC_s=(I*a)+(E*energy_p)+(MC_s); % Net Annual costs

%Additional equipment investment

If=11250000;      % Investment cost of 3 stage evaporator
in NOK
Is=63269910;

Et=1182*5000;    % Operating Energy demand with combined
equipment

MC_t=(If+Is)*(5/100); % Maintenance cost 5 percent

AC_t=(If*a)+(Is*a)+(Et*energy_p) +(MC_t); % Net Annual costs

B=(E*energy_p-Et*energy_p)+(MC_s-MC_t); % Net annual savings
(annual cost reduction plus maintenance)
Io=(If+Is)-I;    %Additional investment costs

% Payback time determination
PB_3EV_SD=Io/B

% 3 stage evaporator with drum Drying

r=5/100;           % Rate of interest taken 5 %
n=20;             % Number of years
a=(r/(1-(1+r)^-n)); % Annuity factor
E=2958*5000;      % Operating Energy demand per year
energy_p=0.36;    % Energy price in NOK

I=61666110;       % Process with Drum dryer investment
cost
MC_s=I*(5/100);   % Maintenance cost 5 percent of
investment cost

AC_s=(I*a)+(E*energy_p)+(MC_s); % Net Annual costs

```

```

%Additional equipment investment

If=11250000;           % Investment cost of 3 stage evaporator
in NOK
Is=61666110;

Et=1158*5000;         % Operating Energy demand with combined
equipment

MC_t=(If+Is)*(5/100); % Maintenance cost 5 percent

AC_t=(If*a)+(Is*a)+(Et*energy_p) +(MC_t); % Net Annual costs

B=(E*energy_p-Et*energy_p)+(MC_s-MC_t); % Net annual savings
(annual cost reduction plus maintenance)
Io=(If+Is)-I;         %Additional investment costs

% Payback time determination
PB_3EV_DD=Io/B

% 3 stage evaporator with Vacuum freeze Drying

r=5/100;              % Rate of interest taken 5 %
n=20;                 % Number of years
a=(r/(1-(1+r)^-n));  % Annuity factor
E=3315*5000;         % Operating Energy demand per year
energy_p=0.36;       % Energy price in NOK

I=68615910;          % process with Drum dryer investment
cost
MC_s=I*(5/100);      % Maintenance cost 5 percent of
investment cost

AC_s=(I*a)+(E*energy_p)+(MC_s); % Net Annual costs

%Additional equipment investment

If=11250000;           % Investment cost of 3 stage evaporator
in NOK
Is=68615910;

Et=1163*5000;         % Operating Energy demand with combined
equipment

MC_t=(If+Is)*(5/100); % Maintenance cost 5 percent

AC_t=(If*a)+(Is*a)+(Et*energy_p) +(MC_t); % Net Annual costs

B=(E*energy_p-Et*energy_p)+(MC_s-MC_t); % Net annual savings
(annual cost reduction plus maintenance)
Io=(If+Is)-I;         %Additional investment costs

```

```

% Payback time determination
PB_3EV_VFD=Io/B

% Process with MVR evaporator and spray Drying

r=5/100;           % Rate of interest taken 5 %
n=20;             % Number of years
a=(r/(1-(1+r)^-n)); % Annuity factor
E=3183*5000;      % Operating Energy demand per year
energy_p=0.36;    % Energy price in NOK

I=63269910;       % Process with Spray dryer investment
cost
MC_s=I*(5/100);   % Maintenance cost 5 percent of
investment cost

AC_s=(I*a)+(E*energy_p)+(MC_s); % Net Annual costs

%Additional equipment investment

If=9000000;       % Investment cost of MVR in NOK
Is=63269910;

Et=629*5000;     % Operating Energy demand with combined
equipment

MC_t=(If+Is)*(5/100); % Maintenance cost 5 percent

AC_t=(If*a)+(Is*a)+(Et*energy_p) +(MC_t); % Net Annual costs

B=(E*energy_p-Et*energy_p)+(MC_s-MC_t); % Net annual savings
(annual cost reduction plus maintenance)
Io=(If+Is)-I;    %Additional investment costs

% Payback time determination
PB_MVR_SD=Io/B

% MVR evaporator with Drum Drying

r=5/100;           % Rate of interest taken 5 %
n=20;             % Number of years
a=(r/(1-(1+r)^-n)); % Annuity factor
E=2958*5000;      % Operating Energy demand per year
energy_p=0.36;    % Energy price in NOK

I=61666110;       % Drum dryer investment cost
MC_s=I*(5/100);   % Maintenance cost 5 percent of
investment cost

AC_s=(I*a)+(E*energy_p)+(MC_s); % Net Annual costs

```

```

%Additional equipment investment

If=9000000;           % Investment cost of MVR in NOK
Is=61666110;

Et=606*5000;         % Operating Energy demand with combined
equipment

MC_t=(If+Is)*(5/100); % Maintenance cost 5 percent

AC_t=(If*a)+(Is*a)+(Et*energy_p) +(MC_t); % Net Annual costs

B=(E*energy_p-Et*energy_p)+(MC_s-MC_t); % Net annual savings
(annual cost reduction plus maintenance)
Io=(If+Is)-I;        %Additional investment costs

% Payback time determination
PB_MVR_DD=Io/B

% MVR evaporator with Vacuum freezee Drying

r=5/100;             % Rate of interest taken 5 %
n=20;               % Number of years
a=(r/(1-(1+r)^-n)); % Annuity factor
E=3315*5000;        % Operating Energy demand per year
energy_p=0.36;      % Energy price in NOK

I=68615910;         % Vaccum freeze dryer investment cost
MC_s=I*(5/100);    % Maintenance cost 5 percent of
investment cost

AC_s=(I*a)+(E*energy_p)+(MC_s); % Net Annual costs

%Additional equipment investment

If=9000000;           % Investment cost of MVR in NOK
Is=68615910;

Et=611*5000;         % Operating Energy demand with combined
equipment

MC_t=(If+Is)*(5/100); % Maintenance cost 5 percent

AC_t=(If*a)+(Is*a)+(Et*energy_p) +(MC_t); % Net Annual costs

B=(E*energy_p-Et*energy_p)+(MC_s-MC_t); % Net annual savings
(annual cost reduction plus maintenance)
Io=(If+Is)-I;        %Additional investment costs

% Payback time determination
PB_MVR_VFD=Io/B

```

Appendix-6, a
Economic analysis Summary table

1. Economic data of drying process with alternatives combination of freeze conc. and drying methods.

Cost in NOK	Process with Direct Spray drying	Process with Freeze conc+spray drying	Process with Direct Drum drying	Process with Freeze conc+Drum drying	Process with Direct Vacuum freeze drying	Process with Freeze conc+vacuum freeze drying
Net investment cost	63269910	83651535	61666110	82047735	68615910	88997535
Energy value in kWh	3183	1245.3	2958	1124	3315	1230
Energy cost per year	5729400	2241540	5324400	2023200	5967000	2214000
Maintenance cost (5%)	3163496	4182577	3083306	4102387	3430796	4449877
PB time (years)		5.3		5.7		4.8
Depreciation cost per year	3005321	3973448	2929140	3897267	3259256	4227383

2. Economic data of drying process with alternatives combination of 3 stage evaporator (3SEV) and drying methods.

Cost in NOK	Process with Direct Spray drying	Process with 3 stage evap+spray drying	Process with Direct Drum drying	Process with 3 stage evap+Drum drying	Process with Direct Vaccum freeze drying	Process with 3 stage evap+vaccum freeze drying
Net investment cost	63269910	76634910	61666110	75031110	68615910	81980910
Energy value in kWh	3183	1182	2958	1158	3315	1163
Energy cost per year	5729400	2127600	5324400	2084400	5967000	2093400
maintenance cost per year	3163496	3831746	3083306	3751556	3430796	4099046
PB time (years)		3.7		4.2		3.4
Depreciation cost per year	3005321	3640158	2929140	3563978	3259256	3894093

3. Economic data of drying process with alternatives combination of mechanical vapor recompression (MVR) and drying methods.

Cost in NOK	Process with Direct Spray drying	MVR+spray drying	Direct Drum drying	MVR+Drum drying	Direct Vaccum freeze drying	MVR+vaccum freeze drying
Net investment cost	63269910	73961910	61666110	72358110	68615910	79307910
Energy value in kWh	3183	629	2958	606	3315	611
Energy cost per year	5729400	1132200	5324400	1090800	5967000	1099800
Maintenance cost per year	3163496	3698096	3083306	3617906	3430796	3965396
PB time (years)	2.17		2.37		2.03	
Depreciation cost per year	3005321	3513191	2929140	3437010	3259256	3767126

Appendix-7

"Transcritical two stage CO₂ system EES code"

"Evaporating pressure"

Pe=25

" Pressure inside intermediate pressure receiver"

Pin=40

"Condensing pressure"

Ph=100

"Calculated Heat load at evaporator"

Qe=107

"Thermodynamic properties at state point 1"

T1s=t_sat(R744,P=Pe)

T1=T1s+5

h1=enthalpy(R744,T=T1,P=Pe)

s1=entropy(R744,T=T1,P=Pe)

s2=s1

"Compressor efficiency"

eff=0.75

"Thermodynamic properties at state point 2"

h2s=enthalpy(R744,s=s2,P=Pin)

h2=(h2s-h1)/eff+h1

" Temperature of Intermediate pressure receiver calculated from pressure"

Tin=28.8

"Thermodynamic properties at state point 3 and 4"

h3=enthalpy(R744,T=Tin,P=Pin)

s3=entropy(R744,T=Tin,P=Pin)

h4s=enthalpy(R744,s=s3,P=Ph)

T4=temperature(R744,P=Ph,h=h4)

h4=(h4s-h3)/eff+h3

"Properties of hydrolysates at gas cooler"

Tw1=10

Pw1=1

Tw2=50

"Calculated properties of hydrolysates"

h1w=enthalpy(Water,T=Tw1,P=Pw1)

h2w=enthalpy(Water,T=Tw2,P=Pw1)

"Thermodynamic properties at remaining state points"

h5=h1w+h4-h2w

T5=temperature(R744,P=Ph,h=h5)

T6=15

h6=enthalpy(R744,T=T6,P=Ph)

$h_7 = h_6$ "Expansion process "

$h_8 = \text{enthalpy}(R744, x=0, P=Pin)$

$h_9 = h_8$

$T_9 = \text{temperature}(R744, P=Pe, h=h_9)$

"Mass flow rate at lower side"

$m_{R_low} = Q_e / (h_1 - h_9)$

"Mass flow rate at higher side"

$m_{R_high} = (m_{R_low} * (h_2 - h_8)) / (h_3 - h_7)$

"Work done by compressor 1 at lower side"

$w_{c1} = m_{R_low} * (h_2 - h_1)$

"Work done by compressor 2 at top side"

$w_{c2} = m_{R_high} * (h_4 - h_3)$

"Net work done by both compressors "

$w_{tot} = w_{c1} + w_{c2}$

"Heat load at gas cooler "

$Q_g = m_{R_high} * (h_4 - h_5)$

"Heat load at sub cooler "

$Q_m = m_{R_high} * (h_5 - h_6)$

"Refrigeration COP"

$COP_R = Q_e / w_{tot}$

Appendix-8

"High Temperature Heat pump system EES code"

"Evaporating pressure"

Pe=6.3

"Thermodynamic properties at state point 1 to 2"

T1=temperature(R290,P=Pe,x=1)

h1=enthalpy(R290,P=Pe,x=1)

T2=10

h2=enthalpy(R290,P=Pe,T=T2)

s2=entropy(R290,T=T2,P=Pe)

s2=s3

"Compressor efficiency"

eff=0.75

"Propane condensing pressure at cascade HX "

Pc=22

"Thermodynamic properties at other state points "

h3s=enthalpy(R290,s=s3,P=Pc)

h3=((h3s-h2)/eff)+h2

h4=enthalpy(R290,x=0,P=Pc)

h5=h1+h4-h2

h6=h5 "Expansion process "

"Interstage heat exchanger pressure "

Pin=6.2

"Thermodynamic properties at other state points "

h7=enthalpy(R600,x=1,P=Pin)

h8=enthalpy(R600,T=T8,P=Pin)

s8=entropy(R600,T=T8,P=Pin)

s9=s8

T8=75

" Butane Condensing pressure "

Ph=23

"Thermodynamic properties at other state points "

h9s=enthalpy(R600,s=s9,P=Ph)

h9=((h9s-h8)/eff)+h8

h10=enthalpy(R600,x=0,P=Ph)

h11=h7+h10-h8

h12=h11 "Expansion process "

T3=temperature(R290,P=Pc,x=1)

T4=temperature(R290,P=Pc,x=0)

T9=temperature(R600,P=Ph,h=h9)

T6=temperature(R290,P=Pe,h=h6)

T7=temperature(R600,P=Pin,x=1)
T12=temperature(R600,P=Pin,h=h12)

"Heat Load "
Qc=350

"Butane mass flow rate "
mh=Qc/(h9-h10)

"Propane mass flow rate "
ml=mh*(h7-h12)/(h3-h4)

"Cooling load at evaporator "
Qe=ml*(h1-h6)

"Work done by compressor 1 "
W1=ml*(h3-h2)

"Work done by compressor 2 "
W2=mh*(h9-h8)

"COP of heat pump "
COP_h=Qc/(W1+W2)

Appendix-9

"Scientific Paper and Award"

Application Of Refrigeration Technologies For Energy Efficient Production Of Fish Protein Hydrolysates

Prem Kumar SHERMAN^(a), Ignat TOLSTOREBROV^(a), Kristina N. WIDELL^(b), Armin HAFNER^(a), Tom Ståle NORDTVEDT^(b)

^(a) Norwegian University of Science and Technology
Trondheim, 7491, Norway, premks@stud.ntnu.no

^(b) SINTEF Ocean
Trondheim, 7465, Norway, Kristina.Widell@sintef.no

ABSTRACT

Fish protein hydrolysate (FPH) is one of the most efficient and sustainable way to recover the valuable nutrients from fish remaining materials and has a widespread application. However, the production of FPH demands intensive heating and cooling loads in the temperature range between 0 and 90 °C. In addition, the stabilization of FPH using conventional moisture removal techniques like spray drying and evaporators is energy intensive due to low solid content. This study investigates application of refrigeration technologies and heat pumps to determine sustainable and energy efficient methods for processing and stabilization of FPH. The freeze concentration, vacuum-concentration and freeze-drying processes were investigated in combination with energy recovery at high temperatures (heating and sterilization). The overall comparison of production lines with respect to the energy savings of different techniques was presented. **Keywords:** Fish protein hydrolysates (FPH), Industrial drying techniques, vacuum freeze concentrator, vacuum drying, Heat pump drying, Energy savings.

1. INTRODUCTION

Fishing sectors produce significant amount of fish rest raw materials which greatly contribute to environmental impacts owing to its disposal factor. These by products are used for low value products in the market. However, the high protein source of fish waste and its by-products can be used to produce valuable products like Fish Protein Hydrolysates (FPH) ([Desai et al., 2022](#)).

The liquid state of FPH has a high water content, which is relatively unstable and reduces shelf life. Hence long-term storage and transport is not possible. The removal of moisture from FPH is complicated and expensive. Drying can be performed using spray dryers, drum dryers which remove the moisture down to 1-3% ([Petrova et al., 2018](#)). Conventionally, spray dryers are widely used in industries, but they are large energy consumers, with energy consumption up to 11.5 MJ/kg of water removed ([Mujumdar 2007](#)). With the efficient techniques the specific energy consumption was reduced upto 5.5MJ/kg of evaporated water ([Mansour et al., 2011](#)). Several studies reported vacuum freeze-drying method is suitable for temperature sensitive products.

Evaporation methods can be used for concentrating the FPH as well. Among the energy efficient techniques, multistage evaporation (MSE) method, Mechanical vapor recompression (MVR) method, energy reduction is mentioned. Han et al. ([2021](#)) experimentally investigated the MVR system and concluded that with two effect evaporator 40% more energy saving was achieved when compared with single-stage MVR system. Jeantet et al. ([2015](#)) studied the energy consumption in the processing of dairy and feed powders by vacuum evaporation and spray drying methods and established calculation models in computing the energy consumption in the dairy industry. They observed that, to produce 1 kg of dairy powders the energy costs were 6.1 MJ/kg powder for pregelatinized starch and soy protein concentrate respectively.

Concentration processes must be performed before the final stages of product drying to lower the drying cost. Freeze concentration technique is performed to lower the overall energy consumption rate in the production of FPH. Miyawaki et al. ([2005](#)) in their research work reported, that the freeze concentrators

consume energy of around $\sim 0.3\text{MJ/kg}$ of water to freeze. Heat pumps are energy efficient technologies which can be used to provide integrated cooling and heating. Using heat pumps, waste heat from other processes can be recovered and can be upgraded and reused effectively. Studies related to integrated heat pump application system in the production of fish protein hydrolysates process is limited. From the above literature review, it is identified that research findings related to energy conservation and application of heat pumps in the production of fish protein hydrolysates are available in scanty. Hence, in this present study, the main objective is to identify the energy use in each process, identifying the process with high energy use and suggesting the energy reduction measures.

2. EXPERIMENTAL METHODS

The process flow diagram of the production of fish protein hydrolysates with different concentration and drying alternative techniques is given in Figure 1. To have a better view on energy use, the concentrating methods are compared in combination with drying methods. Conventional methods like spray drying and evaporators are compared with methods like freeze concentration, vacuum freeze drying, and heat pump assisted drying. The energy study involves a detailed investigation of freeze concentration, evaporation in the concentrating process and drying using spray drying method, vacuum freeze drying, rotary drum drying, heat pump assisted drying.

The study was performed for 1000 Kg/h of rest raw material (RRM) and 1000 kg/h of water (1:1 ratio). At all levels, the mass flow and energy flows were analysed. The initial composition of RRM is given in Table 1: (Petrova 2018). Two types of RRM (chilled and frozen) were used in the production of hydrolysates. The frozen RRM is first thawed from a lower temperature of $-18\text{ }^{\circ}\text{C}$ to $10\text{ }^{\circ}\text{C}$. Once the RRM is thawed, the next step involves grinding and mincing with water. The pre-treatment process was same for all the processing methods. During the hydrolysis process, the solution was heated to hydrolysis temperature of $50\text{ }^{\circ}\text{C}$ and the enzymes were added to the RRM mixture.

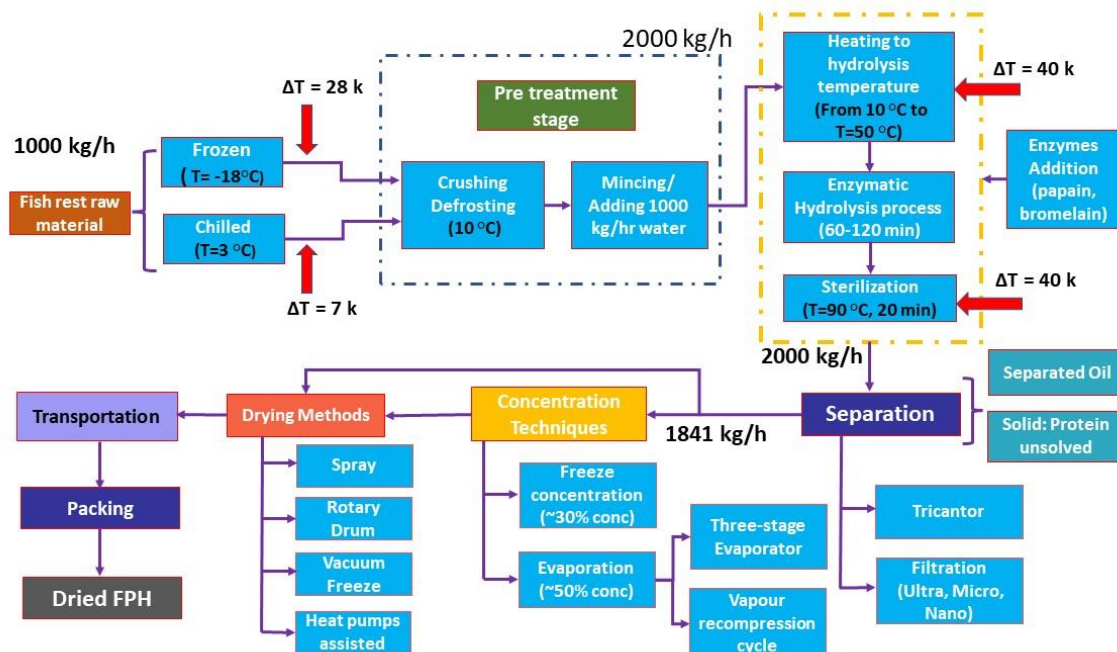


Figure 1: General process flow diagram in production of fish protein hydrolysates

Heating the mixture to the hydrolysis temperature consumes significant amount of energy. After the completion of the hydrolysis process, the temperature of the solution is pasteurized at temperature of $90\text{ }^{\circ}\text{C}$ and the mixture was stirred for another 15-20 mins. The RRM water - mixture is then fed into the separation

process. In the calculation, it was considered to have approximately 7% solids with 6.5% protein content in the FPH after separation. The protein unsolved mixture has 80% protein and 20% water. The composition of the final LPH after separation is given in Table 1.

Table 1: Composition of rest raw material and hydrolysates after separation

RRM initial composition (1000 kg/h)	Percent	Liquid FPH after separation (1841 kg/h)	Percent
Water (W)	77.7	Water	93
Protein (P)	14.6	Protein	6.583
Fats (F)	0.4	Fats	0.217
Ash (A)	7.3	Ash	0.2

2.1. Freeze concentration process.

Freeze concentration is a technique that involves freezing and removal of water by fractional crystallization of water into ice. The hydrolysates were initially cooled to +4 °C from 90 °C in the freeze concentration process. In the process, the inlet mass flow rate was 1841 kg/h, the hydrolysates are concentrated at 30 % solids from the initial feed temperature of +4 °C to the final freezing temperature of -3 °C. Above the freezing temperature, the enthalpy change can be calculated as follows, by evaluating C_p above freezing point.

$$\Delta h_T = (T - T_f) * C_p \quad \text{Eq. (1)}$$

T and T_f represents initial and final freezing temperature in degree Celsius or kelvin. The specific heat C_p value was calculated as the sum of C_p values of individual products. Below the freezing point, the change in enthalpy, Δh was calculated as follow,

$$\Delta h_{T, \text{frozen}} = (T - T_f) * (C_p - (x_w - x_{un,w})) * \left(\frac{L}{T} + (C_{p,w} - C_{p,ice}) \right) \quad \text{Eq. (2)}$$

Where L represents the latent heat of ice (333.5 kJ/kg), $C_{p,w}$, $C_{p,ice}$ represents the heat capacity of water and ice respectively which was calculated as a function of temperature, the total change in enthalpy is given by,

$$\Delta h_{total} = \Delta h_T - \Delta h_{T, \text{frozen}} \quad \text{Eq. (3)}$$

Net heat load to be removed to freeze the product in kW was calculated as follow, Where M is the mass flow rate in kg/s.

$$Q_c = M * \Delta h_{total} \quad \text{Eq. (4)}$$

During the process, the heat required to melt the ice formed in freeze concentration process must be accounted. The Carnot COP and refrigeration work operating at $T_h = 0$ °C and $T_l = -40$ °C are calculated. Where T_h and T_l represents the higher and lower temperature, respectively.

2.2. Evaporation using three stage evaporation and mechanical vapor recompression.

In the evaporation process, the final solid content in concentrate was considered to be 50% for calculation. Higher solid content increases the viscosity of the product, and the evaporation process is more difficult to perform as studied in laboratory experiments. The mass flow rate of hydrolysates into the evaporator at concentration stage was at 1841 kg/h. In three stage evaporator, the vapor from the previous stage was used as a heating medium in the next stage which reduces the energy demand. The inlet temperature of hydrolysates was considered in two cases in the multistage evaporator, case 1: 90 °C, since the process is continuous and the temperature after the separation is expected to be 90 °C with no heat loss. In case 2, the hydrolysates are processed to storage temperature of 0°C. The amount of heat required to evaporate the water is given by the heat energy required to raise the feed temperature to boiling point (100 °C) and the latent heat required to evaporate from liquid to vapor which is given by,

$$Q_{net} = M * C_p * \Delta T + M_v * \Delta H \quad \text{Eq. (5)}$$

For a three-stage evaporator, the total heat value is divided by the number of stages (three) for approximation. The mass flow rate out of the evaporator and the vapor removed are calculated using energy

and mass balances. Heat load to be removed from the condensing vapor is given below, where h_3 is the enthalpy of vapor at third effect and h_{liq} is the enthalpy of the liquid at condensing temperature and pressure (0.2 bar and 30 °C).

$$Q_c = M_v(h_3 - h_{liq}) \quad \text{Eq. (6)}$$

In mechanical vapor recompression system, the vapor from the feed solution is heated using a compressor or a blower fan which increases the pressure and the temperature sufficiently for energy transfer. The energy possessed by the vapor is reutilized for heating the feed. The cycle operates at higher pressure 1.5 bar. A reheater can also be employed at the exit of the compressor based on the temperature requirements. The required heat energy to evaporate the moisture and to concentrate the feed is provided by the necessary work input to the system. The work input in kJ/kg in the vapor compression cycle is provided by,

$$W = \frac{h_{2s} - h_1}{n_{is}} \quad \text{Eq. (7)}$$

2.3. Drying Techniques

In spray drying, the heat input (Q_t) required to evaporate the water includes (i) the heat required for sensibly heating the liquid-phase and evaporating the water, (ii) heat required for heating the solids in the feed, (iii) the amount of heat required to raise the temperature of the remaining water in the product. Additional heat required for heating the air from ambient temperature has to be considered as follows, where T_1 , T_2 is the inlet and exit air temperature respectively.

$$Q_{net} = 1.25 * Q_t * \left[\frac{T_1 - T_{air}}{T_1 - T_2} \right] \quad \text{Eq. (8)}$$

In rotary drum drying, the heat source air temperature was 300 °C and the hydrolysates are concentrated to ~98% solids. The required heat is provided by the exchange of heat between the hot air and the product. The following assumptions are included in the analysis, (i) Heat to raise the temperature of the feedstock solid. (ii) Heat lost in residual moisture; (iii) heat carried away by the amount of moisture present in the exit feed. (iv) The heat required to raise water temperature to saturated temperature. (v) The heat required to raise the temperature of the water to vapor temperature, is given by the product of the mass of vapor to the latent energy, (vi) heat loss and additional energy required for heating the air.

In vacuum freeze-drying, the sublimation of the product occurs at -20 °C inside the freezing chamber at pressure ~1.0 mbar. The product is frozen from initial feed temperature to temperature of -20 °C. After this sublimation of ice occurs, which results in the direct phase change of ice into vapor without liquid phase. The heat energy required during the process will be the difference in enthalpy between the saturated solid state to the saturated gas state of water at -20 °C and 1 mbar. The freezing load is provided by the refrigeration capacity to transform water vapor to ice on the evaporating surface. It is given by the difference in enthalpy of saturated gas at -20 °C to the solid at -40 °C at the same pressure. Other additional energy was considered in the vacuum freeze-drying is the work input to the compressor to provide the necessary cooling capacity at sufficient temperature. The Carnot COP of the refrigeration capacity is calculated at $T_h = 30$ °C and $T_l = -50$ °C. The work input of the vacuum pump to maintain relatively low pressure during the entire drying process was also calculated.

Heat pump assisted drying can provide greater energy savings for the drying process. The heat rejected from the heat pump system is used to heat air to high temperatures up to 150 °C. In our study high temperature heat pumps were considered. High temperature heat pumps can be used for drying the products effectively. Also, better products quality with a low energy consumption in controllable drying environment are achieved. Examples of heat pump assisted drying include heat pump assisted solar drying, fluidized bed drying, microwave drying, atmospheric freeze drying, and chemical heat pump assisted drying. Heat pumps works on the principle of vapour-compression cycles or absorption-compression cycles. Natural refrigerants like Ammonia, CO₂ are widely used in the refrigeration industry due to their better thermodynamic properties and reduction in environmental impacts. CO₂ booster and ejector systems are the developments in CO₂ refrigeration which increases the system performance. The simple heat pump cycle consists of a compressor,

condenser, evaporator, and expansion valve. COP indicates how efficiently the heat pump is running. From an industrial point of view, higher COP reduces energy costs.

3. RESULTS & DISCUSSION

3.1. Concentration using freeze concentration

The heat load to be removed from the hydrolysates was calculated to 135.5 kW. The energy required to freeze 1 kg of water was found to be .26 MJ/Kg. The results are in accordance with studies stated by Osato (2005). The fraction of ice removed from the feed hydrolysates was equivalent to be 76.7%. Using numerical models, the initial temperature at which nucleation of ice occurs was calculated to be -0.6 °C. The heat load to melt 1411 kg/h of ice formed was calculated at 137 kW considering sensible heat above and below freezing and latent heat when the phase change occurs. In freeze concentration, apart from the energy required for freezing the LPH and melting the ice, the refrigeration work must be considered. The refrigeration work calculated during Carnot process was 30.4 kW with evaporation temperature -40 °C and condenser temperature 0 °C. The Carnot COP is 5.8. The freeze concentration method leads to reduced energy consumption, here the main principle is the crystallization of liquids, the energy required to crystallize the liquids is lower when comparing the energy for vaporizing the liquid, as the latent heat to change liquid to gas phase is higher than the latent energy to phase change from liquid to solid.

Using freeze concentration method, the hydrolysates are concentrated to 30% solid content with a mass flow rate of 430 kg/h. Further, the drying processes were performed in order to remove water completely. In the drying calculation after freeze concentration, the LPH was concentrated to 98% solids in spray, drum and vacuum freeze drying. The hydrolysates initial temperature was -1°C and the amount of water vapor removed at 298 kg/h. The drying process consumes high energy between 1.5-1.67 kWh/kg of water removal as seen below in Figure 2. The obtained calculation results are in the range with standard values at 0.8 to 5.5 kWh/kg of water removal. The high energy required during the concentrating process is due to the energy needed in raising the feed temperature close to the boiling point temperature and the latent energy for changing the liquid phase to the vapor phase.

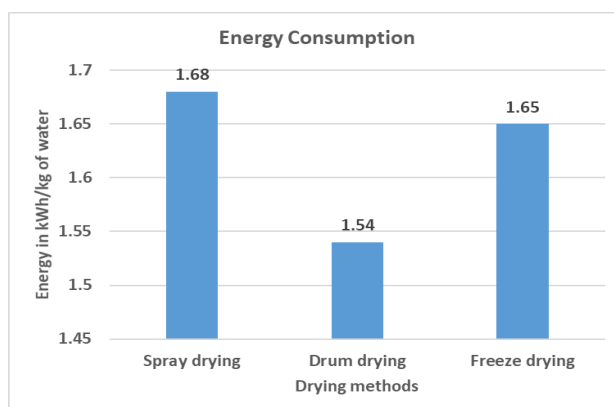


Figure 2. Energy consumption in drying process

3.2. Concentration by three stage evaporators

Multistage evaporators and vapor recompression methods are studied to identify how energy reduction can be achieved at concentration steps. The heat load calculated during the three-stage evaporator process was 338 kW when the process is continuous with hydrolysates flow temperature at 90 °C. If the hydrolysates are stored to storage temperature, the total heat load during the process was 399 kW. The concentrated hydrolysates flow at exit of the evaporator is 257.7 kg/h and the amount of vapor removed is 1583 kg/h. It was estimated that the vapor evaporated at the last stage was 527.6 kg/h calculated from total evaporating

vapor with the concentrating level at each stage. The condenser was maintained at a lower temperature of 30 °C with a pressure of 0.2 bar. Cooling Load for condensing the vapor at last stage was calculated to be 364 kW. The process was further dewatered by drying methods and the corresponding heat loads are calculated as shown below,

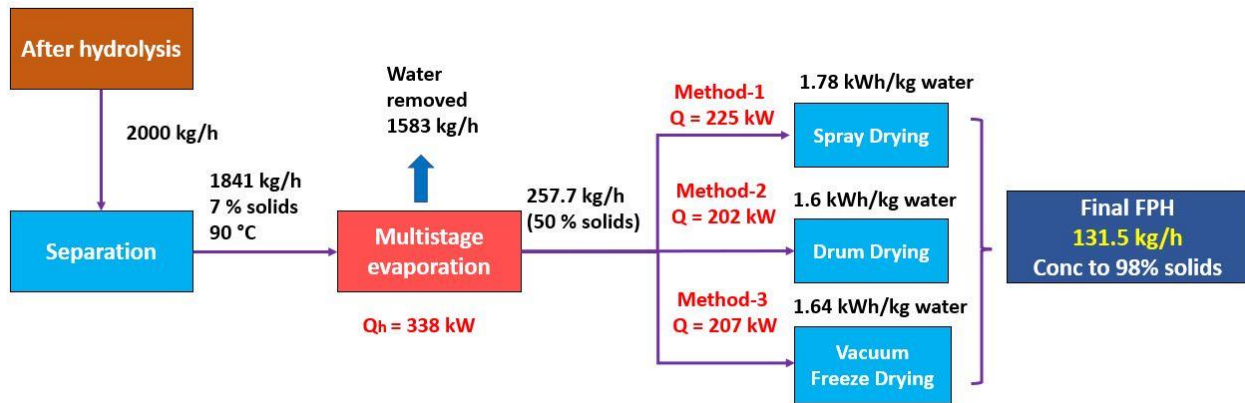


Figure 3. Process flow diagram with three stage evaporators

3.3. Mechanical vapor recompression

The work input of the system was calculated at 103.1 kJ/kg to raise the pressure from 1 bar. The heating capacity out of the system Q_c was 2310.7 kJ/kg. The compressor removes the vapor from the evaporator and increases the pressure. Energy for evaporation was returned to the system. The pressure difference of the compressor is small resulting in low energy input. Hence the COP of the system is very high at 22. The system can be operated with increase in pressure and the corresponding heat output is large. On the other hand, the work input to raise the system pressure is higher. In this process, only during starting, steam was consumed and further no external steam input was required. The process is reliable in operation, compact equipment, does not require any external heating source and higher thermodynamic efficiency.

3.4. Heat pump assisted drying

When heat pumps are integrated into the drying system, the energy efficiency of the process is increased. In the spray dryer the exhaust air has sufficient heat, which is surplus energy that can be utilized as a heat source to the heat pump. The high-temperature air is heated at the condenser side, hence lowering the amount of energy that the heaters in driers are using. The high temperatures heat pump studied in this work was used to heat the air to a temperature up to 150°C. In spray and drum drying, a significant amount of the energy was consumed by heating the drying air to the desired high temperature. Hence, calculation was performed to understand the influence of inlet air temperature on the energy consumption in the spray dryer. The heat transfer was very inefficient by heating the air from 15°C to 200°C, hence the temperature lift must be reduced. The energy variation, with respect to the inlet air temperature for spray dryer, is given below. It is observed that the inlet air temperature plays a significant role in energy consumption.

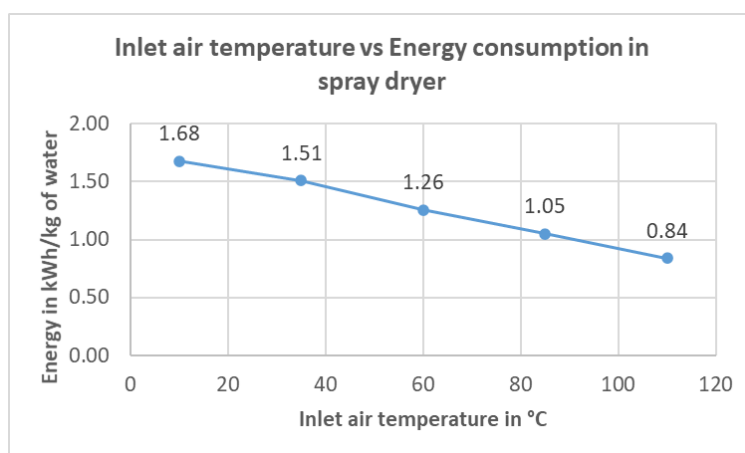


Figure 4. Spray dryer energy consumption against inlet air temperature

When the air temperature increased from 10°C to 110°C, the energy required to evaporate per kg of water was reduced to 0.84 kWh/kg ~ 3020 kJ/kg of water which is a 50% reduction in energy consumption in the spray drying process which is seen in above Figure 4. Since using high temperature heat pump, with ammonia or CO₂ as a working fluid, the energy recovery can be achieved to sufficiently heat the air to a higher temperature, this reduces the energy need for heating the air. Waste heat recovery can be an efficient option to heat the drying air which reduces the overall energy consumption. Heat pump assisted drying consumes less energy, since the heat pump cycle has higher COP. Using heat pumps the waste heat can be recovered more effectively. Implementing high temperature heat pumps in the process of production of FPH helps to cover heating and cooling needs in an economical way.

3.5. Overall energy consumption

The total energy requirement when concentrating 1000 kg/h of rest raw material to 131.5 kg/h (98% solids) is given below in Table 2. It is observed from the table, that the direct drying of FPH consumes significant amount of energy use. Hence, concentrating techniques before the final drying process should be implemented to reduce the energy demands. When concentrating 30% solids of FPH by freeze concentration and then final concentrating with drying methods, results in lower energy consumption around 1120-1245 kWh for 1 ton of rest raw material. Which is 60 % energy savings when compared with direct drying methods.

Table 2: Process wise Energy requirement (kWh) per 1 ton of RRM

		Freeze concentration	Three effect evaporators	Mechanical vapor recompression	Direct drying
Drying method used	Spray drying	1245.3	1182	629	3183
	Drum drying	1124.3	1158	606	2958
	Vacuum freeze drying	1230	1163	611	3315

Concentrating to 50 % solids using mechanical vapor recompression (MVR) method followed by drying has very low energy requirements of 606-630 kWh when processing 1 ton of RRM. For heat sensitive products, the freeze concentrating process can be widely used, as the process operates at lower temperatures. Lower process operating temperature leads to improved process efficiency and enhances the product quality.

4. CONCLUSION

In this research work, the energy consumption in the production of fish protein hydrolysates for 1 ton/h of RRM was investigated in detail. To stabilize the FPH, removal of moisture by direct drying process consumes significant amount of energy around 3000 to 3300 kWh. Freeze drying, spray drying and drum drying

consume high amount of energy, between 1.5 to 1.88 kWh/kg of water. On the other hand, when performing concentrating process before final drying reduces the overall energy consumption. Freeze concentration can be used as an effective process in combination with drying and has an energy consumption of 1120-1250 kWh. With freeze concentration method 30% solids was concentrated. The main advantage is low temperature operation and reduce further energy costs. Also, in this study three stage evaporation and mechanical vapor recompression was studied with drying methods. The results showed a significant energy reduction when compared with direct drying process, the mechanical vapor recompression process consumes less energy when comparing other methods, since it works on energy recovery principle. High temperature heat pump assisted drying was studied with heat recovery, which is an effective way of integrating the cooling and heating demands.

ACKNOWLEDGEMENTS

The authors gratefully acknowledge the Research Council of Norway and industrial project partners for the financial support for carrying out the present research [NFR project No. 294662, CoolFish].

NOMENCLATURE

Abbreviations

<i>FPH</i>	Fish Protein Hydrolysates
<i>RRM</i>	Rest Raw Material
<i>Hx</i>	Heat exchanger
<i>CO₂</i>	Carbon dioxide
<i>COP</i>	Coefficient of performance
<i>ERS</i>	Energy Recovery Scheme
<i>MEE</i>	Multi Effect Evaporator
<i>MVR</i>	Mechanical Vapor Recompression
<i>BPR</i>	Boiling Point rise
<i>SMER</i>	Specific Moisture Extraction Rate

Greek symbols

ΔH_{vap}	Latent heat of vapor [kJ/kg]
ρ	Density [m ³ /kg]
η_c	Carnot efficiency -

Symbols

<i>H</i>	Enthalpy [kJ/kgK]
<i>C_p</i>	Specific heat capacity [kJ/kgK]
<i>W_c</i>	Work Carnot [kW]
<i>Q_{net, t}</i>	Heat Transfer rate/Heat input [kW]
<i>m_f</i>	Feed Mass flow rate [kg/h]
<i>m_v</i>	Mass flow rate of vapor [kg/h]
<i>E</i>	Energy Consumption [kWh]
<i>L_{ice}</i>	Latent heat of ice [kJ/kg]
<i>T_{a1}</i>	Inlet air temperature [°C]
<i>T_{a2}</i>	Exit air temperature [°C]

Subscripts

<i>l</i>	liquid
<i>v</i>	vapor
<i>w</i>	water

REFERENCES

- Desai, A. S., Brennan, M., Gangan, S. S., Brennan, C., 2022. Sustainable Fish Production and Processing. Chapter seven - Utilization of Fish Waste as a Value-Added Ingredient: Sources and Bioactive Properties of Fish Protein Hydrolysate, Pages 203-225. <https://doi.org/10.1016/B978-0-12-824296-4.00004-9>
- Petrova, I., Tolstorebrov, I., Eikevik, T. E., 2018. Production of fish protein hydrolysates step by step: technological aspects, equipment used, major energy costs and methods of their minimizing. International Aquatic Research. volume 10, pages 223–241. <https://link.springer.com/article/10.1007/s40071-018-0207-4>
- Himaya, S. W. A., Ngo, D. H., Ryu, B., Kim, S. K., 2012. An active peptide purified from gastrointestinal enzyme hydrolysate of Pacific cod skin gelatin attenuates angiotensin-1 converting enzyme (ACE) activity and cellular oxidative stress. Food Chemistry, 132 (4) pp. 1872-1882. <https://doi.org/10.1016/j.foodchem.2011.12.020>
- Mujumdar, A. S., 2007. Principles, classification, and selection of dryers. In: Mujumdar AS (ed) Handbook of industrial drying. CRC Press, Boca Raton. https://luchosoft.com/pdf/Hand_Book_Of_Industrial_Drying_2006.pdf

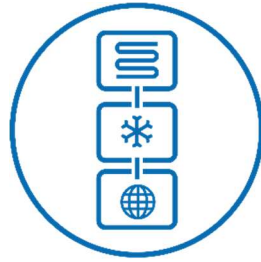
- Mansour H., Busairi A. B., Baker C. G. J., 2011. Energy consumption of a pilot-scale spray dryer. *Dry Technology* 29(16):1901–1910.
- Miyawaki, O., Liu, L., Shirai, Y., Sakashita, S., Kagitani, k., 2005. Tubular ice system for scale-up of progressive freeze-concentration. *Journal of Food Engineering* Volume 69, Issue 1, Pages 107-113.
- Han, D., Chen, J., Zhou, T., Si, Z., 2021. Experimental investigation of a batched mechanical vapor recompression evaporation system. *Applied Thermal Engineering*, Volume 192, 116940. <https://doi.org/10.1016/j.applthermaleng.2021.116940>
- Schuck, P., Jeantet, R., Tanguy, G., Me´jean, S., 2015. Energy Consumption in the Processing of Dairy and Feed Powders by Evaporation and Drying. *Drying Technology*, 33: 176–184. <https://DOI:10.1080/07373937.2014.942913>



IOR.org.uk

REFRIGERATION AIR CONDITIONING HEAT PUMPS

Student Author Prize Winner



7th IIR Conference on Sustainability
and the Cold Chain

ICCC 2022
ONLINE
APRIL 11-13

Prem Kumar Sherman

For the paper

**Application Of Refrigeration Technologies For Energy Efficient Production Of
Fish Protein Hydrolysates**

organised by

THE INSTITUTE OF REFRIGERATION
on behalf of the
International Institute of Refrigeration
Conference of IIR Commissions D1, D2 and C2

Date and Venue
11th - 13th April 2022
Online Virtual Conference

Signed:

IOR Chief Executive